EXTRA-ORDINARY HALL EFFECT AND MAGNETIZATION IN NICKEL-RICH Ni-Fe-Cr AND Ni-Fe-V ALLOYS

A Thesis Submitted
In Partial Fulfilment of the Requirements
for the Degree of
DOCTOR OF PHILOSOPHY

By

ANUP KUMAR GANGOPADHYAY

to the
DEPARTMENT OF PHYSICS
INDIAN INSTITUTE OF TECHNOLOGY, KANPUR
DECEMBER, 1983

PHY-1983-D-GAN-EXT

87521

Dedicated

to

my parents

CERTIFICATE

This is to certify that the work reported in this thesis entitled, "Extra-ordinary Hall Effect and Magnetization in Nickel-rich Ni-Fe-Cr and Ni-Fe-V Alloys" has been carried out by ANUP KUMAR GANGOPADHYAY under our supervision. No part of this work has been submitted elsewhere for a degree.

(Rajat Kumar Ray)
Professor
Department of Physics
Indian Institute of Technology
Kanpur-208016

December, 1983

(Alak Kumar Majumdar)
Assistant Professor
Department of Physics
Indian Institute of Technology
Kanpur-208016

ACKNOWLEDGEMENTS

It gives me a great pleasure to express my deep feeling of gratitude to Drs. R.K.Ray and A.K. Majumdar for their constant guidance, help and encouragement to bring the work to a logical conclusion. My sincerest thanks to Dr. Majumdar for suggesting the problem at a crucial stage and to Dr. Ray for helping me to form a healthy attitude towards research, which, I believe, will go a long way to further my scientific career. It was really a pleasure working with them in an atmosphere of 'camaraderie'.

My heartful of thanks to Dr.T.N.Srinivasan for his kind help and valuable advice at various stages of this work. I am also indebted to him for learning some useful experimental "tricks". I feel specially obliged to Mrs. A.Sinha for supplying a few samples and to Prof. L. Berger for sending some valuable data. I deeply appreciate the kind gesture shown by Drs.A.K.Majumdar and R.D. Greenough in allowing me to use some of their unpublished data.

To Mr.V.P.Gupta goes my heartful of thanks for taking more than professional interest in preparing the alloys. The help and co-operation extended by Dr.N.V.Nair and Dr.K.P.Gupta for this purpose is also gratefully acknowledged.

My sincere thanks to Dr.A.K.Nigam and Mr.S.B.Roy for their help and co-operation at various stages of the work.

I gratefully acknowledge the co-operation I enjoyed from the staff members of the Low Temperature Laboratory, -M/S. S.D.Sharma, S. Singh, N. Ahmed, Janki Prasad, Ram Ashrey, U.S. Tewari, Jawaharlal and Ram Prakash. My special thanks to the members of the Glass Blowing Workshop and also of the Physics Electronics Workshop for timely help, whenever requested.

I highly appreciate the wonderful roles played by M/S. V.P. Gupta (drawing), U.S.Mishra (typing), L.S.Rathaur and H.K. Pandya (cyclostyling) and others in their respective arenas to enable me to present the work in a decent form.

The warmth and friendship and many stimulating discussions (academic and.....) I enjoyed in the company of M/S. S.B.Roy, P.K. Khowash, D. Chowdhury and P. Thakur will always remain a cherishing memory.

Last but not the least, I would like to express my sincere thanks to numerous friends (or foes, if I have any), who directly or indirectly, knowingly or unknowingly, made my stay in this campus an enjoyable occassion.

-ANUP KUMAR GANGOPADHYAY

CONTENTS

LIST OF TABLES

LIST OF FIGURES

SYNOPSIS

EXTRA-ORDINARY HALL EFFECT AND MAGNETIZATION IN NICKEL-RICH Ni-Fe-Cr AND Ni-Fe-V ALLOYS

A Thesis Submitted
In Partial Fulfilment of the Requirements
for the Degree of
DOCTOR OF PHILOSOPHY

By
ANUP KUMAR GANGOPADHYAY
Department of Physics
INDIAN INSTITUTE OF TECHNOLOGY, KANPUR, INDIA
December 1983

The Hall resistivity of a ferromagnet consists of two parts: i) The ordinary part, which arises due to the Lorentz force acting on the current carriers, ii) The extra-ordinary part arising from the asymmetric scattering or some transverse displacement of the current carriers due to their interaction with the scattering centres in the metal. Some kind of spin-orbit coupling is believed to provide this interaction. The extra-ordinary Hall co-efficient R_s shows a change of sign on alloying in various binary and ternary Ni and Fe based alloys. Generally this sign change of R_s is also accompanied by a sign change in the co-efficient of linear magneto-striction λ_s and an associated maximum in the ferromagnetic anisotropy of resistivity (FAR). Since very few systematic studies have been made to investigate the sign change of R_s in ternary alloys, we took up the two alloy systems, Ni-Fe-Cr/V for our present study. The two systems, specially Ni-Fe-Cr, seemed to be of additional interest because of the already existing data showing

a non-linear change in the average magnetic moment $\bar{\mu}$ on alloying. There seemed to be a possibility that the split-band (S.B.) model, developed by Berger to explain the sign change of R_s and λ_s in Ni and Fe based alloys, may not hold good for the Cr system. As it happens quite often, though the beginning was made with this limited aim, some interesting results at the initial stages of the work subsequently drew our interest also to a systematic and comprehensive study of the magnetic properties of the two ternary systems in the Ni-rich region.

After briefly introducing the subject in Chapter I, a short review is given to highlight both the experimental and theoretical findings obtained so far. This is followed by a discussion on the S.B. model and its importance in connection with the sign change of R_s and λ_s in various binary and ternary alloys. The Chapter ends by spelling out the motivations behind the present investigation.

Chapter II starts with the experimental techniques involved in sample preparations and characterizations. Next is discussed the procedures followed for magnetic measurements using a PAR model 155 vibrating sample magnetometer. Finally the design and fabrication of the cryostat along with the necessary circuitry used for the measurements of Hall effect and resistivity in the range 77-473K is discussed. Special attention is given to the design of the sample holder which allows one to use pressure contacts.

In Chapter III are presented the results of magnetic measurements after developing the theories used for data analysis. At the same breath the results are also discussed. The magnetic measurements consist of: i) T_c measurement, ii) study the change in magnetization of seven Ni-Fe-Cr alloys and four Ni-Fe-V alloys from 77K upwards and their interpretation in terms of the spin-wave theory, iii) change in saturation magnetization at OK (obtained by extrapolation) with composition, iv) study of susceptibility above T_c for three Ni-Fe-Cr and two Ni-Fe-V alloys, v) Arrott plots for a few alloys from 77K to near their respective T_c's. The results of the magnetic measurements can be summarized as follows:

(1) Though a $T^{3/2}$-term along with a T^4-term could well account for the decrease in magnetization with temperature, the values of the spin-wave stiffness constants were found to be always less than the corresponding neutron scattering results. This discrepancy was found to be due to the existence of other than spin-wave excitations, which appeared to be like Stoner's single particle excitations for itinerant weak ferromagnets, following a T^2-law. The co-efficient for T^2-term increases with increasing Cr concentration.

(2) Reduced magnetization, when plotted against reduced temperature, falls much faster than Brillouin functions.

(3) The ratio of the number of Bohr magnetons per atom, obtained from the Curie constant and the one from the low

temperature saturation magnetization, was always found to be greater than unity. This ratio increased fast with the addition of Cr/V (i.e. decreasing T_c).

(4) Arrott plots were found to be fairly good straight lines for the alloys with lower T_c over a wide range of temperature. All these evidences indicate that with increasing Cr/V concentration, both the ternary systems behave more like itinerant weak ferromagnets.

Chapter IV starts with the results of the extra-ordinary Hall co-efficient measurements at 77 and 300K of about fifteen alloys in the Cr series and twelve in the V one. From these data we could establish the position of of the $\gamma_{HS} \simeq 0$ ($\gamma_{HS} = \frac{R_s M_s}{\rho^2}$ is the extra-ordinary Hall conductivity) line for both the series. The informations that could be obtained from our measurements are the following:

(i) For both the alloy series, $\gamma_{HS} \simeq 0$ line lies far away from both the experimental $\lambda_s \simeq 0$ line as well as the $\lambda_s \simeq \gamma_{HS} \simeq 0$ line predicted from the S.B. model. Deviation was found to be more in the case of Cr series than the V one.

(ii) Both $(\gamma_{HS})_{exp.} \simeq 0$ and $(\lambda_s)_{exp.} \simeq 0$ lines showed considerable curvature, contrary to what one expects from the S.B. model. An attempt was made to explain the curvature by empirically introducing the non-linearity in the experimental $\bar{\mu}$ vs. concentrations curves, in the equation for $\gamma_{HS} \simeq \lambda_s \simeq 0$ line, predicted from the S.B. model.

Some possible reasons have been discussed to explain the failure of the S.B. model in the light of the results obtained from magnetic measurements. The Chapter ends with an attempt to explain the residual resistivity of the alloys with the help of the "two-current" model for conduction in transition metals.

The conclusions that could be drawn from our present study are summarized in Chapter V and the scope for future work has been discussed.

Chapter I

Hall Effect in Ferromagnets

It is well known that Hall effect in any material is basically a manifestation of the Lorentz force acting on the charged particles in a magnetic field. Due to this, the carriers get deflected and produce a transverse field along the y-direction (under the usual Hall geometry the magnetic field is along the z-direction and the current flows along x-direction). This field is proportional to the current density J_x and the magnetic induction B. Thus

$$E_y = R_o J_x B \qquad (1.1)$$

where R_o is the Hall constant which is inversely proportional to the carrier concentration and the dominant carrier type (electron/hole) determines its sign. Deviation from Eqn.(1.1), reflected in the non-linear behaviour of Hall voltage and magnetic induction, can arise mainly due to the following reasons:

i) A transition from low-field ($\omega_c \tau < 1$) to high-field ($\omega_c \tau > 1$) limit by either increasing the magnetic field or lowering the temperature/impurity concentrations, or both. Here $\omega_c = \frac{eH}{m^*}$ (m^* = effective mass of the carriers) is the cyclotron frequency and τ is the mean relaxation time.

ii) If contribution to R_o comes through some mechanism, other than the Lorentz force, considerable deviation from

linearity might be observed. This is the case particularly in materials having some kind of long range magnetic order or even in those having short range magnetic ordering (viz. spin glasses).

Our present interest lies with the materials in the second category and that component of the Hall effect, which arises from magnetization. Figure 1.1 shows the typical behaviour of Hall resistivity ρ_H ($\rho_H = E_y/J_x$), as a function of magnetic induction in a typical ferromagnetic material. The similarity of this curve to that of magnetization clearly shows that in a ferromagnet the additional term should be proportional to magnetization. Indeed the Hall resistivity in a ferromagnet can be described as

$$\rho_H = R_o\ B + R_s M \qquad \text{(SI units)} \qquad (1.2)$$

The first term is the usual Lorentz or ordinary term and the second one is called the extra-ordinary term with R_s as the extra-ordinary Hall constant. It is quite obvious that in the high fields when the material has reached "technical saturation", further increase of ρ_H can be only through the first term and hence the high field part is linear in B. As shown in Figure 1.1, the slope of the high field straight line part gives R_o and the extrapolation of this straight line gives an intercept of $R_s M_s$ on the ρ_H-axis. Though this method of separation of the ordinary and the extra-ordinary terms is justified, a word of caution is necessary. For materials having a large high field susceptibility, specially near the Curie temperature T_c, even the

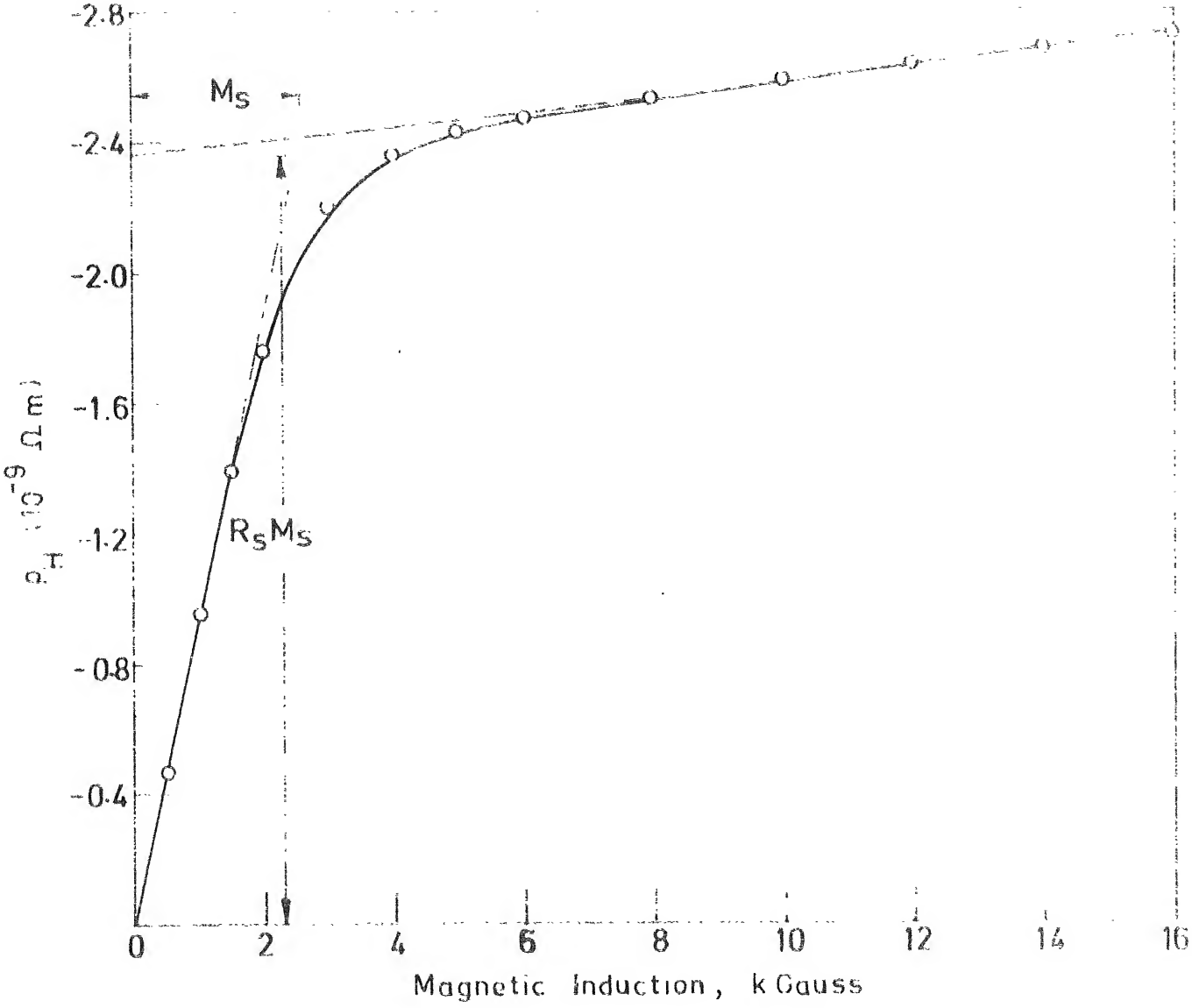

FIG. 1.1 TYPICAL BEHAVIOUR OF THE HALL RESISTIVITY OF A FERROMAGNETIC MATERIAL

extra-ordinary term can have appreciable contribution to the high field slope of ρ_H vs. B curves and hence the value of R_o obtained by the above method will be erroneous. In that case a knowledge of the high field susceptibility is necessary and R_o can be extracted from the slope only when the contribution of the second term is evaluated.

In general, R_s is at least one order of magnitude higher than R_o and hence in a ferromagnet the extra-ordinary term dominates. Another important distinction is that R_s has been found to be strongly temperature dependent in contrast to a weak temperature dependence of R_o. There exists a correlation between R_s and the electrical resistivity ρ,

$$R_s \propto (\rho)^n \qquad (1.3)$$

where $2.0 > n > 1.5$ at higher temperatures in the usual ferromagnetic materials like Ni[1] and Fe[2]. In transition metals and alloys, R_s usually follows the relationship

$$R_s = a\rho + b\rho^2 \qquad (1.4)$$

where 'a' and 'b' are constants dependent on the material.

Above the magnetic ordering temperature (T_c or T_N), though the extra-ordinary term ($R_s M_s$) vanishes since the material no longer possesses spontaneous magnetization, there is no reason to suppose that the co-efficient R_s also becomes zero. As can be seen from Eqn.(1.2), the quantity $\partial\rho_H/\partial H$ should be proportional to the susceptibility and the temperature dependence should come mainly through the susceptibility if

R_o and R_s are assumed to be weakly temperature dependent in the paramagnetic region. Theory[3] as well as experiments on Ni and Ni-Mo alloys[4] and also on Dy[5], Tb[6], etc., confirm this. These data also show a smooth variation of R_s across T_c (T_N).

1.1 Theories for Extra-ordinary Hall Effect

Last thirty years have seen a burst in theoretical activity in search of a plausible explanation for this phenomenon. It is amply clear by now that no single theory is capable of explaining all the characteristics of this effect in a large variety of materials. Since good reviews[7,8] on this account already exists in the literature, and very few new developments have come up since then, we have no intention to present the same here. Rather we will try to present briefly the salient points involved in those theories which have been able to stand the test of time.

The experimental relationship between R_s and ρ naturally drew the attention of theoreticians in search of a scattering mechanism which can produce a voltage having the odd nature (with respect to current and magnetic field directions), characteristic of the Hall voltage. An interaction which depends on spin and can have the antisymmetric character needed for this kind of scattering, is the spin-orbit interaction. All the theories developed so far agree on this basic point that some kind of spin-orbit interaction is

responsible for the extra-ordinary Hall effect. Divergence starts with the nature of the spin-orbit (henceforth termed as S.O.) interaction. Similar to other branches of magnetism, here also the theories can be broadly classified into two categories: i) itinerant, ii) localized.

1.1.1 Theories Based on Itinerant Models

In the original work of Karplus and Luttinger,[9] assuming d-electrons to be itinerant in character with unequal population for spin-up and spin-down electrons (to account for the magnetization), it was shown that an extra-ordinary term with co-efficient proportional to the square of the electrical resistivity can arise under the influence of "intrinsic" (d-spins interacting with its own orbital angular momentum) S.O. interaction. As a result of this S.O. interaction, the electron wave-functions acquire a left-right asymmetry and a net current is produced under the influence of an electric field, along a direction perpendicular to both the electric field and the average direction of the spin of the electrons. But Smit[10,11] criticised their theory on the ground that in a perfectly periodic lattice this mechanism cannot produce any net current but can only polarize the Bloch States. Deviation from periodicity due to lattice imperfections or impurities can only produce a finite current. Though in a later paper Luttinger[12] found some cancellation effect, he could not accept all the criticisms of Smit. The controversy

still remains unresolved. Smit[13] has shown that in the steady state all scattering-independent effects vanish and only surviving mechanism is that of skew scattering. But Smit's theory is also subjected to criticism as it predicts a sign change of the Hall angle ($R_s M_s/\rho$) with the nature of the impurity scattering potential (attractive or repulsive), which is not consistent with his own experimental results. Another important aspect is that these theories obviously cannot be applied to rare-earth systems whose electrons contributing to magnetic moment are well localized.

There are other theories also by Irkhin and Shavrov,[14] which considered the scattering of electrons by phonons and obtained similar kind of relationship ($R_s \propto \rho^2$) as for impurities. Kondorskii[15] arrived at a relationship similar to Eqn.(1.4) by considering the scattering by both impurities and phonons. His own experimental results[15] for a number of Ni-Fe, Fe-Mo, and Fe-Al alloys follow Eqn.(1.4) over a wide range of temperatures and concentrations.

1.1.2 Theories Based on Localized Models

Kondo[16] proposed a different model where the charge carriers are S-electrons with equal population for spin-up and spin-down electrons and the d/f-electrons are localized at the lattice sites with their total spin contributing to the magnetization. At finite temperatures, the periodic potential of the lattice is disturbed due to thermal disordering of the magnetic moments and the S-electrons get scattered under the

influence of d/f-spin-S-spin interaction (RKKY type). Though anisotropic (which disappears when the ground state of the d/f-electrons is nondegenerate) in nature this interaction itself cannot give rise to skew scattering and hence no extraordinary Hall current. Only when the "intrinsic" S.O. interaction of the d/f-electrons is taken into account, a Hall current appears. According to his calculations, the Hall resistivity is given by

$$\rho_H = \text{Constant} < (M - \langle M \rangle)^3 > \qquad (1.5)$$

where $< (M - \langle M \rangle)^3 >$ is a three-spin correlation function which describes the spin-fluctuations due to thermal disorder and account for the temperature variation of ρ_H. At T=0 this function vanishes and in the paramagnetic range (above T_c) it can be exactly evaluated to give $\rho_H \propto \chi H$ and hence in agreement with the experimental results. In the intermediate temperature range Kondo evaluated this function and showed that except for the low temperature minimum observed in pure Fe,Ni and Co[2,17], all other experimental aspects agree qualitatively well with this theory. But an important criticism of this theory, as pointed out by Kondo himself, is that no skew scattering can arise if the orbital angular momentum of the d/f-electrons is quenched as in transition metals and Gd.

To circumvent this, Abel'skii and Irkhin[18] and also Kagan and Maksimov[19] invoked a mixed type of S.O. interaction (S-orbit/d(f)-spin) along with the intrinsic S.O. interaction and evaluated the three spin-correlation

function under the molecular field approximation to obtain for $S = \frac{1}{2}$

$$\rho_H \sim M_s^2(0) - M_s^2(T) \qquad (1.6)$$

where $M_s(T)$ is the spontaneous magnetization at temperature T. Maranzana[20] also evaluated the correlation function under molecular-field approximation to obtain ρ_H in terms of the derivatives of Brillouin functions. The results are essentially similar to those of Kondo. An expression for ρ_H for antiferromagnets was also obtained by him.

1.1.3 Scattering Mechanisms

From the picture that has emerged so far, two distinct scattering mechanisms appear to be responsible for the extraordinary Hall effect, viz. i) skew scattering, and ii) side-jump.

As proposed by Smit[11], the S.O. interaction lifts the left-right symmetry with respect to a plane containing the electron's spin and its incident velocity and hence the scattering probability towards left and right of this plane no longer remains equal. This asymmetric or skew scattering results only when the scattering probability is calculated in the second Born approximation. But calculations with plane waves (i.e. free electrons) as unperturbed wave-functions give results which are too small to account for the experimental results. The correct order of magnitude is obtained only when the influence of the periodic part of the S.O. interaction on wave-functions is taken into account[21]. In the case of noble metals containing rare earth impurities with localized

4f electrons, skew scattering arises from the orbital exchange terms[22]. Fert and Jaoul[23] proposed a different skew scattering theory based on S-d-S scattering of the free electrons. Whatever be the model, skew scattering always predicts R_s to be proportional to the electrical resistivity. It is dominant when the electron mean free path is large, i.e. in dilute alloys and/or at low temperatures.

Another mechanism is the side-jump, proposed by Berger[24], which arises when scattering of wave packets are considered in the presence of S.O. interaction. It has a purely quantum mechanicalorigin which can be visualized as follows. When an electron wavepacket is approaching a scattering potential, before and after scattering the motion of the center of mass can be well described as moving along straight lines. But the two trajectories before and after collision might not meet at the center of the scattering potential; the new trajectory might be displaced from the one before scattering by a finite amount. Thus at every scattering the electron wavepacket experiences a finite displacement (calculated to be about -10^{-10} 10^{-11}m. for band electrons) along y-direction which contributes to the extra-ordinary Hall effect. This results because the scattering potential distorts the wave function locally and thereby creates a local current density. It also experiences a longitudinal displacement which however does not influence the Hall effect. The magnitude of the side-jump has been found to be independent of the range, strength, and nature (i.e. impurities, phonons, etc.) of the scattering potential. This

mechanism dominates when the mean free path of the electrons is small i.e. for concentrated alloys and/or at high temperatures. R_s arising from side-jump should be proportional to the square of the electrical resistivity. More sophisticated calculations for side-jump have been carried out by Lyo and Holstein[25] and also by Nozieres and Lewiner[26] in the first Born approximation and their results confirm Berger's findings.

1.2 Sign of the Extra-ordinary Hall Co-efficient (R_s)

The theories discussed so far, mainly try to explain the relationship between R_s and the resistivity ρ, or the temperature variation of R_s. The first successful theory to account for the sign of R_s in common ferromagnetic materials like Fe, Ni and Co was due to Kondorskii[27]. It is well known that both R_s and the ordinary Hall co-efficient R_o have the same sign in Fe and Ni (both are positive in Fe and negative in Ni at room temperature). So earlier it was assumed that it is only the carrier type which determines the sign of both R_s and R_o. But in the case of Co, R_s changes from the low temperature negative value to a room temperature positive value at around 220K, whereas R_o remains negative throughout[17]. Later measurements on purer single crystals of Fe also show that R_o changes sign around 77K (from negative to high temperature positive values), although R_s remains positive throughout[2]. These facts along with the data for R_o and R_s in some alloys (e.g. Ni-Fe, where R_s changes from negative to positive values around 18 at.% Fe whereas R_o only around 95 at.% Fe[28])

clearly shows that R_o and R_s can have different signs, in general. Guided by these facts, Kondorskii[27] suggested a theory which involves a detailed knowledge of the Fermi surface of the metal to predict the sign of R_s.

According to Kondorskii, in ferromagnets, due to the exchange splitting of the spin-up and spin-down bands, the occupation of the two sub-bands are different. The contribution to R_s by the carriers in different sub-bands (i.e. with different spins) will be different; the carrier type (electron or hole-like) in a particular sub-band will be decided by the topology of that part of the Fermi surface. So the overall sign of R_s will be determined by the dominating carriers and their spins. He arrived at an expression for R_s as

$$R_s = \frac{C}{I_s \sigma^2} \Sigma_n M_n K_n S_n \qquad (1.7)$$

where I_s is the spontaneous magnetization, σ is the electrical conductivity, M_n is the average z-component of the magnetic moment of an electron in the n^{th} band ($M_n = \pm \mu_B$; which is positive for electrons in the up-spin band), $K_n S_n$ is some integral carried over the n^{th} spin zone S_n, and C is some constant for a given metal. Thus if the quantity $\Sigma_n K_n S_n$ for the electronic part of the Fermi surface dominates over that of the hole-part, the main carriers of extra-ordinary Hall effect can be termed as electron-like and vice versa. Accordingly he formulated that R_s will be positive if the dominant carriers are electron-like and are from the up-spin

band and negative if they are electron-like and are from the down-spin band. For holes, the signs will be just the opposite of those for electrons. Using the above criterion and from the knowledge of the Fermi surface of Ni, Kondorskii found that the main contributions in Ni are from electron-like carriers from the unfilled down-spin band and hence R_s is negative. But for iron, the predominant current carriers are electrons from the up-spin band and holes from the down-spin band, both of which contribute to a positive value of R_s.

Though successful in explaining the signs of R_s in Fe and Ni, the application of this kind of theory requires detailed knowledge of the Fermi surface, which is often not available, specially for alloys. To explain the sign change of R_s with composition in various Ni and Fe based alloys, Berger[29] proposed a split-band model, which we will discuss in detail in the next section. Before, that, we would also like to point out that recently in a series of papers[30-32], Kondorskii have applied Coherent Potential Approximations to calculate the extra-ordinary Hall co-efficient in binary disordered alloys at around OK. They have discussed the effect of both impurity type and impurity concentrations on R_s (at OK) taking into consideration both the periodic and aperiodic part of the S.O. interaction. Though theoretically sound, theform of R_s is such that direct comparison of experimental results with their equations is not possible. Hence we will not discuss those theories further.

1.2.1 Split-band (S.B.) Model

Two basic approaches were developed to tackle the problem of transition metal alloys where both the constituents could belong either to the same series or one of them could be a noble metal. The first approach is the rigid-band model due to Mott[33], and the second one is the virtual-bound-state model due to Friedel[34]. In the former case, the constituents are assumed to form common d-bands as well as S-p bands; and the addition of impurity simply changes the position of the Fermi level, connected with band filling, depending on the valence difference between the host and the impurity atoms. A typical example is that of Ni-Cu alloys, where by the addition of Cu (having one excess electron than Ni) the Fermi level is pushed up and around 60 at.% of Cu the Fermi level coincides with the top of the Ni 3d-band, marking the disappearance of ferromagnetism. The rigid-band model holds good if the impurity potential is not strong, which is true when the constituents have small valence difference. But if the impurity lies far away from the host in the periodic table (e.g., Cr, V, etc. in Ni), the perturbation around the impurity in the alloy might be strong enough to "split up" an impurity state above the Fermi level. If this state lies just above the Fermi level, it can resonate with the continuum states. Such a state is called a virtually-bound state, as suggested by Friedel[35]. Since then it has been widely used to explain the deviation of saturation magnetization at OK from the Slater-Pauling curve for alloys like Ni-Cr, Ni-V, etc. Also the "period-effect" where

resistivity, thermopower, electronic specific heat co-efficient, etc. show periodicity as one starts adding transition metal impurities, starting from the left of the 3d (or 4d, 5d) series, to a given host, finds suitable explanation in the framework of the virtual-bound state model (the "period- effect" will be discussed further in Chapter IV, Section 4.5).

The split-band model (from now onwards it will be termed as S.B. model) is just an extension of the virtual-bound state model applied to fairly concentrated alloys and was suggested by Berger[29] to explain the sign change of R_s in various Ni-based alloys. According to this model, each constituent of the alloy has its own 3d band, distinct in the energy scale. In the case of ferromagnetic alloys, the bands are further split due to exchange interaction energy and so these sub-bands are also distinctly separate for various constituents. In a binary alloy $A_{1-x}B_x$, as x is increased, the bands for the element B grow in size and those of A shrink. This has a good theoretical support in the CPA calculations for the band structure of various Ni and Fe based alloys by Hasegawa et al.[36-38]. According to the CPA calculations, distinctly separate bands for constituents A and B are possible if the average energy of an electron at site A (E_A) and site B (E_B) differ by more than the band width W of the host metal[39]. Usually this condition is fulfilled if the valency difference between the constituents is sufficient ($\gtrsim 2$). But in the case of ferromagnetic materials the energy at a site i (i = A,B) is made of i) electrostatic and ii) exchange parts. So large valency difference between

the host and the impurity may not always ensure complete splitting since the two energies may be of different sign. For the same reason the difference $E_A - E_B$ will also be different for spin-up and spin-down electrons. As for example in Ni-Fe alloys $E_{Fe} - E_{Ni} = -0.06$ for the spin-up electrons and for the spin-down electrons it is 0.56, given in units of half the band width[37]. So, due to the addition of Fe in Ni, the spin-up band remains almost unaltered, whereas the spin-down band gets considerably deformed and almost splits up into two different sub-bands.

There are fairly good experimental evidences in support of such band splittings. Ultraviolet photo-electron spectroscopy (UPS) and reflectivity data for Cu-Ni alloys[40] show a rapid increase of the number of states between the top of the Cu d-band and the Fermi level with the addition of Ni, signifying the growth of a separate band for Ni. Later measurements on the same system[41] not only confirms the above findings but also show a qualitative agreement with the CPA calculation of density of states for Cu-Ni alloys[42]. UPS studies even in amorphous Cu-Zr and Pd-Zr[43] alloys show the splitting of the d-bands, though the shapes of the d-bands are completely different from those of the constituent elements.

1.2.2 Split-band (S.B.) Model and the Sign Change of R_s in Alloys

It was found long back[44] that the extra-ordinary Hall constant R_s changes sign in Ni-Fe and Ni-Co alloys almost for

the same electron to atom ratio (~ 27.7). This led to a theory[44], under the rigid band approximation, according to which the sign change of R_s was associated with the Fermi level crossing some degeneracy in the Ni band. But, subsequently in Cu-Ni-Fe alloys it was found that no such correlation exists between R_s and the electron to atom ratio. To explain these results Berger[29] suggested an extreme model where all the three constituents have distinctly separate sub-bands in the ternary alloy with the bands for Cu lying at the bottom and those for Fe at the top. The sign change of R_s was identified with the Fermi level crossing the top of the Ni spin down band (or where the spin-down bands of Ni and Fe meet). This model was further extended for Ni-Fe-Me (Me = Cr, V, Ti, W, Mo, etc.) alloys and the band picture suggested for them is as shown in Figure 1.2. Of the three constituents, the bands for Ni are at the bottom since it is most attractive to electrons. On the other hand due to the large valence difference between Me and Ni, the bands for Me are split up from the host and are formed on top. Both the sub-bands (↑and ↓) for Fe have been shown here as separate from the corresponding sub-bands for Ni. But as discussed earlier, the spin-up band for Ni is affected little on alloying with Fe and hence the above picture, where the spin-up bands for Fe and Ni have been shown to be separate, seems to be somewhat extreme. However, since the spin-up bands are full and lie below E_F, their role is of no importance in transport properties and in the present context it is of no consequence whether they are split or remain as a

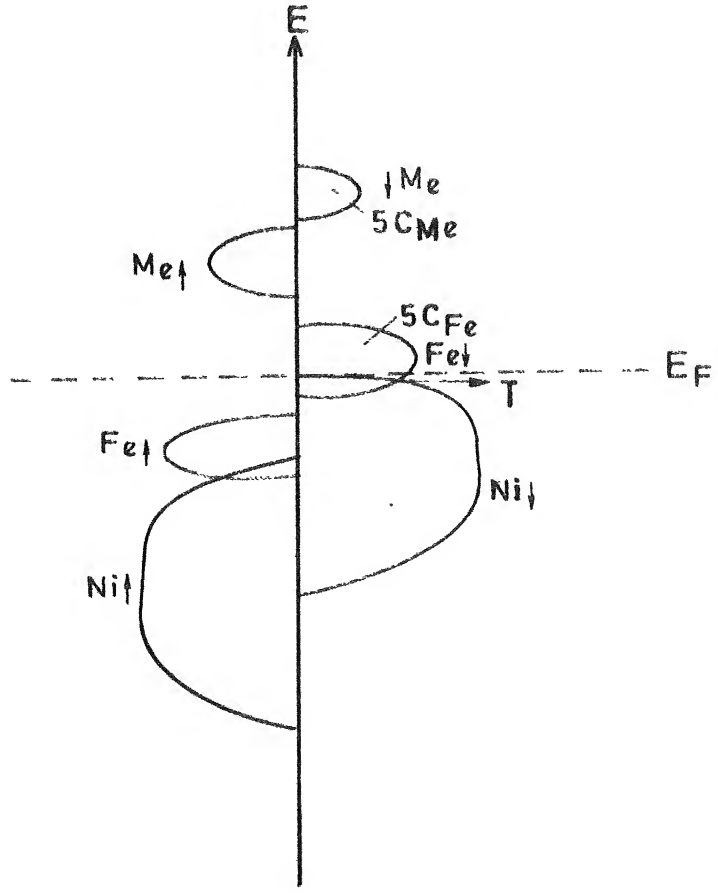

FIG. 1.2. SCHEMATIC DENSITY OF STATES FOR Ni-Fe-Me (Me = V, Cr etc) ALLOY SYSTEM ACCORDING TO SPLIT-BAND MODEL

single band. We call T as the point where the spin-down sub-bands for Fe and Ni meet. According to Berger's theory, the sign change of R_s is associated with the Fermi level (E_F) crossing T. Now the total number of states in a given 3d-sub-band is five times the concentration of the corresponding atoms. Hence the Fermi level cross-over will take place when the total number of holes in the ternary alloy system is equal to 5 C_{Fe} (C_{Fe} = concentration of Fe atoms), i.e. when

$$5C_{Fe} = 0.55 + 2C_{Fe} - (10 + Z)\, C_{Me}$$

$$\text{i.e.} \quad 3C_{Fe} + (10+Z)\, C_{Me} = 0.55 \qquad (1.8)$$

where 0.55 is the number of holes/atom in Ni, C stands for concentration and Z is the valence difference between Me and Ni (e.g. Z = -4 for Cr and -5 for V). It is to be noted that for counting the contribution of electrons/holes by Cr/V atoms, instead of simply taking the valence difference (Z) between Ni and Cr/V, a factor (10+Z) has been used. Because of the position of the Cr/V bands above E_F, they empty out all electrons into the Ni spin-down band, the number of which is given by (10+Z) (See Reference (34)). But instead of Ni-Fe-Cr/V alloys, if one considers Ni-Fe-Cu system, then the sub-bands for Cu will lie below those of Ni. In that case band filling will be guided by the valence difference (Z = +1 in this case) only and so the sign change in Ni-Fe-Cu system will be determined by Eqn.(1.8) with the term $(10+Z)C_{Me}$ replaced by simply C_{Cu}.

The reason for the sign change in R_s is the following[45]. We recall that some S.O. interaction is necessary for the origin of extra-ordinary Hall effect. Now the S.O. coupling parameter, in contrast to that of free electrons ($\lambda_{SO} = \hbar^2/2m^2c^2$), for 3d-band electrons, is given by[21]

$$\lambda_{SO}(E_F) = A_{SO} \chi\, d^2 \sum_n \frac{|\text{matrix element}|^2}{E_n - E_F} \qquad (1.9)$$

where A_{SO} is the atomic S.O. parameter for 3d electrons, χ ($\simeq 0.1$) is an overlap integral between nearest neighbour atomic 3d-states, 'd' is the nearest neighbour distance of atoms, and E_n is the energy of a band state n. As can be seen from Eqn.(1.9), the sign of λ_{SO} and hence R_s will be determined by the quantity in the denominator. When the Fermi level E_F is in the upper half of the band, the states at E_F mostly mix up with those of lower energy, thus rendering the denominator $(E_n - E_F)$ effectively negative. The case is reversed when E_F is at the lower half of a band. Hence R_s should change sign when E_F crosses the boundary between the two sub-bands.

Such a change of sign has been experimentally observed in various binary and ternary alloys. According to Eqn.(1.8) the sign change in binary Ni-Fe alloys should occur when $3C_{Fe} = 0.55$, i.e. around 18 at.% Fe, which is in close agreement with the experimental findings[46]. In Fe-V alloys, though a sign change is not expected as both the spin-up and spin-down bands are partially full, still some anomaly was observed[47] around the composition predicted by the S.B. model.

The other systems where S.B. model has been found successful are Ni-Fe-Cu[29], amorphous $Fe_{80-x}Co_xB_{20}$ ($0 \leq x \leq 80$ at.%), $Co_{40}Ni_{40}B_{20}$, $Fe_{80-x}Ni_xB_{20}$[48] ($60 \geq x \geq 0$), etc.

1.2.3 Other Quantities Associated with the Sign Change of R_s

The following properties are also expected to show some characteristic features as R_s changes sign:

i) The electronic specific heat co-efficient γ is expected to show a minimum as R_s passes through zero. This is simply because the change of sign of R_s is associated with the Fermi-level crossing a minimum in the density of states, according to the S.B. model. Such a minimum has actually been observed in Ni-Fe,[49] and also a quasi-minimum in Fe-V[47,50] alloys. But for other systems, where the S.B. model has been found to be applicable, due to the absence of enough systematic data for γ around $R_s \simeq 0$ compositions, this hypothesis could not be verified.

ii) According to the S.B. Model, R_s and the linear co-efficient of magnetostriction λ_s are both supposed to change sign simultaneously. As shown earlier by Berger[51] in his deformation potential theory of magnetostriction, λ_s depends on the z-component of the orbital angular momentum ($\langle L_z(E_F) \rangle$) at the Fermi level. Since $\langle L_z(E_F) \rangle$ should pass through zero when Fermi level lies at the boundary between Ni and Fe spin-down bands, λ_s should also show a similar behaviour. Experimental findings definitely speak in its support. In fact the S.B. model has been found to be more successful in explaining the sign change of λ_s. In crystalline Ni-Fe[52,53],

Ni-Fe-Cu[54], Ni-Fe-Cr[55], Ni-Fe-V[56], etc. and also in amorphous $(FeCoNi)_{80}B_{20}$[57], $Fe_{80-x}Co_xB_{20}$ and $Fe_{80-x}Ni_xB_{20}$[58] alloys the sign change of λ_s do occur at compositions close to those expected from the S.B. model. It should also be mentioned that theoretically calculated $< L_z(E_F) >$ for Ni-Fe alloys[49] also passes through zero almost at the same composition where $(\lambda_s)_{exp.} \simeq 0$.

iii) Another transport property which shows a characteristic maximum as R_s changes sign is the ferromagnetic anisotropy of resistivity (FAR), $\frac{\Delta\rho}{\rho_o} = \frac{\rho_{11} - \rho_\perp}{\rho_o}$, where ρ_{11} and $\rho_\perp$ are respectively the longitudinal and transverse magnetoresistances and ρ_o is the electrical resistivity in the de-magnetised state. The study of a large number of binary alloys like Fe-Ni, Co-Ni, Cu-Ni, etc. by Smit[59] and of Cr-Ni, V-Ni, etc. by Van Elst[60] have shown that a large maximum (in some cases $\simeq 20\%$) in $\Delta\rho/\rho_o$ occurs for alloys having an electron/atom ratio of 27.7 and sign change of R_s, λ_s etc. also occur for the same compositions[44]. A similar behaviour has also been observed in ternary Ni-Fe-Cu alloys[29]. But the reason for the presence of such a maximum is not so obvious. Earlier Berger[44] had shown that a maximum in $\Delta\rho/\rho_o$ can occur when the Fermi level crosses some degeneracy (or near degeneracy) in the 3d-band states. Under the influence of the S.O. interaction, the 3d atomic orbitals become anisotropic with respect to the direction of the spin (i.e. magnetization) and thus the scattering cross-section of a 4S electron (to the 3d states) become anisotropic. This anisotropy reaches a

maximum when the Fermi level lies near the degeneracy. Being a transport property, $\Delta\rho / \rho_o$ is guided mostly by the electrons at the Fermi level and hence the position of the Fermi level strongly influences its $(\Delta\rho/\rho_o)$ behaviour. But in the later papers[47,49], it has been shown that the sign change of λ_s and γ_{HS} and the associated maximum in $\Delta\rho/\rho_o$ can be explained even without assuming the presence of a degeneracy in the 3d-band states.

1.3 Motivation Behind the Present Investigation

As discussed in Section 1.2.2, the sign change of R_s has been studied in very few ternary systems. Though amorphous ternary systems like $Fe_{80-x}\ Co_x\ B_{20}$ and $Fe_{80-x}\ Ni_x\ B_{20}$[48] have been studied, effectively these are also binary type since the third constituent (B) merely acts as a glass forming element whose concentration is kept constant throughout. However, the study of the sign change of λ_s in ternary alloy systems have been done in a more comprehensive manner. Though a systematic study was made about the sign change of λ_s in ternary Ni-Fe-Cr/V[55,56] alloys long back, the corresponding data for R_s are completely lacking. So it was felt worth-while to establish the $R_s \simeq 0$ line experimentally for these two ternary systems. Other than providing new informations regarding R_s, it would also have given a serious test to the S.B. model. These two systems, particularly Ni-Fe-Cr appeared all the more interesting because of the already existing magnetization

data by Menshikov et al.[61]. Their data show appreciable non-linearity in $\bar{\mu}$ (average number of Bohr magneton/atom) vs. concentration curves. But in the S.B. model, inherent is the assumption that the number of holes/electrons contributed by one atom of Cr/V/Fe is a constant and is independent of concentration, implying a linear relationship between $\bar{\mu}$ and concentration. So the non-linearity in $\bar{\mu}$ vs. concentration curves raised some doubt about the applicability of the S.B. model to this system.

As it happens more often than not in a scientific investigation, starting with a limited aim, the field of interest broadens out with the subsequent progress of the work. Ours was no exception to this. In the beginning, magnetic measurements were carried out to find M_s, the saturation magnetization, to complement the Hall effect data. This will be clear if one recalls that the Hall effect measurements supply $R_s M_s$ only. Subsequent analysis of our magnetization data revealed that at low temperatures, other than spin-wave excitations also contributed to the decrease in magnetization and this extra contribution appeared to be coming from Stoner single-particle excitations corresponding to that of an itinerant weak ferromagnet. This naturally led to the study of paramagnetic susceptibility of a few alloys and derivation of the average number of Bohr magnetons per atom from the Curie-constant. A comparison of the above parameter, obtained from the susceptibility data and the one from the low temperature saturation magnetization measurements can give additional information

regarding the itinerant or localised character of the d-electrons[62] Also there are other criteria that a weak itinerant ferromagnet should satisfy and our investigation progressed accordingly. Details about this can be found in section 3.5. To summarise, data from magnetization measurements helped us to understand the band structure and hence the sign change of R_s in these alloys in a better manner.

Chapter II

Experimental Procedure

In this chapter we will discuss briefly the experimental methods used in general, with proper emphasis on the special techniques involved, if any. We begin with sample preparation and characterizations, followed by measurements of magnetization, electrical resistivity and the extra-ordinary Hall effect.

2.1 Sample Preparation

About a dozen samples of both the ternary alloy series (Ni-Fe-Cr and Ni-Fe-V) were prepared by induction melting of required amount of constituent elements of "specpure" grade (5N purity), obtained from Johnson-Mathey, Inc. (England). The pure metals were in the form of rods for Ni and Fe and in the form of beads for Cr and V. Desired amount of metals (typically around 10 gms) were cut, cleaned with organic reagents and weighed carefully. Except for sample numbers 9,24 and 29 in the Ni-Fe-Cr series and 18,19,20 and 30 in the Ni-Fe-V series, which were obtained from A.Sinha, the rest were prepared by us.

The meltings were performed in a water-cooled coil-type induction furnace, with a maximum power of 7 KW fed by a "Ajax Magnethermic converter" which converts line current of 50 c/s to one of 20 to 40 Kc/s (depending on power consumption). Samples were placed in a high quality alumina crucible which in turn was placed in a graphite susceptor and the whole thing in

a vacuum-sealed quartz tube of 100 mm. diameter. The sample zone was evacuated to 10^{-3} Torr, repeatedly flushed with high purity argon gas, evacuated and finally filled with argon at less than atmospheric pressure. In the subsequent heating process, temperature was monitored by an optical pyrometer. After completion of melting, power was switched off to allow the melt to cool-down in the furnace. Small pieces were cut from the top and bottom of the ingot thus obtained, and their Curie temperatures were determined separately to give an idea about the homogeneity of the samples. Usually for a good melt the two values differed by a few degrees only.

For further homogenization, the samples were put in a quartz capsule, evacuated, repeatedly flushed with argon gas and finally sealed with a partial pressure of argon gas (a few mm.) inside. These capsules were kept in a furnace at around 1150°C for 48 hrs. and then quenched in water. This water-quenching is necessary to retain the high-temperature random substitutional disorder in the polycrystalline samples and to prevent any possible clustering. These cylindrical samples were swaged, cold rolled and cut into various shapes (cylindrical for magnetic measurements and in the form of rectangular strips for transport property measurements) and sizes. Finally to remove the strains introduced in the various cold-working processes, they were annealed at 900°C for 24 hrs. under argon atmosphere (a few mm) and water-quenched.

To check the actual composition of the alloys, spectrometric analysis were performed with the help of a model 751

Atomic Absorption Spectrophotometer (Instrumental Lab.Inc.,USA). For this, the samples were dissolved in concentrated HNO_3 for analysis of Cr/V and in concentrated HCl for Fe, diluted to ppm. ranges ($<5\mu g/ml$. for Fe and Cr and $<75\mu g/ml$ for V), sprayed by an atomiser in the oxidizing flame of N_2O-C_2H_2 mixture and the absorptivities were measured. This could be compared against a calibration curve (which is linear in the specified ranges) drawn earlier using standard solutions of known concentrations. The accuracy of this method is within about 4% of the actual concentrations. In some cases, the composition of two different pieces of the same sample were determined and were found to be within the accuracy of our measurement. This further ensures the homogeneity of the samples, at least in the macroscopic scale. Also chemical analysis was done for some of the samples and the results were found to be consistent with the spectroscopically determined values.

The actual compositions were found not to differ much from the nominal compositions except that the Ni-Fe-Cr alloys were found, in general, to be poorer in Cr content and the corresponding vanadium alloys to be slightly richer in vanadium. The higher temperature and longer melting time required for the latter type of alloys probably led to the evaporation of some Ni and Fe, resulting in an alloy, richer in vanadium content. Taking all possible factors into consideration, we claim that the compositions presented for our alloys are correct to within 6 to 7 percent of the given compositions of the minor constituents.

A few samples were also selected at random for X-ray powder diffraction analysis, using an automatic scanning General Electric X-ray diffractometer (XRD-6) with Cu-K_α radiation as the source. All the samples investigated showed f.c.c. structure with little variation of lattice parameter with composition (3.52 to 3.56°A). Addition of Cr in Ni-Fe influences the lattice parameter in a manner similar to those of V.

2.2 Measurement of Magnetic Properties

All magnetic measurements were carried out with a Princeton Applied Research Inc. (USA), model 155 vibrating sample magnetometer (VSM). By using a model 153 variable temperature cryostat in conjunction with the VSM, measurements were made from 77 to 300K. The high temperature measurements in the range of 300K to 1050K were carried out, using a model 151 high-temperature oven-assembly in place of the cryostat. The magnetic field with a maximum of 18KOe was provided by a 15-inch Varian electromagnet with a 2.5 inch pole gap.

The VSM gives directly the magnetic moment of the sample in a 3-digit digital display. But using the null-method, which provides four ten-step potentiometers to annull the signal voltage (proportional to the magnetic moment of the sample), moments could be read up to four digits. By a suitable choice of sample mass, changes in moment of 1 part in 10^4 can be detected under ideal conditions (i.e. with minimum fluctuations). But in practice, the accuracy was limited to about 2 parts in 10^4. The apparatus was always calibrated against a standard Ni-sample

of known moment, before any measurement.

The high temperature oven-assembly was provided with a 20W bifilar-wound heater which could be energised by a constant current power supply. By suitably controlling the heater current, the sample zone temperature could be raised, lowered or held constant. The sample temperature could be read by a chromel-alumel thermo-couple, attached near the sample and could be held steady within 0.5K, if desired. For low temperature measurements, the cryostat was equipped with a gallium-arsenide diode as well as a copper-constantan thermo-couple. Since our measurements were limited to 77K and above and the Ga-As sensor was slightly away from the sample, to avoid any possible temperature lag between the actual sample temperature and the measured one, thermo-couple read temperatures were preferred. This temperature could be easily read within 0.5K at lower temperatures and with slightly better accuracy at higher temperatures. A novel feature of the cryostat is that the sample zone is connected to the liquid-zone only through a fine capillary, which could be closed or opened from outside. This allows one to easily remove or insert the sample during the experiment. It should, however, be mentioned that because of using the cryostat (which was basically designed for use with liquid helium) with liquid nitrogen, some problems cropped up. Because of the bubbling of liquid nitrogen, some fluctuations were observed in magnetic moment measurements near 77K. However, this disappeared immediately when all liquid nitrogen in the sample chamber evaporated out and measurements above about 85K were perfectly in order.

2.3 Measurement of Transport Properties: Design and Fabrication of the Cryostat

A cryostat was designed for the measurement of resistivity and Hall effect in the temperature range of 77 to 473K. It is a simple arrangement generally used for low temperature transport property measurements, except for the sample holder. A schematic diagram of the cryostat is shown in Figure 2.1. Essentially it consists of two concentric cylindrical chambers with proper arrangements to maintain vacuum/inert gas atmosphere at a partial pressure inside. In the innermost chamber, the sample holder is connected at the end of a non-magnetic thin walled stainless steel tube (length ~47 cm.) of 1.2 cm. O.D., through a threaded brass connector. The other end of this tube is soldered at the centre of the top flange of the cryostat and extended further by a copper tube. Through a side tube connected to this top part, the sample chamber can be evacuated or kept at a partial pressure of some inert gas (argon/helium). A little amount of exchange gas helps attaining thermal equilibrium quickly. As shown in the figure, all the electrical leads are fed through the inner stainless steel tube and ultimately come out through a low melting point vacuum seal made by CENCO, U.S.A.

The sample chamber is surrounded by another non-magnetic thin walled stainless steel (S.S.) tube of 2.2 cm. O.D. and is connected to the inner tube through a brass flange and O-ring joint. A 40 Ω Kanthal heater is wound uniformly and non-inductively on the outer stainless steel tube and is electrically insulated by a thin layer of teflon tape wound

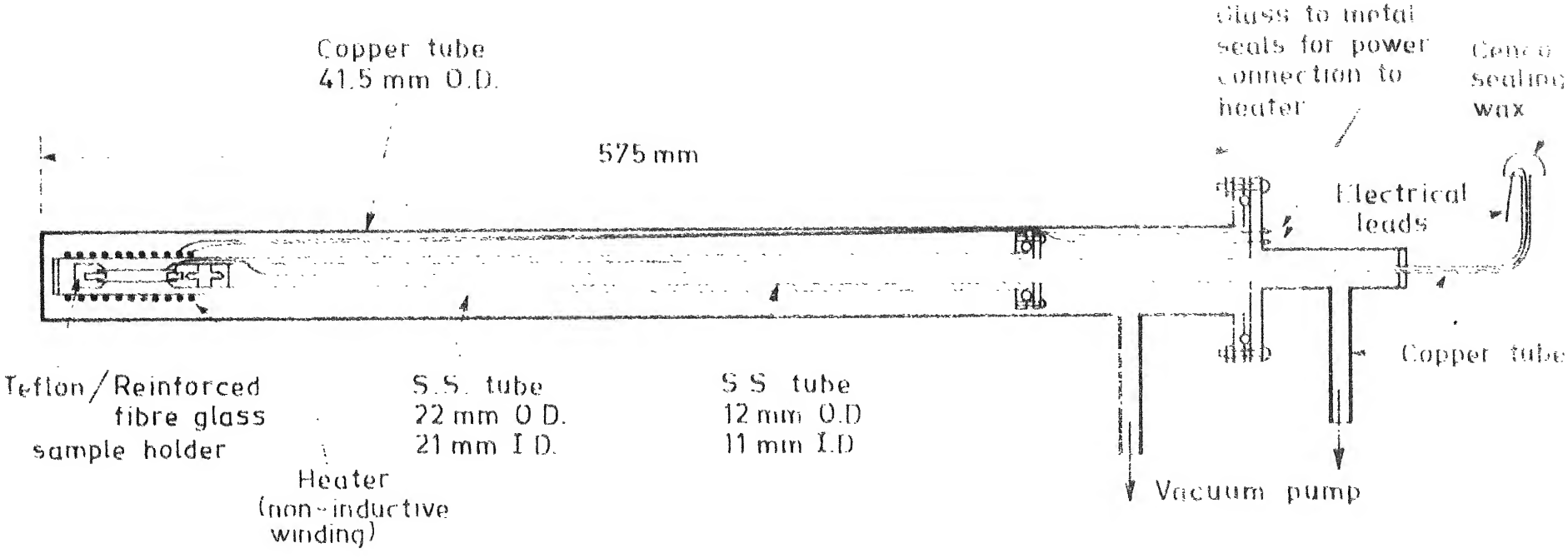
Copper tube
41.5 mm O.D.
575 mm
Glass to metal
seals for power
connection to
heater
Electrical
leads
Copper tube
Teflon / Reinforced
fibre glass
sample holder
S.S. tube
22 mm O.D.
21 mm I.D.
S S tube
12 mm O.D
11 mm I.D
Heater
(non-inductive
winding)
Vacuum pump

Fig. 2.1

around it. The O-ring joint lies sufficiently far away from the heater to prevent any damage to the O-ring, even when the heater is energised. Poor thermal conductivity and thinness of the stainless steel tube help meeting this end. This kind of two chamber arrangement allows one to keep sufficient amount of exchange gas in the sample chamber without disturbing the vacuum in the outer chamber. The heater is energised through 22 gauge copper wires, coming out from the top flange of the cryostat through glass-metal seals. A number of teflon spacers were used to isolate the outer stainless steel tube from the sample holder.

The outermost tube is of copper of 4.15 cm. O.D. and about 57.5 cm. in length. The inner assembly, consisting of the sample chamber and the heater is placed inside this copper tube and fixed with brass nuts and O-ring joint. The outer chamber can be evacuated to less than 10^{-3} Torr through a side tube near the top, to thermally isolate the heater. The cryostat is immersed in a liquid nitrogen dewar (not shown in the figure) of proper size and can slide nicely into the 6.25 cm. pole gap of a 15-inch Varian electro-magnet.

2.3.1 Sample Holder

Since the Hall voltage in a metal, even in a moderately high magnetic field is small ($\sim \mu V$ range), special attention was given in designing the sample holder to minimise the influence of other associated voltages. In a normal four-probe d.c. method, the following problems arise when soldered contacts are

used:

i) A large resistive voltage comes into play due to the mis-alignment of the voltage probes. In the presence of a magnetic field, further contribution comes from magneto-resistance. Though these effects can be eliminated by reversing both the magnetic field and current directions, the large resistive voltage seriously affects the resolution of the measurement, unless special arrangement is made to suppress the resistive part of the voltage.

ii) The use of solder material disturbs the current distribution in the sample and secondly changes the mean width of the sample because of the finite width of the solder itself. Since calculation of Hall resistivity involves the thickness of the sample, the calculations could be erroneous unless the thickness of the solder is known. This can be minimised only by using samples of special geometry (for details, see reference (7), p.188).

To avoid the above mentioned problems, we used pressure contacts instead of usual soldered ones. A sectional view of the sample holder is shown in Figure 2.2. For low temperature measurements, the sample holder was made of plastic reinforced fibre glass, a special material developed in I.I.T., Kanpur. The choice of this material is due to its temperature coefficient of expansion being comparable to those of metals, which helps retaining the pressure contacts even at low temperatures. However, above about 373K this material cannot be used. So for

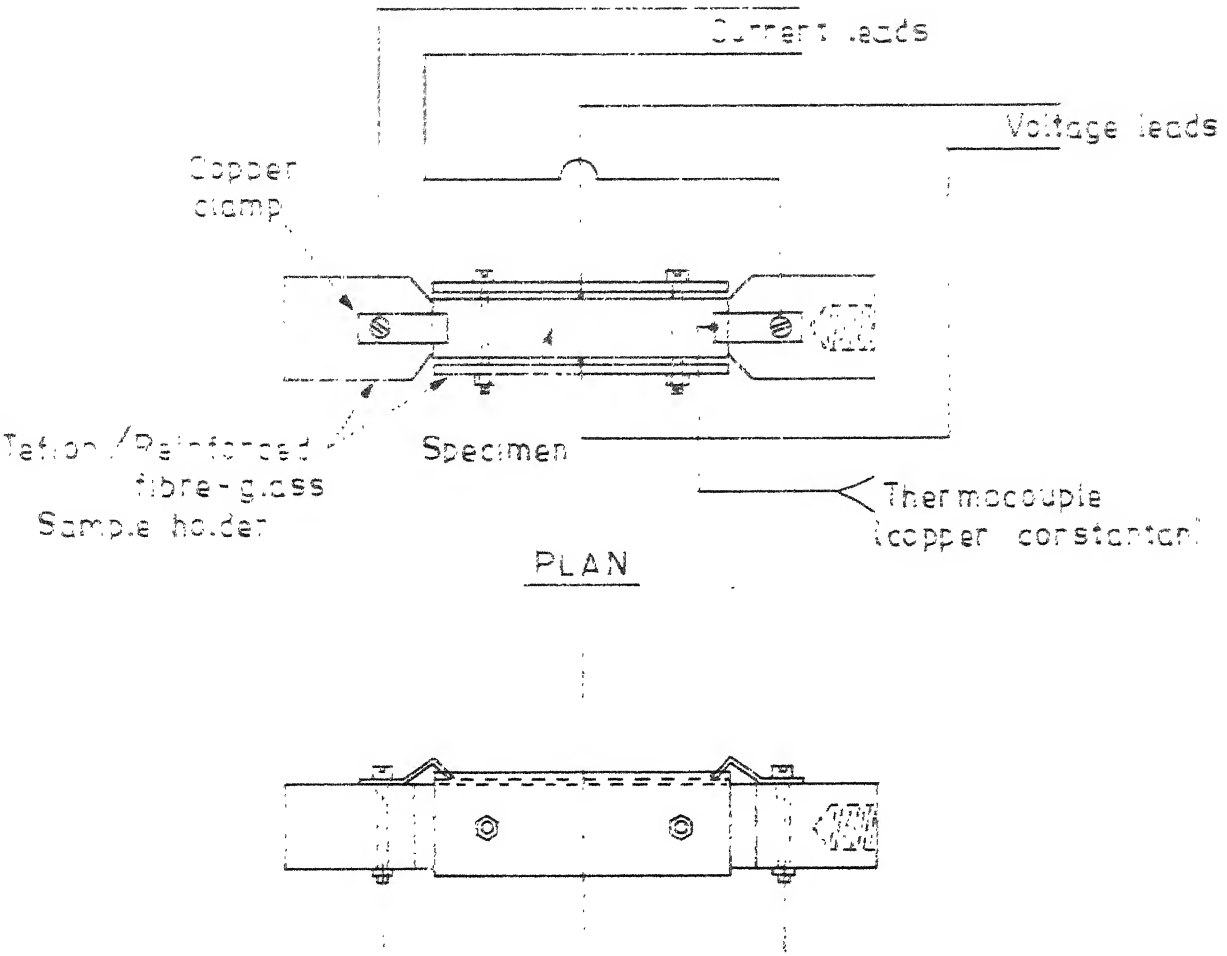
Current leads
Voltage leads
Copper clamp
Specimen
Thermocouple (copper constantan)
PLAN
ELEVATION

Fig. 2.2

measurements above room temperature (upto 473K) a sample holder made of teflon was fabricated. The sample was held firmly in place by two copper (pure) elbows, connected to the sample holder by 1/16" brass nuts. These nuts also provided the binding posts for the current leads (22 gauge copper wires). Thus, other than fixing the sample, the elbows provided an extended current contact to the sample and hence ensured uniform current distribution along its length. The samples were typically of 28x5x0.5 mm. dimension. Such a dimension is necessary as it is well-known[63] that for length/width ratio less than 5, a part of the Hall voltage gets shorted out through the current electrodes. The voltage leads were very fine (to provide minimum area of contact and thus causing minimum disturbance to the current distribution) copper wires (42 gauge), held firmly to the sample by rectangular plastic re-inforced fibre glass blocks, tightened by two 1/16" nuts, as shown in the Figure. Before tightening the screws the wires were manually positioned, with respect to the sample, such that the resistive voltage was minimal (typically $\sim 1\text{-}2\mu$ V). Such an arrangement considerably simplifies the voltage measuring circuitry. A copper-constantan thermo-couple held between one of the copper elbows and the sample provided the sample temperature. Actual contact with the sample eliminated the possibility of any lag between the sample temperature and the measured one.

In a d.c. measurement, Hall voltage is always associated with those arising from Nernst-Ettinghausen and Righi-Leduc

effects[7]. To eliminate these, sufficient amount of exchange gas was kept in the sample chamber and all the connecting leads coming to the sample were wrapped around a binding post. This prevented any longitudinal heat-flow and hence any corresponding transverse temperature gradient or transverse voltage arising respectively from Righi-Leduc or Nernst effects. But no precaution was taken to eliminate the transverse voltage arising from Ettinghausen effect, since the contribution of this is relatively small.

The same sample holder was also used for resistivity measurements. The separation of the voltage leads was measured by a cathetometer-telescope arrangement.

2.3.2 Circuit Diagram and Procedure

In Figure 2.3 is shown the schematic circuit diagram used for Hall voltage measurements. The current was supplied by a Hewlett Packard constant current power supply (model 6114A), through a commutator C_1. Typically 0.5 to 1 ampere was passed through the sample which could be measured by the voltage drop across a standard resistance (1 ohm), connected in series with the sample. Change in current, if any, was less than 1 part in 10^4 during the measurements. Corresponding Hall voltages were measured directly by a model 148 nanovoltmeter (Keithley Instruments Inc., U.S.A.). Since in our pressure contact arrangement, the resistive and thermal voltages were small (a few μV only),no additional accessories

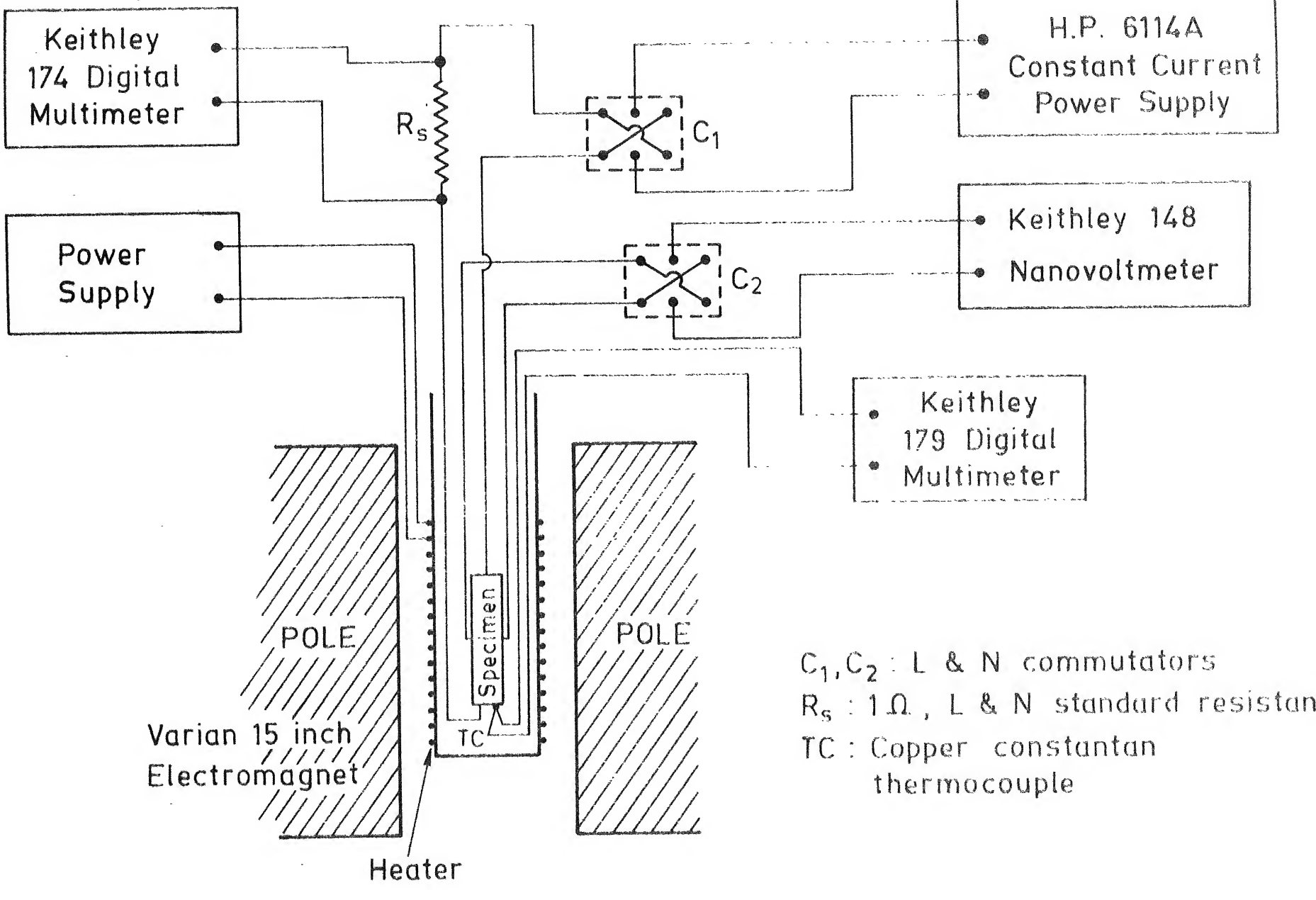
Keithley
174 Digital
Multimeter
R_s
C_1
H.P. 6114A
Constant Current
Power Supply
Power
Supply
Keithley 148
Nanovoltmeter
C_2
Keithley
179 Digital
Multimeter
POLE
Specimen
POLE
Varian 15 inch
Electromagnet
TC
Heater
C_1, C_2 : L & N commutators
R_s : 1 Ω , L & N standard resistan
TC : Copper constantan
thermocouple

(like K-3 potentiometer, etc.) were required to suppress those voltages to resolve the small Hall voltage (typically 10 to 20μV in the highest field for our samples). Even then, to achieve better resolution, a 10-turn helipot was attached to the zero suppressor of the nanovoltmeter. By suppressing the voltages with this zero suppressor, incremental changes in voltage due to incremental magnetic fields were recorded. The sample temperature could be varied or held constant by controlling the heater current and the corresponding thermo-couple output, fed to a model 179 Keithley digital multimeter, gave the sample temperature.

Since the Hall voltage is very small, special precautions were taken to minimise fluctuations. All the electrical leads coming out of the cryostat were properly shielded to protect against external pick-ups and all the accessories were properly grounded. Any movement of the sample in the presence of high magnetic fields could also contribute to large fluctuations. But in our case since the sample was firmly set against the sample holder, this problem did not arise. With all these precautions, a noise level of less than $\pm$10 nano-volts could be achieved even under the worst possible circumstances. To ensure that the sample stands exactly perpendicular to the magnetic field, after suppressing the resistive voltage the whole cryostat was rotated about the vertical axis in the presence of a moderately high magnetic field ($\sim$ a few kG), until a maximum in the incremental voltage was recorded.

To assess the performance of the cryostat, the following checks were performed:

i) Repeated measurements of the same sample at room temperature and at 77K at different times gave reproducible results within our experimental accuracy.

ii) Measurements were carried out on a pure Ni sample at room temperature and the values found were of the right order of magnitude (exact quantitative comparisons were not possible as the values strongly depend on the sample purity).

iii) To ensure that the heater windings were truly non-inductive, search was made to detect any change in the measured voltage as the heater current was switched on.

iv) Calibration of all the measuring instruments were checked with the help of a K-3 potentiometer.

Finally to extract the Hall voltage from the other associated voltages (e.g. resistive, thermal, etc.), voltages were measured at each magnetic field by reversing both the current and field directions and taking their average with proper regard to their signs. The method of extracting the extra-ordinary part from the normal one has already been discussed in Section 1.

The same circuitry was used for resistivity measurements except that the nano-voltmeter was replaced by a model 174 digital voltmeter (Keithley Instruments Inc., U.S.A.), capable of measuring down to 0.1 μv. This provided sufficient accuracy for our present purpose.

Chapter III

Magnetic Properties

In this chapter the magnetic properties of the two alloy systems (Ni-Fe-Cr and Ni-Fe-V) are presented and an attempt has been made to interpret them qualitatively and wherever possible, quantitatively. The experimentally measured quantities are (a) Curie temperature T_c, (b) Magnetization at 77K and above, and (c) paramagnetic susceptibility. The low temperature magnetization data have been analysed in the light of the spin-wave theory and various parameters, like spin-wave stiffness constant D, the mean magnetic moment per atom $\bar{\mu}$ has been extracted from it. $\bar{\mu}$ has also been calculated from the Curie-Weiss constant derived from paramagnetic susceptibility and the large ratio of $(\bar{\mu})_{\text{para}}/(\bar{\mu})_{\text{low temperature}}$, found by us, has been explained in the framework of itinerant 'weak' ferromagnetism.

3.1 Curie Temperature T_c

The magnetization vs. temperature curve, measured in the small residual field ($\sim$ 30 Oe) of the magnet, enabled us to determine T_c. From the slope $-\frac{dM}{dT}$ vs. T curves, as shown in Figure 3.1, one can easily find T_c. A small but systematic difference in the value of T_c determined from heating and cooling data was observed due to a temperature lag between the sample and the temperature sensor. So the mean of the two values was taken.

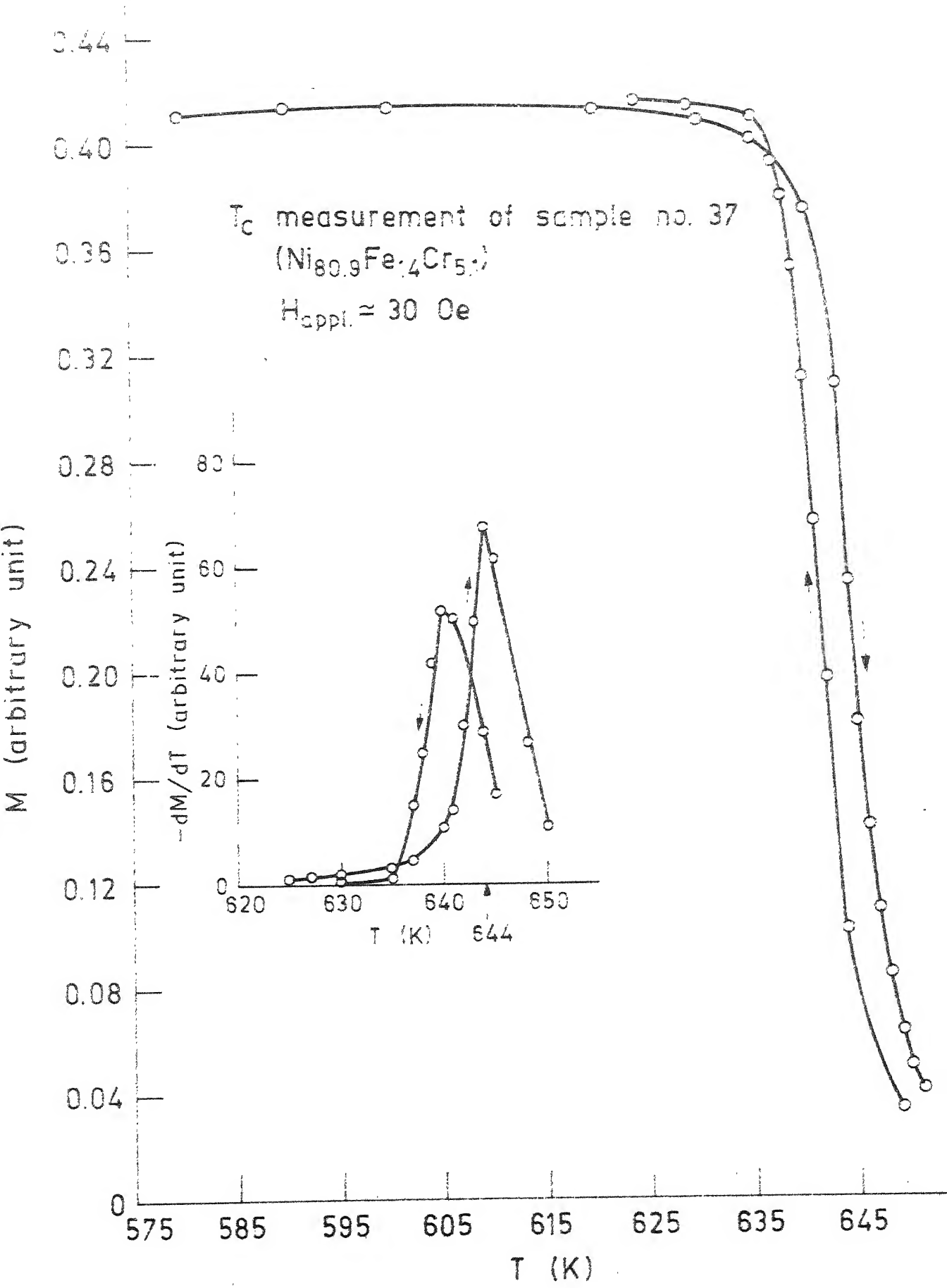
T_c measurement of sample no. 37
(Ni80.9Fe14Cr5.1)
H_appl. ≃ 30 Oe
M (arbitrary unit)
0.44
0.40
0.36
0.32
0.28
0.24
0.20
0.16
0.12
0.08
0.04
0
575
585
595
605
615
625
635
645
T (K)
-dM/dT (arbitrary unit)
80
60
40
20
0
620
630
640
650
T (K)
644

Fig. 31

In Table 3.1A, the T_c values for various compositions of Ni-Fe-Cr alloys are presented; Table 3.1B presents those of Ni-Fe-V. Several pieces, taken from different parts of the melt, were used for measurement and their mean value is given in the tables. The error bars include this factor along with the experimental errors. Thus in a crude way, they provide a good idea about the homogeneity of the samples.

It can be easily seen from our data that even though in a non-linear fashion, addition of Fe enhances the T_c by approximately 10K/at.% of Fe and suppresses it by about 25-30K/at.% of Cr/V. This is consistent with the earlier data of Menshikov et.al.[64] on Ni-Fe-Cr alloys. Though the critical composition for the disappearance of ferromagnetism is only 13 at.% of Cr for binary Ni-Cr[65,66] alloys and about 11.5 at.% of V for Ni-V[67] alloys, from Tables 3.1A and 3.1B it is clear that in the corresponding ternary systems ferromagnetism is retained even up to much higher concentrations of Cr/V. This is because in binary Ni-Cr and Ni-V alloys ferromagnetism disappear when the Fermi level (E_F) crosses the top of the Ni spin-down band. But in the presence of Fe, a new 3d Fe-spin-down band appears above the corresponding Ni sub-band, as has already been discussed in Chapter I (Section 1.2.1) in the context of S.B. model. So in the ternary systems disappearance of ferromagnetism should coincide with E_F crossing the top of the Fe-spin-down band. This additional number of 3d magnetic states due to Fe are responsible for retaining ferromagnetism even at concentrations

Table 3.1A : Curie Temperature for various Ni-Fe-Cr Alloys

Sample No.	Composition of Ni-Fe-Cr alloys (at.%)	T_c (K)
42	78-6-16	185±5
50	72-8-20	93±3
9	85.5-11-3.5	620±3
24	81-11-8	470±4
40	73.5-11.5-15	260±5
29	75.1-12.8-12.1	365±3
48	70-12-18	179±2
34	72.5-13.7-13.8	315±7
26	80-16-4	693±3
28	75-17-8	543±3
33	68.1-17.4-14.5	320±6
35	76.8-21.2-2	778±4
27	75.5-20.3-4.2	717±3
51	67-21-12	470±2
32	69.6-22.8-7.6	635±5

Table 3.1B : Curie Temperature for various Ni-Fe-V Alloys

Sample No.	Composition of Ni-Fe-V alloys (at.%)	T_c (K)
49	78-4-18	90±4
46	82.5-7.5-10	362±3
45	76.8-7.2-16	167±5
19	83-10-7	486±2
20	80.5-10.5-9	417±3
18	85-11-4	609±5
39	77.4-11.9-10.7	393±1
37	80.9-14-5.1	640±4
38	76.5-14-9.5	462±1
36	81-17-2	746±3
30	79.4-17-3.6	691±2
31	74-22-4	741±3

(Cr-V) much higher than in the corresponding binary systems.

3.2 Magnetization

Before presenting the results of magnetization measurements, it seems relevant to spell out the motivations behind any such measurements. As discussed earlier in Section 1.3, a knowledge of M_s is necessary to extract R_s from the Hall effect measurement data. On the other hand, the change in composition of the alloys results in i) a shift of the Fermi level with respect to the Ni-spin-down band due to which R_s changes in magnitude (and sign), and ii) a change in the total number of electrons/holes in the band, thereby changing the spontaneous magnetization at 0K. Thus evaluation of magnetization at 0K, is expected to shed some light on the problem of sign change of R_s. With such ideas in mind M_s was measured at 77K and above for a number of alloys of both the ternary systems.

It is well known that change in M_s at low temperatures occurs through two mechanisms: a) collective excitations or generation of spin-waves, b) single particle or Stoner excitations. In our case it was found that the magnetization data above 77K could be very well explained on the basis of the spin-wave theory, at least for the alloys with higher T_c (> 500K). Since in our present experimental facility, measurements could not be extended below 77K, only a few alloys with sufficiently high T_c were chosen for rigorous spin-wave analysis. In the next few sections the data for such analysis are

presented and discussed.

3.2.1 Spin-wave Theory

It is well known[68] that the specific magnetization $\sigma(H,T)$(emu/g) as a function of temperature T(K) and field H(Oe) can be given by

$$\sigma(H,T) = \sigma(0,0) - \frac{2.612 g\mu_B}{\rho}\left(\frac{k_B T}{4\pi D}\right)^{3/2} Z\left(\frac{3}{2}, \frac{T_g}{T}\right) \qquad (3.1)$$

where g is the Lande splitting factor, μ_B is the Bohr magneton, ρ is the density, k_B is the Boltzmann constant, D is the spin-wave stiffness constant, $T_g = \frac{g\mu_B H_{int.}}{k_B}$ is the spin-wave gap temperature and $Z(\frac{3}{2}, \frac{T_g}{T})$ is a Bose-Einstein integral which can be expanded in powers of T_g/T. The correction term arises, because in the presence of an effective internal field $H_{int.}$ an energy gap of value $g\mu_B H_{int.}$ appears in the spin-wave dispersion relation given by

$$E(q) = g\mu_B H_{int.} + Dq^2 + Eq^4 + ... \qquad (3.2)$$

$H_{int.}$ is given by

$$H_{int.} = H_{appl.} - H_D + H_A + H_W \qquad (3.3)$$

where $H_{appl.}$ is the external magnetic field, H_D is the demagnetizing field, H_A is the anisotropy field, and H_W the Lorentizian field or the spin-wave demagnetizing field. Basically the q^2 term in the spin-wave dispersion relation gives rise to the

$T^{3/2}$ term in Eqn.(3.1) and the higher order q^4 or the anharmonic term to a $T^{5/2}$ contribution. Thus Eqn.(3.1) can be written as

$$\frac{\Delta\sigma(H,T)}{\sigma(0,0)} = \frac{\sigma(H,T)-\sigma(0,0)}{\sigma(0,0)} = \alpha' Z(\frac{3}{2}, \frac{T_g}{T})T^{3/2} + \beta Z(\frac{5}{2}, \frac{T_g}{T})T^{5/2} + .. \tag{3.4}$$

where $Z(\frac{5}{2}, \frac{T_g}{T})$ is another correction term due to T_g,

$$\alpha' = (\frac{k_B}{4\pi D})^{3/2} \quad \frac{2.612\ g\mu_B}{\sigma(0,0)\rho} \tag{3.5}$$

and

$$\beta = \frac{3k_B}{16} < r^2 > \quad \frac{\alpha'}{1.948D} \tag{3.6}$$

with $< r^2 >$ as the mean square range of the exchange interaction.

Since D itself is temperature dependent, some additional higher order terms may also come in, depending on the relationship between D and the temperature T. According to the localized models[69,70] of Dyson and others, at low temperatures magnon-magnon interactions can give rise to a leading $T^{5/2}$ term in D in the long wave-length limit. On the other hand, itinerant models[71,72] of Izuyama et al. and others predict a $T^{5/2}$ term due to magnon-magnon interaction and a T^2 term due to the interaction between spin-waves and thermally excited itinerant electrons. Thus at the low temperature limit,

$$D = D_o\ (1 - D_1T^2 - D_2T^{5/2}) \tag{3.7}$$

Inelastic long wave-length neutron scattering experiments on Fe[73] have shown the presence of both the terms, but with D_2

negative. Whereas experiments on Ni[74,75] indicate the presence of a single term, the T^2 one. Magnetization measurements[76] of Ni also support this result. Thus substitution of Eqn.(3.7) in (3.4) gives

$$\frac{\Delta\sigma(H,T)}{\sigma(0,0)} = \alpha T^{3/2}(1-D_1T^2-D_2T^{5/2})^{-3/2} Z(\tfrac{3}{2},\tfrac{T_g}{T}) + \beta Z(\tfrac{5}{2},\tfrac{T_g}{T})T^{5/2} \qquad (3.8)$$

where

$$\alpha = \alpha' \quad (D = D_o)$$

A binomial expansion of the terms in the bracket generates a $T^{7/2}$ term and a T^4 term. To summarise, in addition to the $T^{3/2}$ term one can have (i) a $T^{5/2}$ term in the presence of an anharmonic term (q^4) in the spin-wave dispersion relation and (ii) a $T^{7/2}$ term and/or a T^4 term, depending on the temperature dependence of D.

3.2.2 Low Temperature Magnetization data for Ni-Fe-Cr Alloys

Magnetization as a function of temperature was measured for a number of alloys at a fixed magnetic field (7-8 kOe) and least squares fits of the data to Eqn.(3.8) were tried using various combinations of the unknown parameters, taking three at a time. These were i) $\sigma(0,0)$, α and β, ii) $\sigma(0,0)$, α and co-efficient of $T^{7/2}$ term, iii) $\sigma(0,0)$, α and co-efficient of T^4 term (γ), iv) $\sigma(0,0)$ and α only. The factors $Z(\frac{3}{2}, \frac{T_g}{T})$ and $Z(\frac{5}{2}, \frac{T_g}{T})$ were calculated at each temperature

using the expressions given by Argyle et.al.[77]. Since magneto-crystalline anisotropy is not known for these alloys (which is supposed to be small in our case since $H_{appl.}$ is small), and there was some uncertainty in calculating the demagnetizing field, exact value of T_g could not be calculated. To circumvent this difficulty, T_g was itself taken as a variable parameter and the T_g value that gave the best fit was taken. In Table 3.2 are given the results of such analysis for one of our samples. The standard deviation (SD) of the least squares fits are also included and the values of the various parameters are given along with their statistical uncertainties. It is amply clear from Table 3.2 that inclusion of higher order terms, other than $T^{3/2}$ is essential. The minimum SD could be achieved when a $T^{7/2}$ (or T^4) term is included along with the $T^{3/2}$ term. A better fit with a $T^{7/2}$ (or T^4) term rather than a $T^{5/2}$ term clearly indicates that the deviation from the $T^{3/2}$-law comes mainly through the temperature dependence of the spin-wave stiffness constant rather than the anharmonicity term in the spin-wave dispersion relation (Eqn.(3.2)). An attempt to include both the $T^{7/2}$ (or T^4) term and a possible $T^{5/2}$ term along with the usual co-efficients $\sigma(0,0)$ and α proved to be futile as it led to an unphysical situation where the co-efficients of some of the higher order terms turned out to be positive. This could be partly because, the inclusion of so many parameters demanded more from our experimental data than what its limited accuracy could permit.

Table 3.2 : Results of various least squares fits of magnetization vs. temperature data, taken at a fixed field of 8 KOe for sample number 26

Sample composition (at.%)	Temp. range in which data have been analysed	$\sigma(0,0)$ (emu/g)	α ($10^{-5}K^{-3/2}$)	β ($10^{-8}K^{-5/2}$)	Co-eff. of $T^{7/2}$ term ($10^{-10}K^{-7/2}$)	Co-eff. (γ) of T^4 term ($10^{-12}K^{-4}$)	Standard deviation of least squares fits (10^{-4}) of $\Delta\sigma/\sigma$
		79.03±0.04	-(1.63±0.03)	-	-	-	10.9
$Ni_{80}Fe_{16}Cr_4$	$0.12T_c$ to $0.33T_c$	78.40±0.02	-(0.33±0.04)	-(4.60±0.14)	-	-	1.7
		78.57±0.01	-(0.97±0.014)	-	-(1.08±0.02)	-	1.2
		78.62±0.01	-(1.09±0.01)	-	-	-(5.92±0.12)	1.15

87521

It seems that even if it exists, the $T^{5/2}$ term plays only a minor role compared to the $T^{7/2}$ (or T^4) term. This is consistent with the inelastic neutron scattering studies in Ni-Fe-Cr alloys by Menshikov et al.[64], where they have not reported the presence of any term higher than quadratic in the spin-wave dispersion relation. But the presence of such a term in binary Ni-Fe alloys detected from magnetization[78,79] as well as from neutron scattering[80] measurements, suggests that probably the addition of Cr in Ni-Fe alloys suppresses the anharmonic term.

Similar analysis was carried out for all the alloys studied, and it was found that a $T^{3/2}$ term along with a $T^{7/2}$ (or T^4) term gave the best possible fit to our experimental data. A distinction between a $T^{7/2}$ and a T^4 term could not be made since both of them gave equally good fit. However, recent magnetization studies[78] and also neutron scattering measurements[81,82] reveal that $D \propto T^{5/2}$ in the Ni-rich region of binary Ni-Fe alloys. Guided by these data it seemed logical to accept T^4 term as the next higher order term instead of a $T^{7/2}$ term in these Ni-rich ternary alloys.

In Figures 3.2 and 3.3 are shown the change in reduced magnetization ($\Delta\sigma(H,T)/\sigma(0,0)$) against $T^{3/2}$ (corrected for the gap temperature), specially to show the effect of increasing Cr concentration. The necessity of a higher order term (other than $T^{3/2}$) is quite obvious from the deviation of experimental data from the expected straight line behaviour.

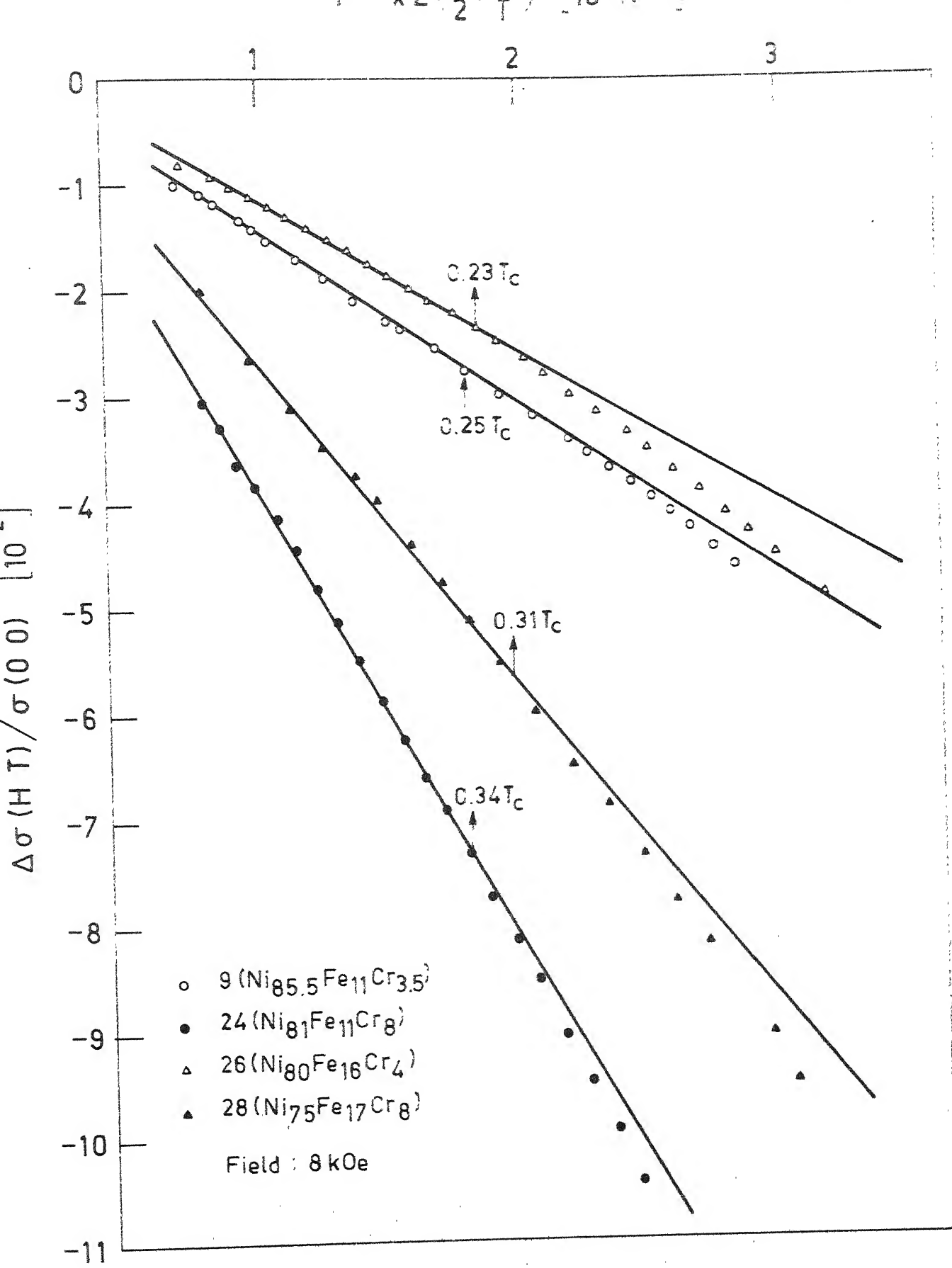
1
2
3
0
-1
-2
-3
-4
-5
-6
-7
-8
-9
-10
-11
$\Delta\sigma(H,T)/\sigma(0,0)$ [10^{-2}]
0.23 T_c
0.25 T_c
0.31 T_c
0.34 T_c
9 ($Ni_{85.5}Fe_{11}Cr_{3.5}$)
24 ($Ni_{81}Fe_{11}Cr_8$)
26 ($Ni_{80}Fe_{16}Cr_4$)
28 ($Ni_{75}Fe_{17}Cr_8$)
Field : 8 kOe

Fig. 3.2

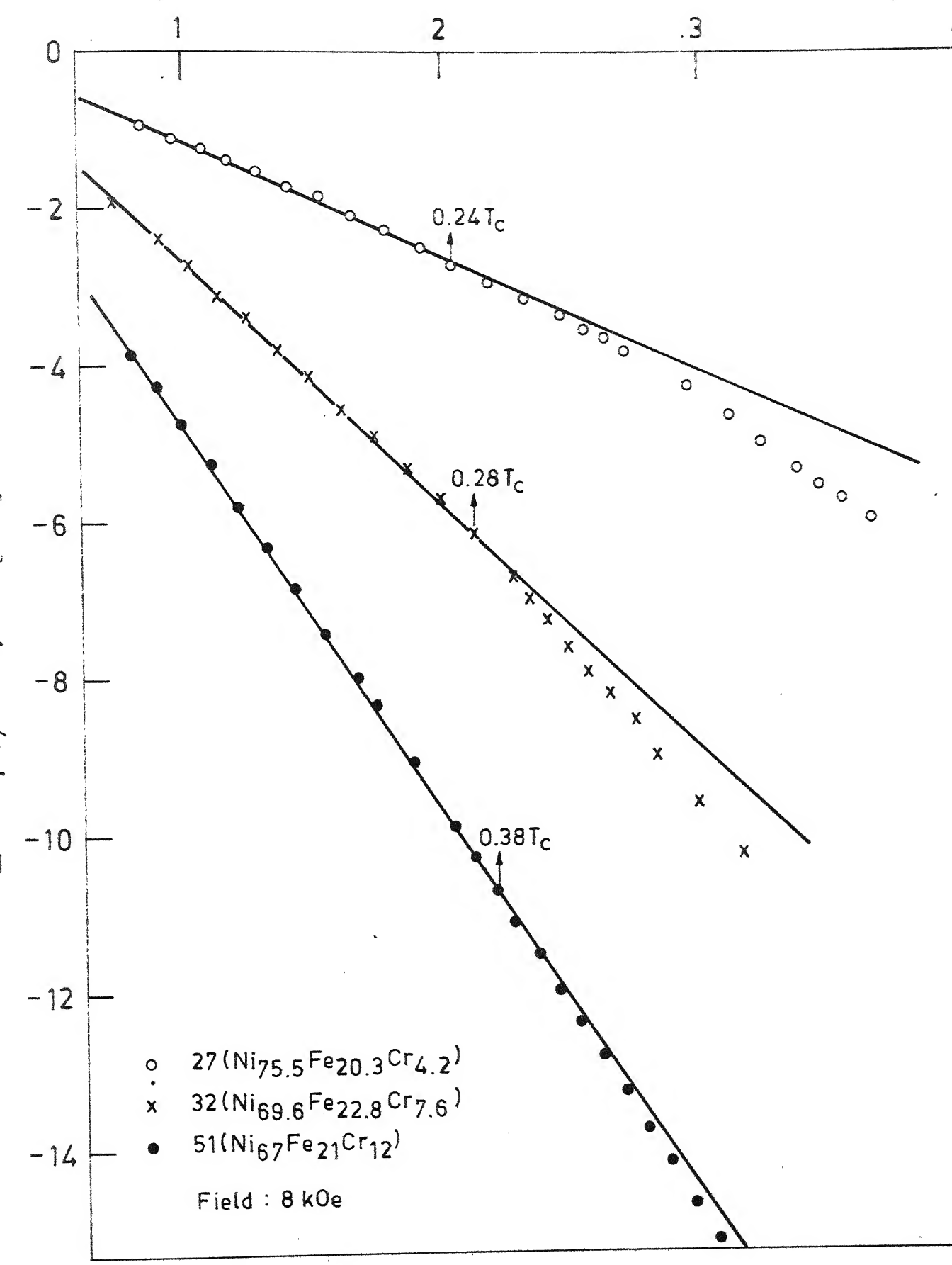
1
2
3
0
-2
-4
-6
-8
-10
-12
-14
0.24 T_c
0.28 T_c
0.38 T_c
27 ($Ni_{75.5}Fe_{20.3}Cr_{4.2}$)
32 ($Ni_{69.6}Fe_{22.8}Cr_{7.6}$)
51 ($Ni_{67}Fe_{21}Cr_{12}$)
Field : 8 kOe

Fig. 3.3

Another interesting point is the gradual increase of the temperature range (in the reduced scale of T/T_c), where the $T^{3/2}$ law holds good, with increasing Cr concentration. Also, noteworthy is the diminishing importance of higher order terms, as can be seen from the smaller deviation of experimental data points from the straight lines with gradual addition of Cr.

In Figure 3.4 are shown the change in the reduced magnetization as a function of reduced temperature (T/T_c). The solid curves are the best fits with $\sigma(0,0)$, α and γ (co-efficient of T^4 term) as the adjustable parameters. Since spin-wave theory is basically applicable to low temperature regions only, the data points above 0.5 T_c were always omitted for the analysis. All the magnetization measurements were carried out in a constant applied field of 8 KOe as pointed out in the figures. In Table 3.3 are shown the values of $\sigma(0,0)$, α and γ for the best fits to our experimental data. The spin-wave stiffness constants, D_o and D_2, derived from the co-efficients α and γ are also presented along with the neutron scattering based values of D_o by Menshikov et al.[64]. Unfortunately, the corresponding neutron scattering data for D_2 are absent in the literature. In the calculations for our D_o, the g values were taken to be 2 and the density ρ were calculated using the lattice parameter data of Menshikov et al.[64]. Their measurements show that in Ni-Fe-Cr system, the lattice parameter increases by about 1% from the corresponding value of pure Ni when the impurity

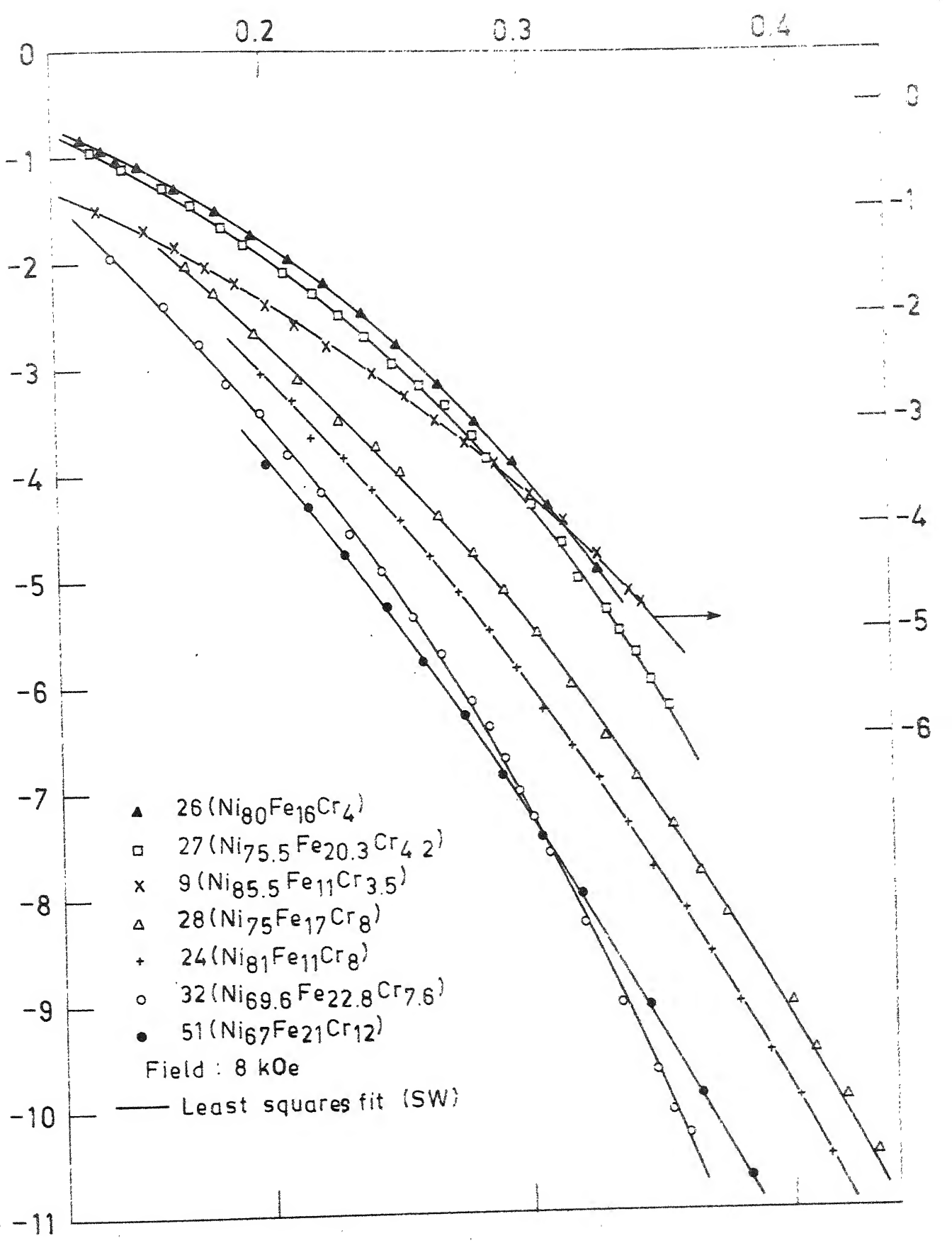
0.2
0.3
0.4
0
-1
-2
-3
-4
-5
-6
-7
-8
-9
-10
-11
▲ 26 ($Ni_{80}Fe_{16}Cr_4$)
□ 27 ($Ni_{75.5}Fe_{20.3}Cr_{4.2}$)
× 9 ($Ni_{85.5}Fe_{11}Cr_{3.5}$)
△ 28 ($Ni_{75}Fe_{17}Cr_8$)
+ 24 ($Ni_{81}Fe_{11}Cr_8$)
○ 32 ($Ni_{69.6}Fe_{22.8}Cr_{7.6}$)
● 51 ($Ni_{67}Fe_{21}Cr_{12}$)
Field : 8 kOe
—— Least squares fit (SW)

Fig. 3.4

concentration (Fe + Cr) reaches around 30 at.% and is rather insensitive to the impurity type (Fe or Cr). Addition of Cr only shows a small decrease in lattice parameter. We claim that the uncertainty in the values of ρ, thus calculated, is within 1%. Actual measurement of density for a few alloys support this claim. Neutron scattering values of D_o for the alloys with 8 at.% of Cr were directly obtained from the data of Menshikov et al.[64] and those of the rest were estimated from the data of nearest available compositions. The following points emerge from the results shown in Table 3.3:

i) Though spin wave theory can very well account for the change in magnetization with temperature over a fairly wide range of temperature (see Figure 3.4), the D_o values determined from magnetization measurements are always less than the corresponding neutron scattering values; at least for the alloys studied.

ii) Though in disagreement with neutron scattering results, our magnetic measurement based values for D_o essentially show the same kind of compositional dependence. For the alloys with fixed Cr concentration, after showing an initial increase, D_o falls off with increasing concentration of Fe. But with the addition of Cr, D_o continuously falls off at a much faster rate.

This finds a suitable explanation in the observation of Menshikov et al.[64] that Cr-Cr interaction is antiferromagnetic and strongest ($\sim$ 227 meV) among all the pair interactions in Ni-Fe-Cr alloys. Fe-Fe interaction is also

Table 3.3 : Results of the least squares-fit for the temperature dependence of magnetization for some Ni-Fe-Cr alloys. The statistical uncertainty in the various parameters are also included

mple mber	Composition of Ni-Fe-Cr alloys (at.%)	Density ρ^* (g/cm^3)	$\sigma(0,0)$ (emu/g)	$-\alpha$ ($10^{-5}K^{-3/2}$)	$-\gamma$ ($10^{-12}K^{-4}$)	D_o (meV-$^oA^2$)	D_2 ($10^{-7}K^{-5/2}$)	D_o (meV-$^oA^2$) from neutron scattering	Standared deviation (10^{-4}) of least squares fit
9	85.5-11-3.5	8.69	65.38±0.02	1.46±0.03	2.6±0.3	222±12	2.7±0.4	310[a]	3.0
4	81-11-8	8.65	52.95±0.03	3.99±0.05	7.2±0.5	131±8	1.2±0.1	180[b]	4.9
6	80-16-4	8.63	78.62±0.01	1.09±0.01	5.9±0.1	239±14	3.6±0.1	315[a]	1.1
8	75-17-8	8.56	66.46±0.08	2.64±0.1	7.0±0.7	150± 10	1.8±0.3	200[b]	10
7	75.5-20.3-4.2	8.61	86.54±0.03	1.11±0.02	5.3±0.2	223±15	3.2±0.2	320[a]	3.2
2	69.6-22.8-7.6	8.50	80.21±0.05	2.58±0.06	8.9±0.6	135±10	2.3±0.2	210[b]	5.9
1	67-21-12	8.42	61.76±0.02	4.77±0.03	2.8±0.3	107±7	0.4±0.05	-	3.8

ρ values were calculated

values estimated from Figure 3 of Reference (64)

values directly read from Figure 3 of Reference (64)

antiferromagnetic, but much weaker (~7 meV) in strength so that its effect can play a major role only when Fe concentration is relatively high; all other pair interactions are ferromagnetic in nature. Thus, addition of even a few percents of Cr could reduce the effective exchange interaction by a considerable amount and thereby reduce D_o.

iii) As Cr is added, α increases much faster than γ. This implies that the $T^{3/2}$-law should hold good over a larger range of temperature (in the scale of T/T_c) for the alloys richer in Cr. This is exactly what we can see from Figures 3.2 and 3.3. Actually this is one of the reasons why spin-wave analysis is meaningful even with the data above 77K for this alloy system. Large values of α also make the measurements easier. It is also important to mention that this kind of validity of the $T^{3/2}$-law over a large temperature range (even up to $T/T_c \simeq 0.5$) have also been found in amorphous ferromagnets[83].

iv) Though the absolute values of D_2 are slightly uncertain, they show a systematic trend of falling with increasing Cr concentration. This is similar to the behaviour found in Ni-Fe alloys where D_2 decreases with increasing Fe concentration[78,81,82]. But the rate of decrease with the addition of Cr in our case, is much faster than those found due to the addition of Fe in binary Ni-Fe alloys.

One might wonder whether the discrepancy in the D_o values obtained from the magnetization and neutron scattering

experiments is a result of using data above 77K (which is more than 0.1 T_c for all the alloys studied) only for our analysis. To check this point, we reanalysed some of the raw magnetization data of Majumdar et al.[84] on metallic glasses (Fe-B-C). The reasons behind choosing their data were two-fold: a) α & T_c for some of their systems were of nearly the same magnitude as those for our alloys, b) the data were readily available. Basically what was done is the following. α was calculated using data, i) from 10K to 180K ($\simeq$ 0.3 T_c), and ii) from 80K to 180K. It was found that the values of α in the two cases differed by not more than 4% and hence the values of D_o, thus calculated, could only differ by about 2.5% (since $D_o \propto \alpha^{-2/3}$). Thus we estimate that the effect of not including data below 77K on D_o, could not be more than 3% and perhaps even less for the alloys with higher T_c. In fact, our error bars given for D_o in Table 3.3, include this factor along with the contribution from other sources. Thus it is clear in the light of the above discussions, that the observed discrepancy between the two values of D_o is a real one rather than just an artifact of the experiments.

Such a difference among magnetization[76], NMR[85], and neutron scattering[75,81] based values for D_o have also been observed in pure Ni. But in the case of Fe, D_o values determined from various type of experiments seem to be in complete agreement[86]. Among the crystalline alloys, Fe-Cr[87] show such anomaly. Whereas in amorphous ferromagnets[83], it seems to be a rule rather than an exception.

Since neutron scattering measurements provide a direct method of measuring D, one should accept the neutron scattering based values as the real ones, rather than those obtained from bulk magnetization measurements. Thus in our case magnetization measurements show that the low temperature magnetization decreases faster than what one should expect from spin-wave excitations only. This probably indicates the existence of other excitations. Aldred[76], in connection with Ni, has shown that Stoner's single particle excitations could account for this additional term. Following the same methodology we have tried to explain the above discrepancy in our case, as will be shown in the following section.

3.2.3 Stoner Excitation

After the classic paper by Stoner[88] on itinerant electron ferromagnetism, numerous workers[89,90] have enriched and developed this new approach of band or itinerant electron ferromagnetism. The basic idea behind this model is that the magnetic electrons, which are itinerant in character, are split into spin-up and spin-down bands, separated by the exchange interaction energy. This splitting is assumed to be proportional to the spontaneous magnetization and, in the low temperature range, the decrease in magnetization with temperature is a result of the excitation of electrons from this spin-up to spin-down states. Wohlfarth et al.[91] have shown that depending on whether the magnetization is due to the electrons (holes) from a single spin band or from both, the temperature

dependence of magnetization will be different. For strong (i.e. when one sub-band is completely full) itinerant ferromagnets, the relative change of magnetization due to single particle or Stoner excitation only, is given by

$$\left(\frac{\Delta\sigma(T)}{\sigma(0)}\right)_{SP} = \frac{2I(T)}{n} e^{-E/k_B T} \qquad (3.9)$$

where $E/k_B T >> 1$, n is the number of holes per atom in the spin-down band, and E is the energy gap between the top of the full sub-band and the Fermi level E_F and I(T) is an integral related to the density of states of the material. Under the assumption of a parabolic band, $I(T) \propto T^{3/2}$ and hence

$$\left(\frac{\Delta\sigma(T)}{\sigma(0)}\right)_{SP} = A\, T^{3/2}\, e^{-E/k_B T} \qquad (3.10)$$

The exponential decrease of σ can be visualized as a result of the existence of the gap E, which necessitates an activation energy to lift the electrons from the filled spin-up states to the empty spin-down states.

On the other hand, for a weak (i.e. when both the sub-bands are only partially full) itinerant ferromagnet the change in reduced magnetization is given by

$$\left(\frac{\Delta\sigma(T)}{\sigma(0)}\right)_{SP} = B\, T^2 \qquad (3.11)$$

where 'B' is related to various band parameters like, the density of states at the Fermi level, their derivatives, band splitting, relative magnetization ζ_0 $\left(= \frac{n\downarrow - n\uparrow}{n\downarrow}\right)$ and so on.

The T^2 dependence is simply a manifestation of fermion excitations due to thermal energy. An additional $T^{3/2}$ term may also arise because of the assumption that molecular field, which splits the spin-up and spin-down bands, is proportional to the total magnetization which in turn decreases as $T^{3/2}$ due to spin-wave excitation.

To search for the existance of any such (Stoner) term, it appeared to be impractical to add Eqn.(3.10) or (3.11) to Eqn.(3.8) and then try for a least squares fit. The reason is that Eqn.(3.8) already contains three unknown parameters and an addition of one or more unknowns will complicate the situation without any appreciable gain. So it appeared more logical to follow the procedure of Aldred[76] of first calculating the expected change in magnetization due to spin-wave only, using the neutron scattering D values and subtracting these from the experimental values, at each temperature. The difference then will simply give the change in magnetization due to single particle excitations only. In such an analysis, implicit is the assumption that the two modes of excitations are independent of each other, which is justified, at least in the low temperature region. Thus, as a first step $(\alpha)_{SW\ only}$ was calculated using the data of Menshikov et al.[64] for D_o. Unfortunately, due to the absence of any such data for D_2, some approximations had to be made to calculate $(\gamma)_{SW\ only}$. We have conjectured that due to the presence of other than spin-wave excitation, D_o values obtained from magnetization

measurements might be less than the corresponding neutron scattering values. Now assuming that D_2 is also affected in the same manner as D_o, and recalling that $\frac{\gamma}{\alpha} = \frac{3}{2} D_2$, one can write $(\frac{\gamma}{\alpha})_{exp.} = (\frac{\gamma}{\alpha})_{SW\ only}$. Since the experimental values of α and γ are known, one can calculate $(\gamma)_{SW\ only}$ by using the value of $(\alpha)_{SW\ only}$. Once $(\alpha)_{SW\ only}$ and $(\gamma)_{SW\ only}$ are known, one can calculate the contribution to magnetization due to single particle excitation from the relation,

$$(\frac{\Delta\sigma(T)}{\sigma(0)})_{SP} = (\frac{\Delta\sigma(T)}{\sigma(0)})_{exp.} - (\frac{\Delta\sigma(T)}{\sigma(0)})_{SW\ only} \qquad (3.12)$$

To see whether this fits into Eqn.(3.10)or (3.11), two kinds of graphical plots were tried: (a) $\log\{(\frac{\Delta\sigma(T)}{\sigma(0)})_{SP} \frac{1}{T^{3/2}}\}$ vs. 1/T and (b) $(\frac{\Delta\sigma(T)}{\sigma(0)})_{SP}$ vs. T^2. It was found that for all the alloys, the second fit was much better than the first one. In Figure 3.5 are shown the results of such a fit. Considering the uncertainties involved in extracting the single particle term, the straight lines seem to be remarkably good. The slope of the straight lines give the co-efficient 'B' of the Stoner term. In Table 3.4 are given the results of such analysis. For comparison data for pure Ni and one Ni-Fe alloy[78] are also included. No such analysis could be performed for sample number 51 since the corresponding neutron scattering data for D_o is not available. However, the values of 'B' given in the above table should be used with a little caution because of the following reasons:

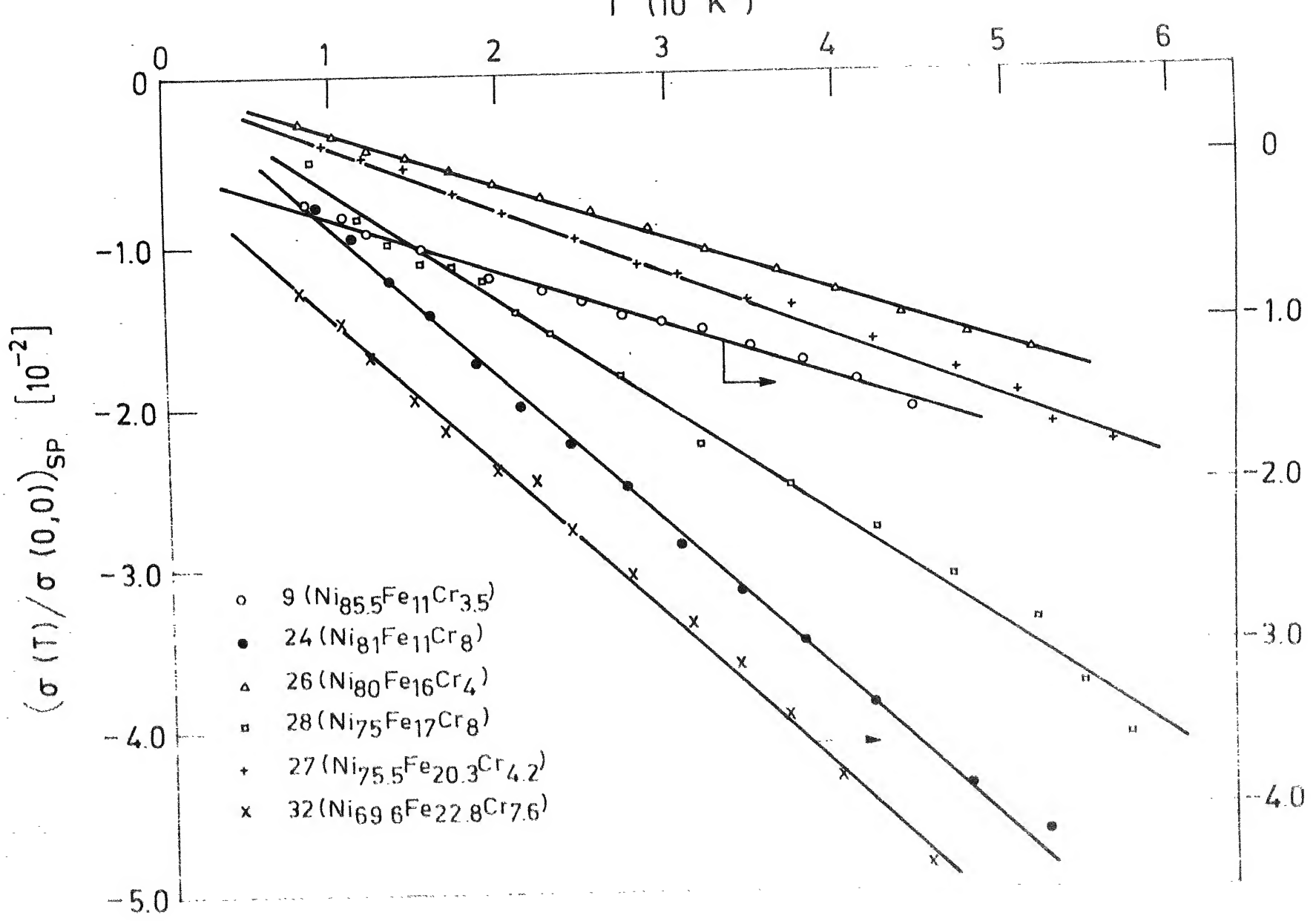
T (10 K)
0
1
2
3
4
5
6
0
-1.0
-2.0
-3.0
-4.0
-5.0
$(\sigma(T)/\sigma(0,0))_{SP}$ $[10^{-2}]$
9 ($Ni_{85.5}Fe_{11}Cr_{3.5}$)
24 ($Ni_{81}Fe_{11}Cr_{8}$)
26 ($Ni_{80}Fe_{16}Cr_{4}$)
28 ($Ni_{75}Fe_{17}Cr_{8}$)
27 ($Ni_{75.5}Fe_{20.3}Cr_{4.2}$)
32 ($Ni_{69.6}Fe_{22.8}Cr_{7.6}$)

Fig. 3 5

i) Since our experimental results could not resolve whether the next higher order term in the spin-wave contribution comes through a $T^{7/2}$ or a T^4 term, the absolute value of $(\gamma)_{exp.}$ is slightly uncertain. This value was used subsequently to estimate $(\gamma)_{SW\ only}$.

ii) As discussed earlier, it is not known how far the assumption made in calculating $(\gamma)_{SW\ only}$, is justified.

iii) Some systematic error also crept in estimating the neutron scattering D_o values for our alloys from the data of Menshikov et al.[64]. Such error could be appreciable because of the sensitive dependence of D_o on the Cr concentration.

Though the absolute values of 'B'are somewhat uncertain, a few broad but definite qualitative features could be identified. From a comparison of the 'B' values for the alloys with increasing Cr concentration but with approximately the same Fe content, it is pretty clear that the addition of Cr enhances the Stoner term considerably. But the change of 'B' with increasing Fe concentration is not very clear. This is since the value of 'B' is sensitive to Cr concentration, a meaningful comparison of 'B' for the alloys with different Fe concentrations can only be possible when their Cr contents are exactly the same. Even then it can be safely concluded that the change of 'B' with Fe concentration is much less compared to that with Cr.

It is evident from the above analysis that Stoner excitations can account for the difference between the

Table 3.4 : Results of the least squares fit of $\left(\frac{\Delta\sigma(T)}{\sigma(0)}\right)_{SP}$ to single particle excitations (Eqn.(3.11))

Sample Number	Composition of Ni-Fe-Cr alloys (at.%)	$B(10^{-7}K^{-2})$	Standard deviation of least squares fit (10^{-4}) to $(\Delta\sigma(T)/\sigma(0))_{SP}$
-	100-0-0	2.8* (3.2)	-
-	89.8-10.2-0	1.12*	-
9	85.5-11-3.5	3.3	4.0
24	81-11-8	9.1	6.2
26	80-16-4	3.2	1.9
28	75-17-8	6.8	12
27	75.5-20.3-4.2	3.9	4.7
32	69.6-22.8-7.6	9.4	6.4

*Reference (78)

The number in the paranthesis is from Reference (86).

magnetization and the neutron scattering determined values of D_o. But the fact that single particle excitations fit more to an itinerant weak rather than strong ferromagnetic description, seems to be a bit puzzling. This is because as shown in Section 1.2.2, according to the S.B. model due to Berger[29], all the spin-up bands (except that of Cr, which is non-magnetic) for Ni-Fe-Cr alloys are situated below E_F and hence the band picture suggests that the system should behave like a strong itinerant ferromagnet. At the same breath it is also pointed out that the existence of a Stoner term in the low temperature excitation of a ferromagnet is not a sufficient proof that the system is an itinerant weak ferromagnet. Because such a term has also been observed in Ni[76,78,86], though from de Haas-Van Alphen measurements[92] it appears to be a strong itinerant ferromagnet. There are other criteria which should be satisfied, before one arrives at a conclusion regarding the strong/weak itinerant behaviour in a particular material. However, from the rapid increase of the Stoner term with increasing Cr concentration and the similarity of this behaviour with Ni-Fe[79] alloys in the Invar region or those of Fe-Pt and Fe-Pd alloys[93] (which are all itinerant weak ferromagnets), one can possibly infer that addition of Cr in Ni-Fe alloys shifts it more towards itinerant weak ferromagnetism. Further evidence in support of this idea will be presented and discussed in Section 3.5.

3.2.4 Low Temperature Magnetization data for Ni-Fe-V Alloys

A few alloys in the ternary Ni-Fe-V system were selected for spin-wave study, mainly to see the effect of addition of vanadium and also the influence of increasing Fe concentration. The choice of alloys were again limited by the experimental constraint of not being able to extend the measurements below 77K. About four alloys of T_c about 500K and above were chosen. Similar to Ni-Fe-Cr alloys, the magnetizations as a function of temperature in a constant applied field of 7KOe were measured and a computer fit of the data were tried for a $T^{3/2}$ term and higher order terms.

In Figure 3.6 are shown the change in reduced magnetization $\Delta\sigma(H,T)/\sigma(0,0)$ as a function of $T^{3/2}$ (corrected for gap temperature). Deviation from the straight line clearly shows the necessity of terms higher than $T^{3/2}$. Similar to corresponding Cr-system, addition of vanadium clearly enhances the $T^{3/2}$ term and the importance of the higher order term decreases accordingly, as can be seen from the lesser deviation from the straight lines for alloys of higher vanadium content; also the range of validity of the $T^{3/2}$-law gets extended in the reduced temperature scale (T/T_c).

In search for the higher order terms, two kinds of least squares fits were tried with: i) $\sigma(0,0)$, α and (co-efficient of $T^{5/2}$ term) and ii) $\sigma(0,0)$, α and γ (co-efficient of T^4 term). Though the second kind of fit was found to be generally better than the first one, the difference

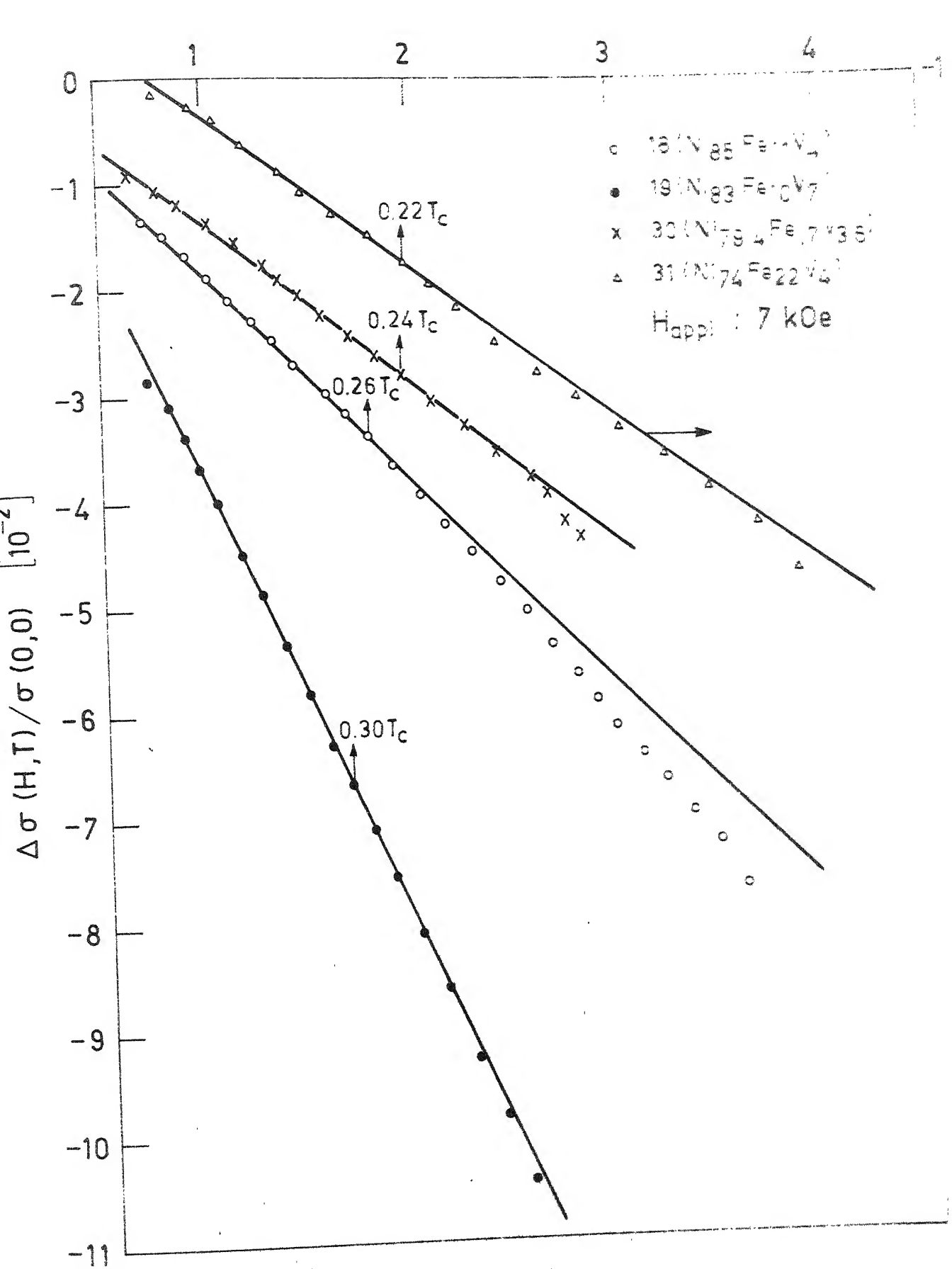
1
2
3
4
0
-1
-2
-3
-4
-5
-6
-7
-8
-9
-10
-11
0.22 Tc
0.24 Tc
0.26 Tc
0.30 Tc
Happl : 7 kOe
Δσ (H,T)/σ (0,0) [10⁻²]

Fig. 3.6

(5% S.D.) was found to be marginal. This is in contrast to Ni-Fe-Cr alloys, where the second kind of fit was always convincingly better than the first one. So there is a possibility that the term β is not negligibly small compared to α in ternary vanadium alloys. Inclusion of β and γ simultaneously was not possible as the limited accuracy of our experimental data do not permit handling of so many parameters together.

In Table 3.5 are shown the results of the least squares fits with different higher order terms, along with the standard deviations. Using the values of α, the spin-wave stiffness constants D_o were calculated and are also included in the table. The values of 'ρ' were calculated in the same manner as discussed in Sec. 3.2.2, using our measured lattice parameter values.

Figure 3.7 shows the change in reduced magnetization with temperature in a constant field of 7KOe for some Ni-Fe-V alloys; the solid curves are the computer fits with the $T^{3/2}$ term along with T^4 term. Although the fits seem to be fairly good, in the absence of any neutron scattering data for D_o, it could not be ascertained whether the magnetization derived values of D_o are the actual ones. In other words, whether the spin-waves are the only excitations responsible for the decrease of magnetization. However, as can be seen from Tables 3.1A and 3.1B, Curie temperatures for Ni-Fe-Cr/V alloys with about the same concentration of Cr/V are of the same order. Since basically both T_c and D_o are related to the

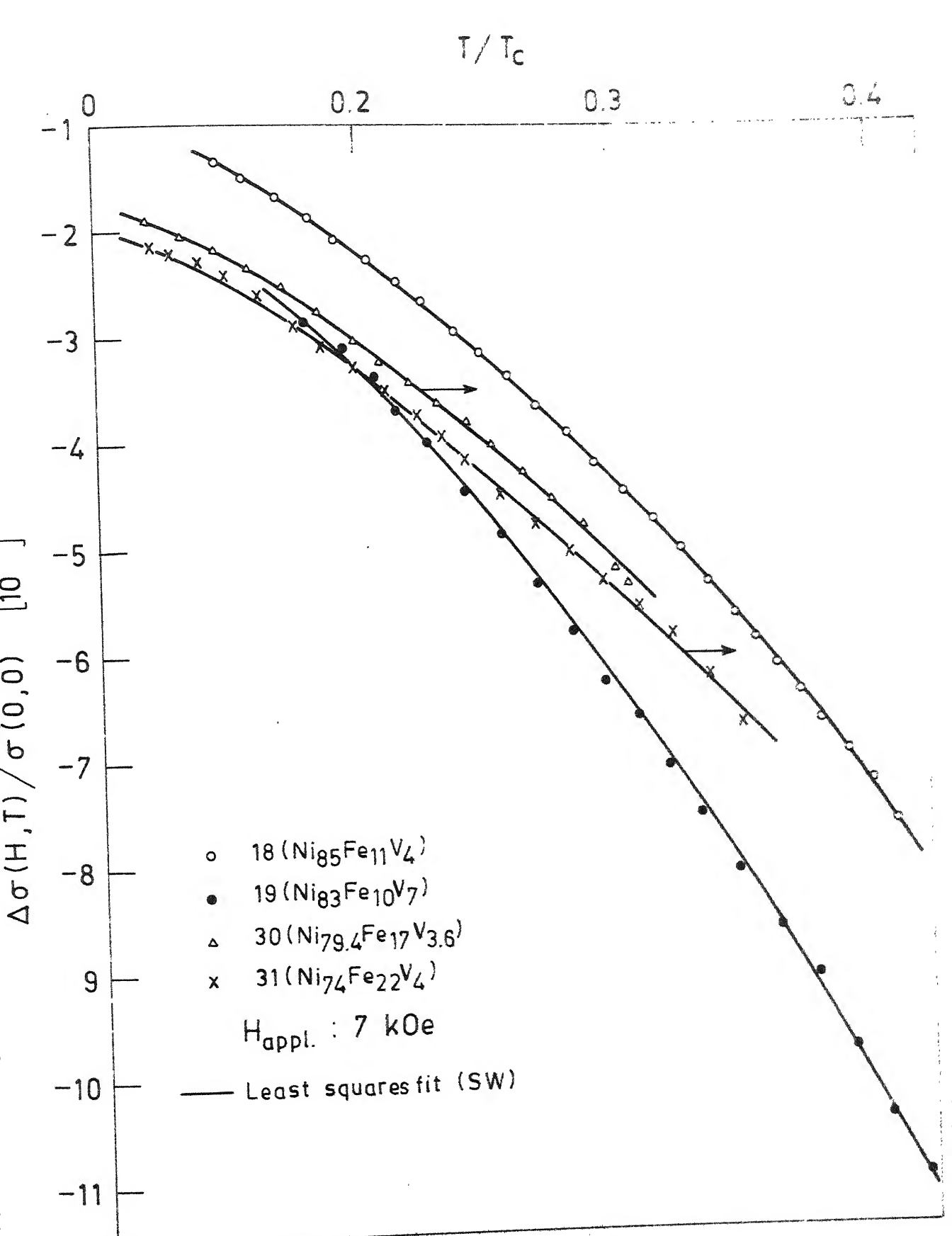
T/ Tc
0
0.2
0.3
0.4
-1
-2
-3
-4
-5
-6
-7
-8
9
-10
-11
Δσ(H,T)/σ(0,0) [10]
18 (Ni85Fe11V4)
19 (Ni83Fe10V7)
30 (Ni79.4Fe17V3.6)
31 (Ni74Fe22V4)
Happl. : 7 kOe
Least squares fit (SW)

Fig. 3.7

Table 3.5 : Results of the least squares fits for the temperature variation of magnetization for some Ni-Fe-V alloys. The statistical uncertainty in the various parameters are also included

Sample Number	Composition of Ni-Fe-V alloys (at.%)	Density ρ^* (g/cm^3)	$\sigma(0,0)$ (emu/g)	$-\alpha$ ($10^{-5}K^{-3/2}$)	$-\beta$ ($10^{-8}K^{-5/2}$)	$-\gamma$ ($10^{-12}K^{-4}$)	D_o (meV-$^oA^2$)	D_2 ($10^{-7}K^{-5/2}$)	Standard deviation of least squares f (10^{-4})
31	74-22-4	8.56	90.2±0.08	1.27±0.13	0.61±0.4	-	199	-	4.7
			90.3±0.06	1.39±0.05	-	0.6±0.3	187	0.3	4.8
30	79.4-17-3.6	8.62	79.2±0.05	1.02±0.1	2.0±0.4	-	250	-	3.8
			79.3±0.03	1.33±0.04	-	2.9±0.5	209	3.3	3.7
18	85-11-4	8.69	61.8±0.02	1.27±0.04	2.9±0.13	-	253	-	2.0
			62.0±0.01	1.80±0.02	-	3.3±0.15	200	1.2	1.9
19	83-10-7	8.65	53.6±0.07	3.01±0.17	4.8±0.6	-	157	-	8.7
			53.8±0.04	3.81±0.06	-	5.7±0.6	134	1.0	7.5

*Calculated values.

average exchange interaction, it is not altogether unjustified to expect that the D_o values for vanadium alloys should be of the same order as the corresponding Ni-Fe-Cr alloys. But a comparison of our D_o values for Ni-Fe-V alloys with those of the neutron scattering derived values for the corresponding Ni-Fe-Cr alloys (Table 3.3) suggest that magnetization derived D_o values are much smaller than expected for this system also. This immediately raises the question whether in Ni-Fe-V alloys also we have other than spin-wave (possibly Stoner-type) excitations at low temperatures. The similarity of the magnetic behaviours (see Section 3.5) in the two systems strongly favours this view-point. The real picture can only emerge when the neutron scattering data are available.

The other features, e.g. a rapid decrease of D_o with vanadium concentration in contrast to a smaller one with Fe concentration, are similar to those of Ni-Fe-Cr alloys. The temperature dependent part of the spin-wave stiffness constant (D_2) also shows a decrease with the addition of vanadium. In fact, the validity of the $T^{3/2}$-law over a larger temperature range is itself a manifestation of the declining importance of the higher order terms.

3.3 Average number of Bohr Magnetons per atom ($\bar{\mu}$)

By extrapolation of the magnetization data (77K and above) to low temperatures, one can obtain the magnetic moment at OK and thereby the average number of Bohr magnetons per atom, $\bar{\mu}$. This procedure is fairly simple and accurate for the alloys with higher T_c and for which spin-wave analysis of magnetization data have been done. For the alloys with lower T_c (< 450K), a $T^{3/2}$-dependence of magnetization was observed (although, over a limited temperature range) above 77K, which justified the extrapolation procedure even for them. This is because of the fact (as discussed in Section 3.2.2) that the alloys with higher Cr content (lower T_c) show a $T^{3/2}$-dependence over a higher temperature range in the rationalized scale (T/T_c). However, this extrapolation procedure is unreliable for alloys with T_c lower than room temperature and hence no such data will be included here. We estimate that the total error in $\bar{\mu}$ is less than 2% for the first method of analysis and is a little more for the second one.

As discussed earlier in Section 1.2.1, to explain the deviation from Slater-Pauling curvesof the various Ni based binary alloys with Ti, V, Cr etc. as impurities, Friedel[34] had introduced the concept of virtual bound state, which was extended by Berger[29] in his S.B. model. Since basically the magnetization is also connected to the number of holes available in the band, similar to Eqn.(1.8), one can express the variation of $\bar{\mu}$ with composition for the ternary systems

Ni-Fe-Me (Me = Cr, V, etc.), by

$$\bar{\mu} = 0.61 + 2\,C_{Fe} - (10 + Z)\,C_{Me} \qquad (3.13)$$

where C stands for the concentration and Z the valence difference between Ni and Me (which is -4 for Cr and -5 for V). Thus experimental values for $\bar{\mu}$ can provide a test for Eqn.(3.13). The experimental results for the two systems are presented in the next two sub-sections.

3.3.1 $\bar{\mu}$ for Ni-Fe-Cr Alloys

Although, a comprehensive study of the variation of magnetic moment with composition over the entire ferromagnetic range of compositions for this alloy series have already been carried out by Menshikov et al.[61], we present here some of the data from our measurements in the Ni-rich region for comparison. This will provide an additional check for the reliability and quality of the samples prepared by us. In Table 3.6 are given $\bar{\mu}$ for various alloys studied along with those of Menshikov et al. and those calculated from Eqn.(3.13). Since some of our compositions were different from those of Menshikov et al.,[61] the corresponding values of $\bar{\mu}$ were estimated from their data for comparison. Considering the uncertainties involved in the interpolation procedure, one can easily see that the two sets of data are fairly in good agreement. But the disagreement with Eqn.(3.13) is too glaring to be ignored. The fact that our experimental values are always larger than the theoretical

Table 3.6 : Average number of Bohr magnetons per atom, $\bar{\mu}$, for various Ni-Fe-Cr alloys

Sample Number	Composition of Ni-Fe-Cr alloys (at.%)	$\bar{\mu}$ (no.of Bohr magnetonons per atom) Present data	Data of Menshikov et al.	According to Eqn.(3.13)	$(Z)_{eff.}$
9	85.5-11-3.5	0.68±0.01(SW)	0.70	0.62	4.3
24	81-11-8	0.55±0.01(SW)	0.57*	0.35	3.5
29	75.1-12.8-12.1	0.46±0.015(E)	0.45	0.14	3.4
26	80-16-4	0.82±0.015(SW)	0.82	0.69	2.8
28	75-17-8	0.68±0.01(SW)	0.70*	0.47	3.4
33	68.1-17.4-14.5	0.48±0.015(E)	0.48	0.09	3.3
35	76.8-21.2-2	0.96±0.015(E)	0.98	0.91	3.7
27	75.5-20.3-4.2	0.89±0.015(SW)	0.89	0.76	3.0
32	69.6-22.8-7.6	0.82±0.015(SW)	0.83	0.61	3.2
51	67-21-12	0.63±0.015(SW)	0.64	0.31	3.3

SW : Data obtained by spin-wave analysis

E : Data obtained by extrapolation, using $T^{3/2}$-law

* : Values directly read from Reference (61).

values and the disagreement between theory and experiment is more for the alloys with higher Cr content, might lead one to suspect whether the value 6 taken for (10+Z) is rather too large. The corresponding value of 5.1 $(= \frac{d\bar{\mu}}{dc}\Big|_{Cr})$[65] even in binary Ni-Cr alloys further strengthens this suspicion. To check this, our experimental values of $\bar{\mu}$ were fitted to Eqn.3.13, replacing (10+Z) by a variable parameter $(Z)_{eff.}$ The values of $(Z)_{eff.}$, thus obtained, are shown in Table 3.6. It is clear from our analysis that i) $(Z)_{eff.}$ is much smaller than the ideal value of 6 for the alloys and ii) $(Z)_{eff.}$, instead of being a constant, is itself composition dependent. But one should bear in mind that the above analysis was confined to Ni-rich region only with the total Fe+Cr concentration never exceeding 30 at.%. However, when one looks into the more comprehensive data of Menshikov et al. (Figure 2 of Reference (61)), a strong non-linearity (implying $(Z)_{eff.}$ to be composition dependent) is also observed in the $\bar{\mu}$ vs. concentration curves. Deviation from linearity is more prominent for the alloys with higher Cr. concentration. It should also be noted that when we replotted their data for $\bar{\mu}$ as a function of C_{Cr} for a series of alloys with constant Fe content, we found that the rate of decrease of $\bar{\mu}$ with Cr-concentration slows down as more and more Cr is added (i.e. $\bar{\mu} \propto C_{Cr}^{n}$, where $n<1$). In other words $(Z)_{eff.}$ is smaller for the alloys with higher Cr-content. Except for a few exceptions (probably due to some uncertainties in determining actual compositions), in

general our data also show similar trend. It should also be pointed out that in the later work on binary Ni-Cr alloys by Acker and Huguenin[95], $(Z)_{eff.}$ have been found to decrease with increasing Cr concentration. Menshikov et al.[61] have tried to explain $\bar{\mu}(c)$ on the basis of "defect theory". When Cr atoms enter into Ni-matrix, some of the nearest Ni-neighbours try to compensate the spin-density around Cr-atoms arising because of the different number of "upward" and "downward" spins of the host and the impurity. This causes a magnetic defect in the N-number of nearest Ni-neighbours, reducing the total magnetization by $(N+1)0.4=5.2\mu_B$/atom (N=12 for f.c.c. lattice and 0.4 is the magnetic moment of pure Cr). Addition of Fe tries to suppress the negative spin polarization effect of Cr atoms. Thus the opposite roles played by the two kinds of impurities in Ni, might provide some qualitative argument in favour of non-linear dependence of average magnetic moment on concentration (Fe or Cr). But according to this theory increasing Cr-concentration should gradually diminish the role played by the Fe atoms and hence one should expect $(Z)_{eff.}$ to increase with increasing Cr-concentration. This is in contrary to what we observe from our as well as from the data of Menshikov et al.[61]. So this aspect of the problem does not seem to fit the "defect theory". We believe, some CPA type calculations (which has successfully been applied to various binary systems by Hasegawa et al.[36-38]) for the band structure of this ternary system will be able to explain these data.

3.3.2 $\bar{\mu}$ for Ni-Fe-V Alloys

We present the data for $\bar{\mu}$ for a few Ni-Fe-V alloys in the Ni-rich region. The same method, as described earlier for Ni-Fe-Cr system, was used for extrapolation of magnetization data above 77K to OK, to obtain $\bar{\mu}$. In Table 3.7 are presented the derived data along with those estimated according to Eqn.(3.13). It can be seen that again Eqn.(3.13) fails to explain the experimental results. To get an estimate of $(Z)_{eff.}$ $(= (10+Z)_{eff.})$, the same kind of analysis as in Cr alloys, have been done. It appears that the average $Z_{eff.}=3.8$ instead of 5 and is itself a function of composition, implying non-linearity in $\bar{\mu}$ vs. concentration curves. Thus, essentially the results are similar to those of Ni-Fe-Cr except for the fact that deviation of $(Z)_{eff.}$ from the ideal value (5) is less for the V-system than for the Cr-ones. For small V-concentrations, $(Z)_{eff.}$ are almost near to the ideal value of 5 and then start decreasing with increasing V-content. This is in contrast to the behaviour of $d\bar{\mu}/dc$ in binary Ni-V alloys[95] where $(Z)_{eff.}$ have been found to be increasing with increasing V-concentration (from initial value of 5 to about 5.7 for C_V = 8 at.%).

Table 3.7 : Average number of Bohr magnetons per atom for various Ni-Fe-V alloys

Sample Number	Composition of Ni-Fe-V alloys (at.%)	$\bar{\mu}$ in number of Bohr magnetons per atom		$(Z)_{eff.}$
		Our data	According to eqn..(3.13)	
46	82.5-7.5-10	0.44±0.015(E)	0.26	3.2
19	83-10-7	0.56±0.01(SW)	0.46	3.6
20	80.5-10.5-9	0.52±0.01(E)	0.37	3.3
18	85-11-4	0.65±0.01(SW)	0.63	4.5
39	77.4-11.9-10.7	0.48±0.015(E)	0.31	3.4
37	80.9-14.0-5.1	0.65±0.015(E)	0.63	4.8
38	76.5-14-9.5	0.55±0.01(E)	0.41	3.6
36	81-17-2.0	0.85±0.015(E)	0.85	5.0
30	79.4-17-3.6	0.82±0.015(SW)	0.77	3.6
31	74-22-4	0.93±0.02(SW)	0.85	3.0

SW : Spin-wave analysed value

E : Values obtained by extrapolation, using $T^{3/2}$-law

3.4 Temperature Variation of Spontaneous Magnetization and Molecular Field Theories

Spontaneous magnetization, M_S, was measured from 77K to their respective Curie temperatures for a few alloys in both the ternary series. As discussed in the preceding section, due to a rapid decrease of the spin-wave stiffness constant with the addition of Cr/V, magnetization in these systems falls off much faster than in Ni or binary Ni-Fe alloys at low temperatures. So it appeared to be interesting to study M_S over the complete ferromagnetic range of temperature, at least for a few alloys. The similarities in some low temperature aspects of the magnetization with those of metallic glasses (viz. validity of the $T^{3/2}$-law over a large temperature range) also raised the possibility of some such similarities in the high temperature behaviour.

At temperatures below about 0.8 T_c, spontaneous magnetizations at any temperature were obtained by extrapolation to zero field of the high field straight line part of the magnetization vs. magnetic field isotherms. At higher temperatures, the well known Arrott[96] plots were used to obtain M_S. This method (Arrott plots) also furnishes a reliable way to determine Curie temperature accurately, since then T_c is the temperature at which M_S vanishes. The above method was applied in determining T_c only for the few alloys under consideration; for the rest, the method used has already been discussed in Section 3.1. The reason is, one needs better accuracy for T_c when the behaviour of reduced

magnetization ($M_S(T)/M_S(0)$) as a function of reduced temperature (T/T_c) is studied, specially near the critical region. Now, according to the molecular field theories, reduced magnetization vs. reduced temperature curves are expected to roughly follow Brillouin functions, except at very low temperatures (due to spin-waves) and near to the critical region, because of the inherent limitations of these theories. Figures 3.8-3.10 show the experimental results for some Ni-Fe-Cr/V alloys along with the Brillouin function curves corresponding to S=1, shown by the dotted lines. It can be readily seen that for all the alloys, magnetization falls much faster than predicted by the theory, over the whole temperature range studied. The theoretical curves for $S = \frac{1}{2}$ have not been shown in the figures partly to preserve clarity and partly because the disagreement with experimental data would have been more for them. Another aspect of our data, as can be seen from Figures 3.9 and 3.10, is that the disagreement between the theory and experiment increases with increasing Cr/V concentrations.

It is well known that though approximate, molecular field theories with $S = \frac{1}{2}$ and S=1 can fairly well explain the magnetization data of crystalline Ni and Fe respectively, within their limitations. But it appears that this kind of theory is rather inadequate for the present systems. As pointed out in Sections 3.2.2 and 3.2.4, the dominance of large spin-wave contribution to the decrease of magnetization up to fairly high temperatures ($\sim 0.5\ T_c$) could be a plausible reason for the disagreement at low temperatures. But the

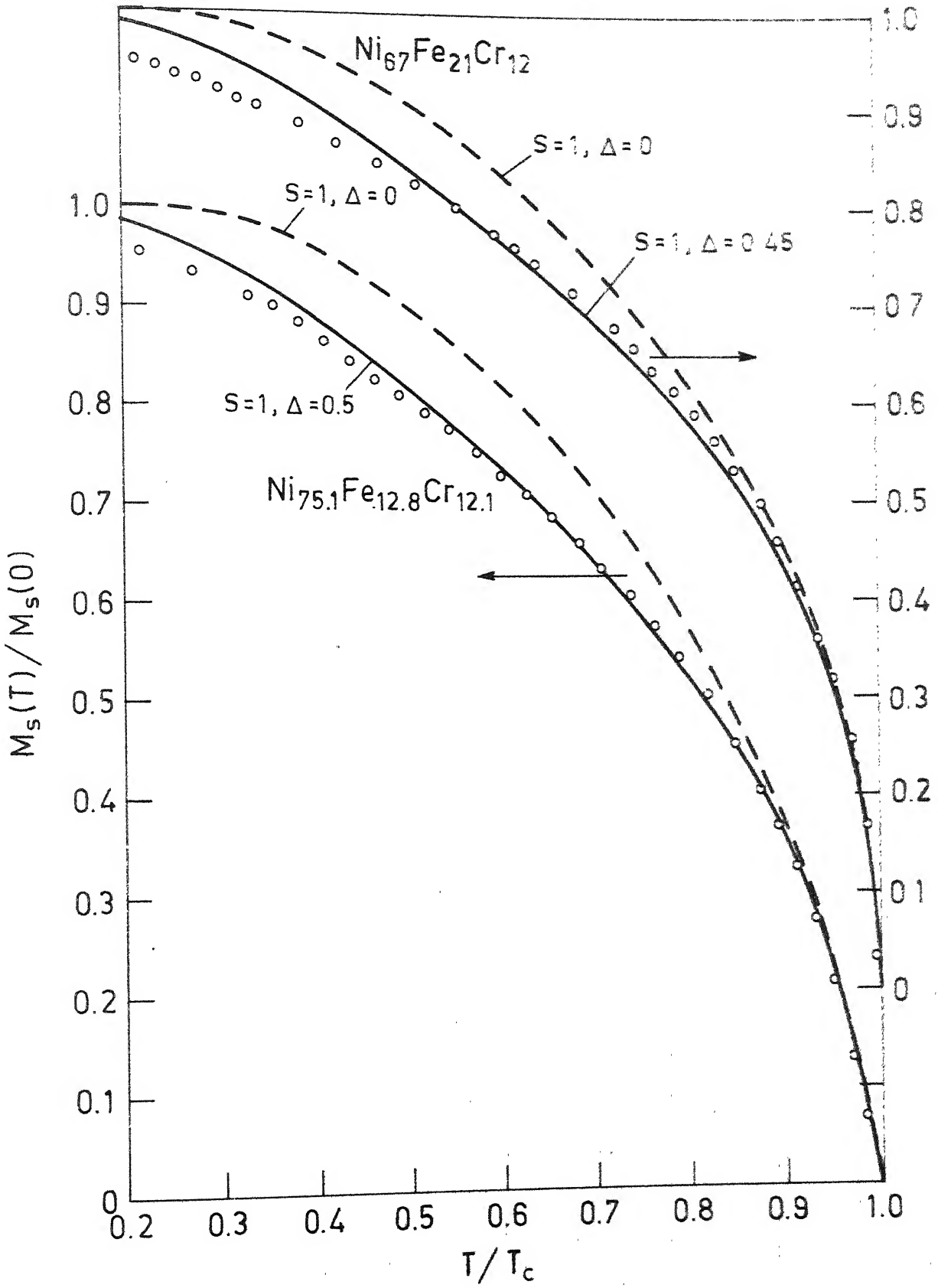
$Ni_{67}Fe_{21}Cr_{12}$
S=1, Δ=0
S=1, Δ=0
S=1, Δ=0.45
S=1, Δ=0.5
$Ni_{75.1}Fe_{12.8}Cr_{12.1}$
$M_s(T)/M_s(0)$
T/T_c
0
0.1
0.2
0.3
0.4
0.5
0.6
0.7
0.8
0.9
1.0
0.2
0.3
0.4
0.5
0.6
0.7
0.8
0.9
1.0

Fig. 3.8

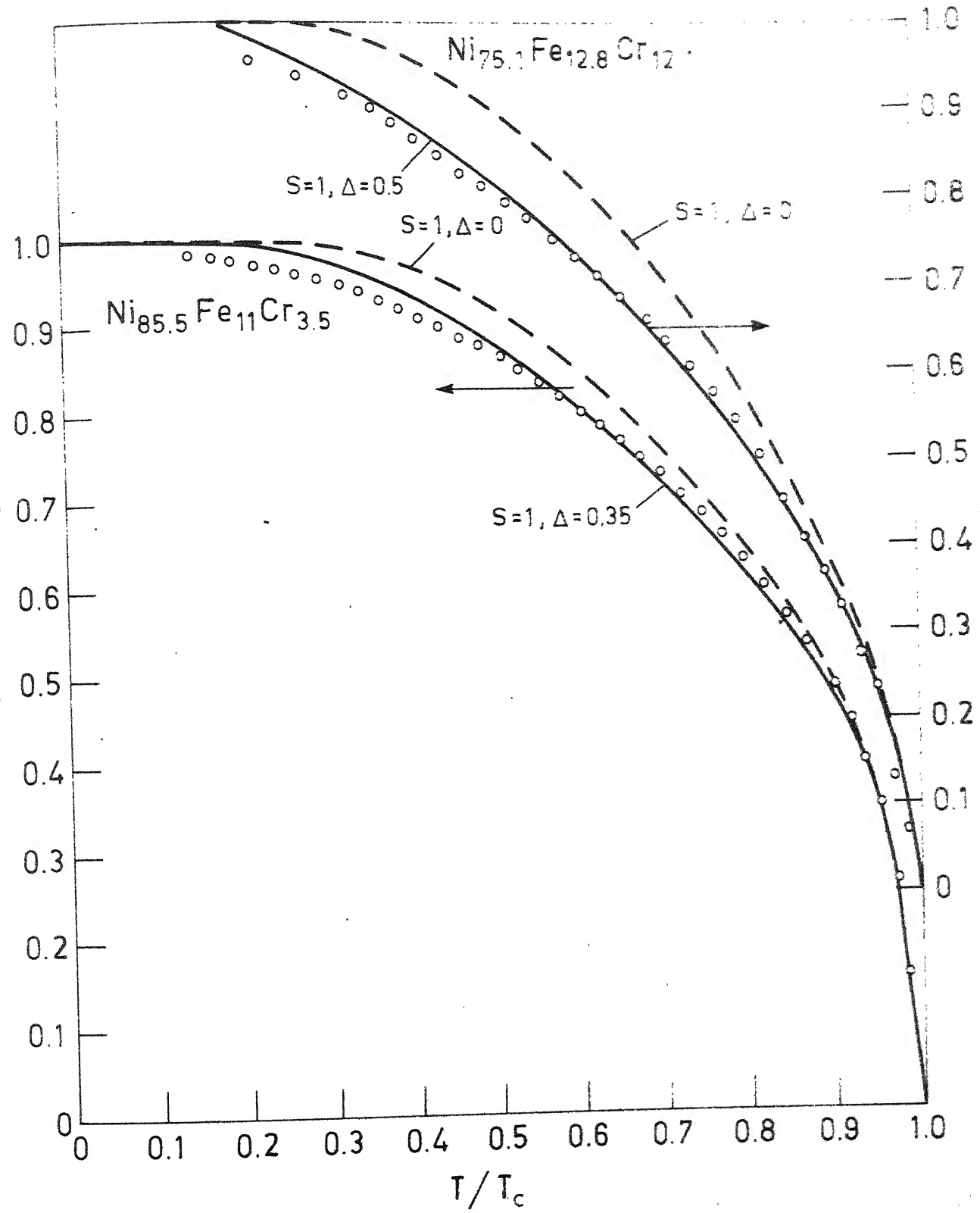
$Ni_{75.1}Fe_{12.8}Cr_{12}$
S=1, Δ=0.5
S=1, Δ=0
S=1, Δ=0
$Ni_{85.5}Fe_{11}Cr_{3.5}$
S=1, Δ=0.35
1.0
0.9
0.8
0.7
0.6
0.5
0.4
0.3
0.2
0.1
0
0.1
0.2
0.3
0.4
0.5
0.6
0.7
0.8
0.9
1.0
T / T_c

Fig. 3.9

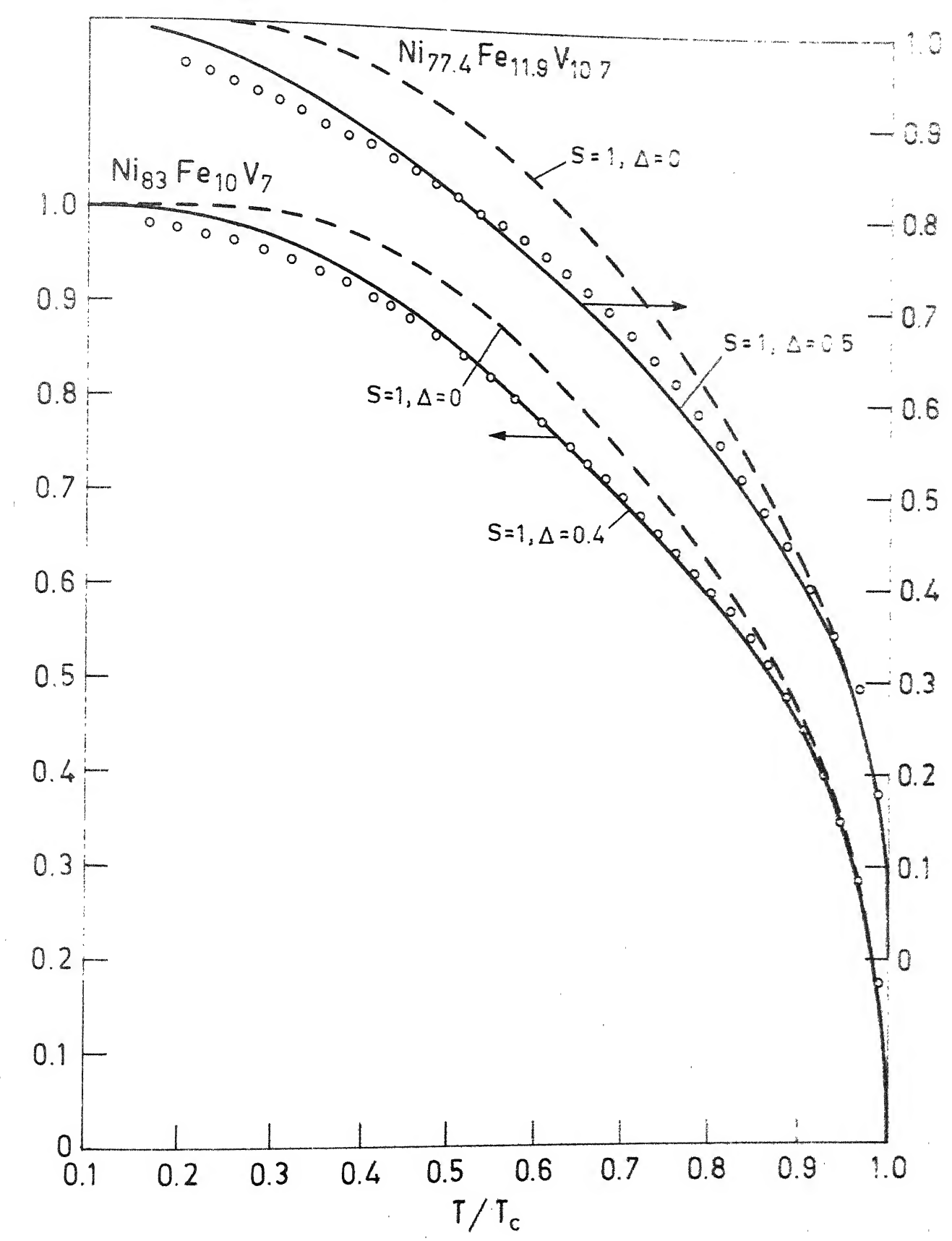
$Ni_{77.4}Fe_{11.9}V_{10.7}$
$Ni_{83}Fe_{10}V_7$
S = 1, Δ = 0
S = 1, Δ = 0.5
S=1, Δ=0
S=1, Δ=0.4
1.0
0.9
0.8
0.7
0.6
0.5
0.4
0.3
0.2
0.1
0
0.1
0.2
0.3
0.4
0.5
0.6
0.7
0.8
0.9
1.0
T/T_c

Fig. 3.10

disagreement at higher temperatures cannot find any logical justification in the framework of the simple molecular field theories. It is also interesting to point out that recent studies of ferromagnetic metallic glasses[97,98] have shown a similar kind of 'diminished curvature' of magnetization in a wide variety of systems. Among the various theories[99,100,101] proposed so far, the ones which incorporate disorder by allowing the exchange interaction to deviate randomly from a mean value, have been found to be more successful in explaining the magnetization behaviour of amorphous ferromagnets. Of these, the theory by Montgomery et al.[100], ascribes the decrease in spin-wave stiffness constant of amorphous materials from their crystalline counterpart, to a rapid rise in the density of spin wave states at lower energies due to disorder and also can explain the depression of Curie temperature; but it fails to explain the diminished curvature of the reduced magnetization curves. On the other hand, the theory propounded by Handrich[99], though handicapped by unchanged T_c even in the presence of disorder (but corrected in a later paper[101]), can very well explain the overall qualitative behaviour of the magnetization curves[97,98]. Though crystalline, the similarity of the magnetization behaviour of the present systems with those of amorphous ferromagnets, prompted us to search for an explanation in the context of those theories.

Because of the simple analytic form, we tried to apply Handrich's theory. According to this, in the presence

of disorder the reduced spontaneous magnetization, under the molecular field approximation, should be given by

$$M_S(T)/M_S(0) = \frac{1}{2}\{B_S(1+\Delta)x + B_S(1-\Delta)x\} \quad (3.14)$$

where B_S is the Brillouin function with $x = \{3S/(S+1)\}(T_c/T) \times \{M_S(T)/M_S(0)\}$ and Δ is a measure of disorder, defined as the r.m.s. deviation from the average exchange interaction between nearest neighbour pairs. In the absence of any disorder, Eqn.(3.14) is simply reduced to $B_S(x)$, as expected. Using Δ as a variable in Eqn.(3.14), the best possible fit could be obtained for S=1, Δ = 0.35 for sample number 9 with 3.5 at.% of Cr and for S=1, Δ = 0.5 for sample number 29 with 12.1 at% of Cr. An equally good fit could also be obtained for S = $\frac{1}{2}$ with different Δ values. The values of S and Δ which give best fits to our experimental curves, are presented in Table 3.8. The solid curves in Figures 3.8 to 3.10 are the best possible fits according to Eqn.(3.14) for S=1. To preserve clarity, the corresponding curves for S= $\frac{1}{2}$ have been omitted. It is clear from the table that whatever be the value of S($\frac{1}{2}$ or 1), Δ always increases with the addition of Cr/V for an alloy series with fixed Fe concentration. But when Fe concentration is increased, maintaining Cr concentration fixed, Δ changes very little as can be seen from Figure 3.8, where the reduced magnetization data for sample number 29 has been presented along with that of sample number 51 for comparison. An increase of Fe concentration by about 8 at.% has reduced Δ only by about 0.05 for

Table 3.8 : Results of best fits of modified Brillouin functions to reduced magnetization data

Sample Number	Composition (at.%)	Values of Δ for best possible fit with	
		S = 1	S = 0.5
9	$Ni_{85.5}Fe_{11}Cr_{3.5}$	0.35	0.4
29	$Ni_{75.1}Fe_{12.8}Cr_{12.1}$	0.5	0.55
51	$Ni_{67}Fe_{21}Cr_{12}$	0.45	0.5
19	$Ni_{83}Fe_{10}V_{7}$	0.4	0.45
39	$Ni_{77.4}Fe_{11.9}V_{10.7}$	0.5	0.5

both S=1 and S = $\frac{1}{2}$. But the corresponding increase of Cr resulted in a change of Δ by 0.15. It should be pointed out that the quantitative agreement between Eqn.(3.14) and our experimental results cannot be claimed to be excellent. But the slight disagreement at lower and higher temperatures is quite expected if the limitations of molecular field theories are kept in mind. Now since Δ is a measure of disorder, the implication of the above results is that the addition of Cr/V in these ternary systems drastically increases disorder, whereas addition of Fe has very little effect; if at all, it tries to suppress disorder. The important question is what kind of disorder can arise from the addition of Cr/V. Since these are all polycrystalline materials and except for a small decrease in lattice parameter no other effect has been observed due to the addition of Cr/V, one can rule out the possibility of any structural disorder. But there is a distinct possibility of higher "magnetic disorder", specially due to the addition of Cr. Neutron scattering studies of Menshikov et al.[64] have shown that out of the six types of pairing interactions in Ni-Fe-Cr alloys, Cr-Cr and Fe-Fe interactions are antiferromagnetic and I_{Cr-Cr} has a very large value, compared to those for other interactions. In that event the exchange integral will vary in a random manner from site to site, depending on the type of nearest neighbour atoms in a random alloy. Because of the large value of I_{Cr-Cr} (~ -227 meV, compared to 52 meV for I_{Ni-Ni}), magnetic disorder will rapidly increase with the addition of Cr, as has

been observed experimentally. On the other hand since I_{Fe-Fe} is very small (- 7 meV) the influence of Fe will be negligible except in the Fe-rich region. But in the case of Ni-Fe-V alloys, in the absence of any such information on exchange interaction, no such explanation could be put forward. However, the similarity of their magnetic behaviour probably suggests the same kind of mechanism in these alloys also.

The results of spin-wave stiffness constant measurements are also consistent with the above picture, since the theory by Montgomery et al.[100] suggests a decrease in D with increasing disorder. If one sticks to the disorder approach to the problem, the above results indicate that for the present systems, "magnetic disorder" is playing similar role as "structural disorder" (or probably both) plays in amorphous magnetic materials. There is another possibility (as will be discussed in the next section) that all these anomalies arise simply because localized theories do not hold good for these ternary systems.

3.5 Itinerant vs. Localized Model

The magnetization behaviour studied so far, reveals two interesting features: i) A rapid increase of the Stoner (T^2) term in the magnetic excitation with the addition of Cr in Ni-Fe alloys. Though the presence of such a term could not be established in Ni-Fe-V alloys due to absence of the spin-wave stiffness constant data obtained from neutron

scattering experiments, still our low temperature magnetization measurements give some indication about the presence of additional excitations other than spin-wave, ii) reduced magnetization for alloys in both the ternary systems falls much faster than predicted by molecular field theories and this discrepancy widens with increasing concentration of Cr/V. These facts, along with the non-integral values of average number of Bohr magnetons/atom ($\bar{\mu}$) and their non-linear dependence on concentration, opened up the possibility of a suitable explanation of our data in the framework of itinerant electron models (IEM) rather than the localized ones.

In the last twenty years some useful criteria have been developed by Wohlfarth and co-workers to distinguish between materials obeying localized models (LM) and those following IEM. One of them is the Rhodes-Wohlfarth plot[62,102], where the ratio q_c/q_s is related to the Curie temperature T_c. Here q_s is the average number of Bohr magnetons per atom derived from the low temperature magnetization data and q_c is the corresponding quantity derived from the Curie-Weiss constant in the paramagnetic region by using the relationship

$$C = \frac{N \mu_B^2 p_{eff.}^2}{3 k_B} \qquad (3.15)$$

where

$$p_{eff.}^2 = q_c (q_c + 2) \qquad (3.16)$$

Here C^{-1} is the slope of the linear part of the inverse susceptibility vs. temperature plots, N is the number of

atoms/gm and k_B is the Boltzmann constant. The basic philosophy of Rhodes-Wohlfarth plot is that in the case of the localized electrons, the effective spin is the actual spin and hence $q_c/q_s = 1$ for all T_c. But in the case of the itinerant electrons, q_s might be less than the maximum possible value and hence $q_c/q_s > 1$. This ratio will be larger, the weaker the ferromagnetism and hence should be related to T_c by

$$\frac{q_c}{q_s} \propto T_c^{-1} \tag{3.17}$$

Recently[102], it has been shown that this kind of plot for a large number of alloys and compounds with diverse constituents show a systematic trend of increasing with decreasing T_c (if not following the same universal curve as predicted by Eqn.(3.17)). However, the Curie-Weiss behaviour above T_c, though observed in almost all ferromagnets including weak itinerant systems like $ZrZn_2$[103,104] and Sc_3In[105], finds little support from the Stoner[88] model or from its later extension by Edwards and Wohlfarth[106]. In the limit of very weak ferromagnetism, Edwards et al. show that

$$\chi = \chi_o \left(1 - \frac{T^2}{T_c^2}\right)^{-1}, \quad T < T_c$$

$$\chi = 2\chi_o \left(\frac{T^2}{T_c^2} - 1\right)^{-1}, \quad (T_F \geq T > T_c) \tag{3.18}$$

where T_F is the effective degeneracy temperature of the Fermion system above which Pauli exclusion principle can no longer restrict the occupation of the bands as all electrons/holes around E_F are thermally excited. Actually this T_F is the temperature corresponding to the energy of exchange splitting of the spin-up and spin-down bands. χ_o is the differential susceptibility at OK, given by

$$\chi_o = Nn(E_F)\mu_B^2 / [In(E_F) - 1] \qquad (3.19)$$

where,

N = number of atoms

$n(E_F)$ = density of states/atom/spin

I = exchange parameter.

Thus according to the Stoner-Wohlfarth theory, $\chi^{-1} \propto T^2$. However, this has not been observed in any weak ferromagnetic system, except Ni_3Al[107]. A Curie-Weiss (CW) behaviour, according to Wohlfarth,[108] is expected only when $T \gg T_F$ which is definitely not the case in the temperature ranges where CW behaviour has been observed in $ZrZn_2$ or other similar systems. The failure of these theories to explain the observed CW behaviour naturally points to the inadequacy of Hartree-Fock approximations, on which these theories were based and developed to describe the finite temperature properties, even for very weak ferromagnets. To describe the CW behaviour, often existence of some local moments were postulated. Though justified in the case of strong ferromagnets,

for weakly ferromagnetic systems this is inadequate. Thus, though from theoretical point of view deduction of local moments from Curie constant is questionable, nevertheless the ratio q_c/q_s serves as an useful indicator for the degree of itinerancy. But as cautioned by Wohlfarth[102], this criterion may not be conclusive if the material shows some unusual spin structure (viz. conical, spiral etc.) below T_c. Common examples are Pd-Fe and Pd-Co alloys which show "giant moment" behaviour.

In this connection it seems relevant to add that though CW behaviour does not find explanation from these theories, dynamical "spin-fluctuation" approach by Moriya et al.[109] can very well explain them, though the mechanism is entirely different. Though CW law is common to both the localized and the weakly itinerant systems, the properties of spin fluctuations are entirely different in the two cases. A unified approach in terms of spin-density fluctuations have also been suggested[90] to explain the properties of materials which lie intermediate between the two extremes (localized and weakly itinerant limits) and whose q_c/q_s ratios lie intermediate between the two (1 and ∞).

Thus we may conclude from the above discussions that measurements of paramagnetic susceptibility can serve an useful purpose in determining the itinerant or localized character of magnetism. Our measurements in the ferromagnetic region for two ternary alloy systems showed some indication of behaving like weak itinerant systems. To check this,

paramagnetic susceptibility measurements were carried out for three alloys in the Ni-Fe-Cr system and two in Ni-Fe-V. Since the q_c/q_s criterion can be applied[102] usefully for alloys with T_c < 500K (to satisfy the condition $T_c < T_F$, T_F being the degeneracy temperature), our choice of alloys were limited by this criterion.

Out of the five samples, two of them (one in each ternary series) have T_c below room temperature. For these two, measurements were carried out above room temperature only. This is partly because the other three alloys studied, showed pure paramagnetic behaviour at temperatures much above T_c (only above $(T-T_c) \geq 100K$). So when our interest lies in the paramagnetic region only, measurements below room temperature for the above two samples would have added little to our knowledge. The deviation from pure paramagnetic behaviour, characterized by non-linear relationship between M and H, is probably due to some kind of short range order or some super-paramagnetic clusters present at temperatures well above T_c. Figure 3.11 shows some characteristic M vs. H graphs above T_c.

In Figure 3.12 is shown inverse susceptibility as a function of temperature, measured in a constant field of 5 KOe, for the alloys under discussion. All the alloys show fairly well defined CW behaviour from a temperature high above their respective T_c to the highest temperature of measurements. The slope of the straight line gives inverse of Curie-Weiss constant (1/C) and its intercept on the temperature axis

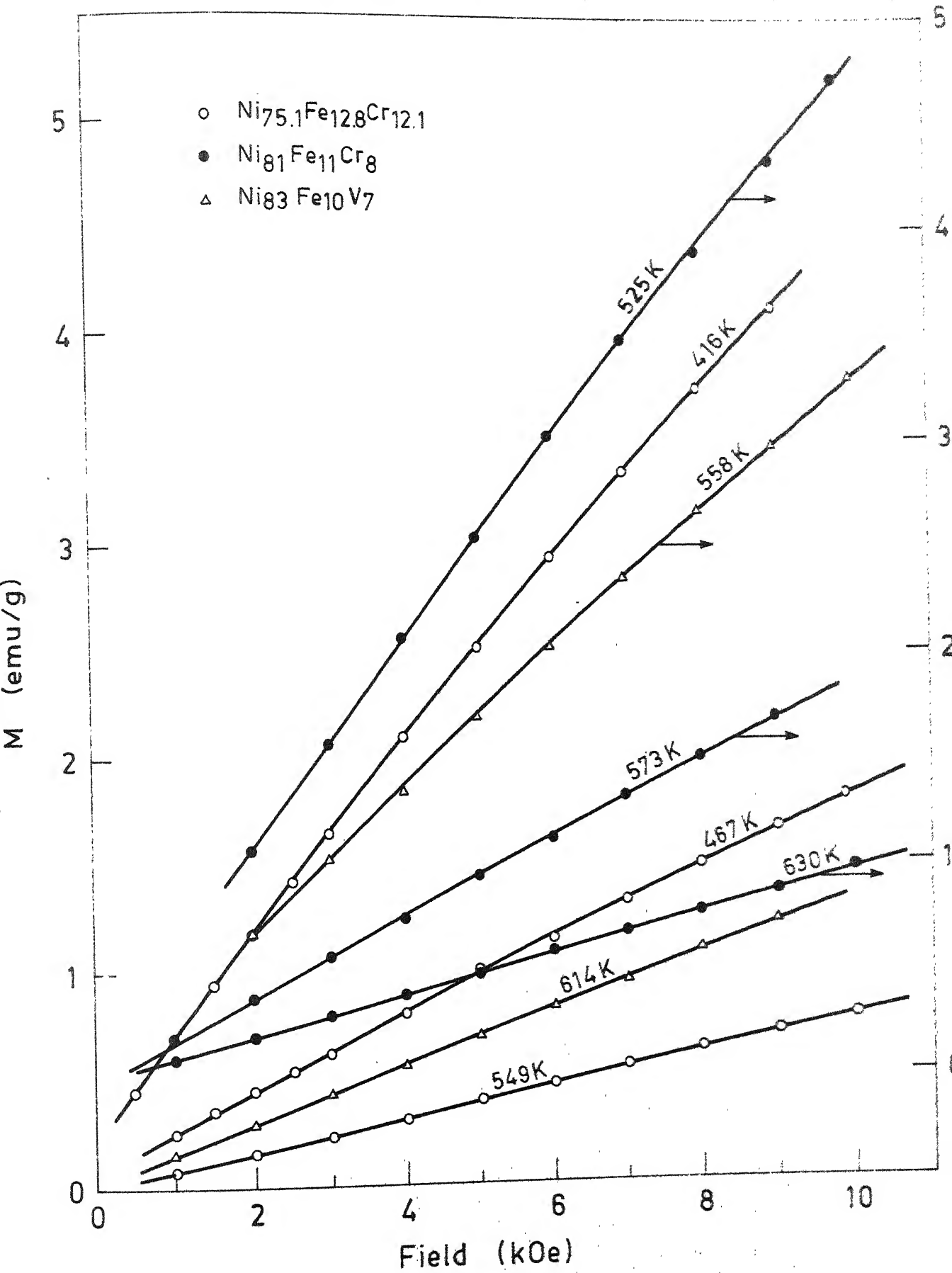
o Ni75.1Fe12.8Cr12.1
● Ni81 Fe11 Cr8
△ Ni83 Fe10 V7
525K
416K
558K
573K
467K
630K
614K
549K
M (emu/g)
Field (kOe)
0
1
2
3
4
5
6
8
10

Fig. 3.11

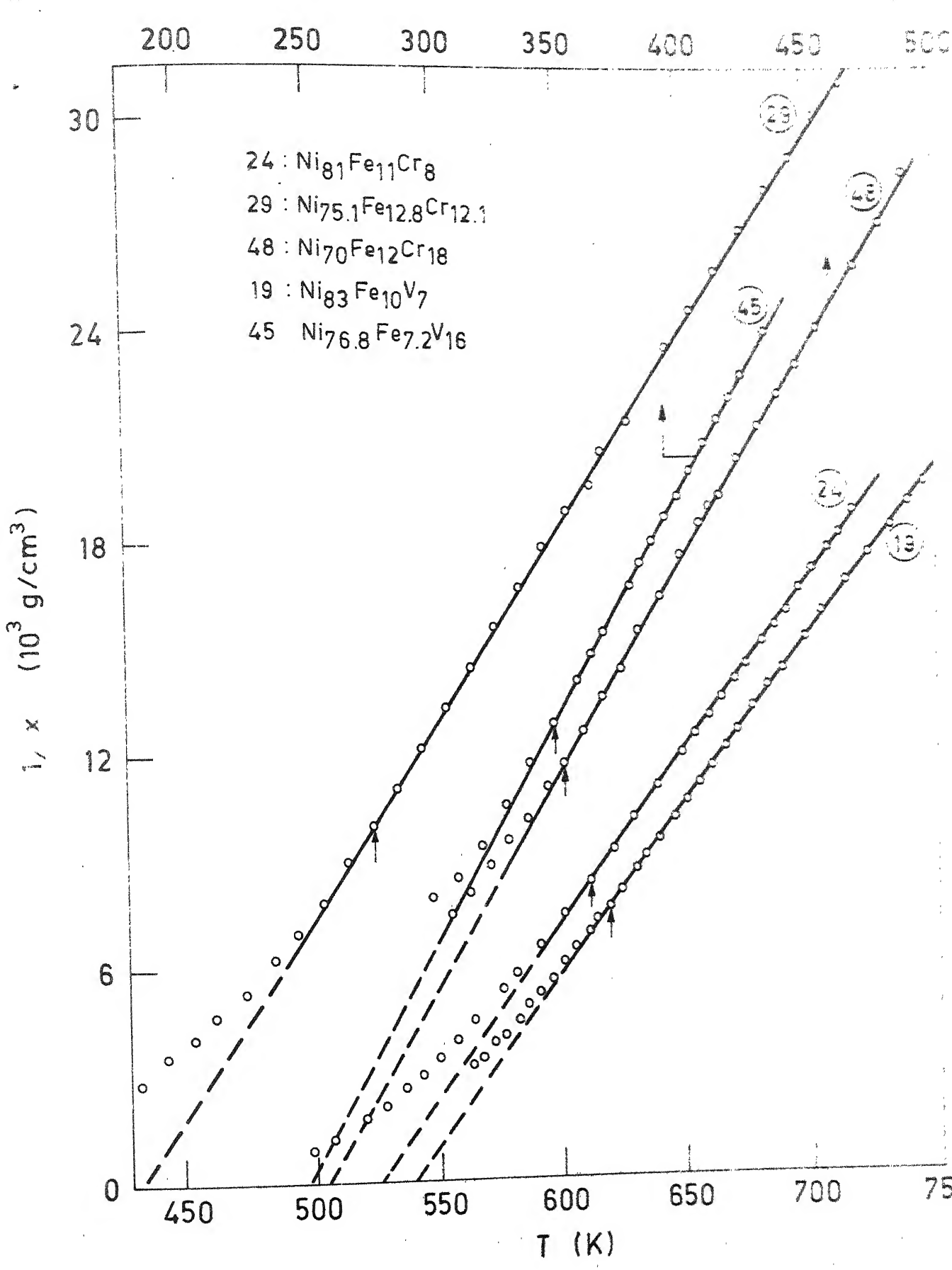
200
250
300
350
400
450
500
30
24
18
12
6
0
24 : Ni81Fe11Cr8
29 : Ni75.1Fe12.8Cr12.1
48 : Ni70Fe12Cr18
19 : Ni83Fe10V7
45 Ni76.8Fe7.2V16
29
48
45
24
19
1
x (10^3 g/cm^3)
450
500
550
600
650
700
T (K)

Fig 3.12

gives θ, the paramagnetic Curie-temperature. The values of q_c, defined by Eqn.(3.16), for the respective alloys were calculated using Eqn.(3.15) and our experimentally determined values of C^{-1}. In Table 3.9 are presented the results of such calculations along with the values of T_c, θ and also T_d, the temperature at which deviation from CW law is observed, for the various alloys under consideration. The values of q_s were taken from Tables 3.6 and 3.7 (actually $q_s = \bar{\mu}$, given in those tables) for sample Nos.24,29 and 19 and the corresponding quantity for sample numbers 45 and 48 were estimated from compositions close to them. For comparison, q_c and q_s values for some typical itinerant weak ferromagnets are also included in the table. It is quite apparent from the table that q_c/q_s indeed show a systematic increase with decreasing T_c i.e. with increasing concentration of Cr/V. The values are also comparable to the literature values of some binary and ternary alloys of different constituents which have T_c close to our alloys. It should also be noted that our q_c/q_s values for Ni-Fe-Cr alloys are nearly the same as those for Ni-Fe-V alloys of comparable T_c. Such experimentally observed systematic behaviour lends strong support to the contention that addition of Cr/V to Ni-Fe alloys drives it more towards itinerant weak ferromagnetism. However, this is in contrast to the case of binary Ni-Fe alloys, which show strong itinerant behaviour in the Ni-rich region and weak in the Invar region[78].

Table 3.9 : Values of T_c, θ, T_d, q_c and q_s for some Ni-Fe-Cr/V Alloys

Sample Number	Alloy Composition (at.%)	T_c (K)	θ (K)	T_d (K)	q_c (μ_B)	q_s (μ_B)	q_c/q_s
24	$Ni_{81}Fe_{11}Cr_8$	470	526	612	1.39	0.55	2.5
29	$Ni_{75.1}Fe_{12.8}Cr_{12.1}$	365	434	524	1.27	0.46	2.8
48	$Ni_{70}Fe_{12}Cr_{18}$	179	255	352	1.19	0.30*	4.0
19	$Ni_{83}Fe_{10}V_7$	486	540	620	1.41	0.56	2.5
45	$Ni_{76.8}Fe_{7.2}V_{16}$	167	248	348	1.14	0.27*	4.2
	+$ZrZn_{1.9}$	26	-	-	0.86	0.16	5.4
	a$(Fe_{0.3}Ni_{0.7})_2B$	307	-	-	1.31	0.50	2.62
	a$(Fe_{0.2}Ni_{0.8})_2B$	105	-	-	0.85	0.24	3.54
↑	b$Fe_{56.5}Cr_{43.5}$	47	60	-	0.957	0.125	7.7
c-phase	b$Fe_{55.1}Cr_{44.9}$	29	53	-	0.788	0.096	8.2
↓	b$Fe_{55.5}V_{44.5}$	160	165	-	1.139	0.222	5.1

* Estimated values from Table 3.7 and Reference (61)

\+ Reference (110)

a Reference (111)

b Reference (112)

One striking feature for all the alloys is the large difference between paramagnetic and ferromagnetic Curie temperatures, θ and T_c. It can be also seen from Table 3.9 that the difference ($\theta - T_c$) increases with increasing concentration of Cr/V. Such large differences have also been observed in Cr-rich Fe-Cr alloys (see table). Similarly the temperature from which the deviation from Curie-Weiss behaviour starts (T_d), also increases with increasing Cr/V concentration. This behaviour was also reflected in the M vs. H isotherms above T_c, as discussed earlier. For all the alloys T_d was found to be close to the temperatures where M vs H isotherms show perfect linearity. So one could attribute this to the presence of some kind of short range ordering up to temperatures close to T_d. But it is amazing to think how any kind of short range order could remain up to such a high temperature, which is about 2 T_c for sample numbers 45 and 48! No straight-forward explanation could be offered for this observation at present.

Materials with weak itinerant character (large q_c/q_s) should also show a host of other properties, viz. their Arrott plots should be a set of parallel straight lines over a wide range of temperature[102]. The Arrott plots are the M^2 vs. H/M isotherms which are found to be straight lines (except for some deviations in the low-field region) for all ferromagnets near T_c. This kind of relationship comes directly from the Landau theory of phase transitions when the free energy is expressed in powers of magnetization[96]

in the limit of $M(T)/M(0) \ll 1$ near T_c. But the slope of such plots are temperature dependent. On the other hand, Edwards and Wohlfarth[106] have shown that in the limit of very weak ferromagnetism ($\zeta_o \ll 1$, where ζ_o is the relative magnetization of spin-up and spin-down electrons),

$$\left\{\frac{M(H,T)}{M(0,0)}\right\}^2 = \left\{1 - \left(\frac{T}{T_c}\right)^2\right\} + \frac{2\chi_o H}{M(H,T)} \qquad (3.20)$$

Hence the Arrott plots at all temperatures below T_F ($T_c \ll T_F$ for weak systems) should be a set of parallel straight lines with slopes equal to $2\chi_o \{M(0,0)^2\}$.

Figures 3.13 and 3.14 show the Arrott plots over a wide temperature range for two Ni-Fe-Cr alloys and one Ni-Fe-V alloy, for which the susceptibility were measured. Except for the deviation at low fields, which is naturally expected due to domain orientation and some possible spatial inhomogeneity in the sample, the plots appear as fairly good straight lines. However, because of the limited field range available, the number of data points in the linear part, specially at lower temperatures, are small. But at higher temperatures the linearity of such plots have been established without any ambiguity. On the other hand, the slopes are definitely not temperature independent. But then, even in $ZrZn_2$, which is thought to be near an ideally weak ferromagnet, the slopes of Arrott plots show considerable temperature dependence; lately, terms higher than M^3 were included in Eqn.(3.20) to give a better agreement[113]. So in our case, the temperature

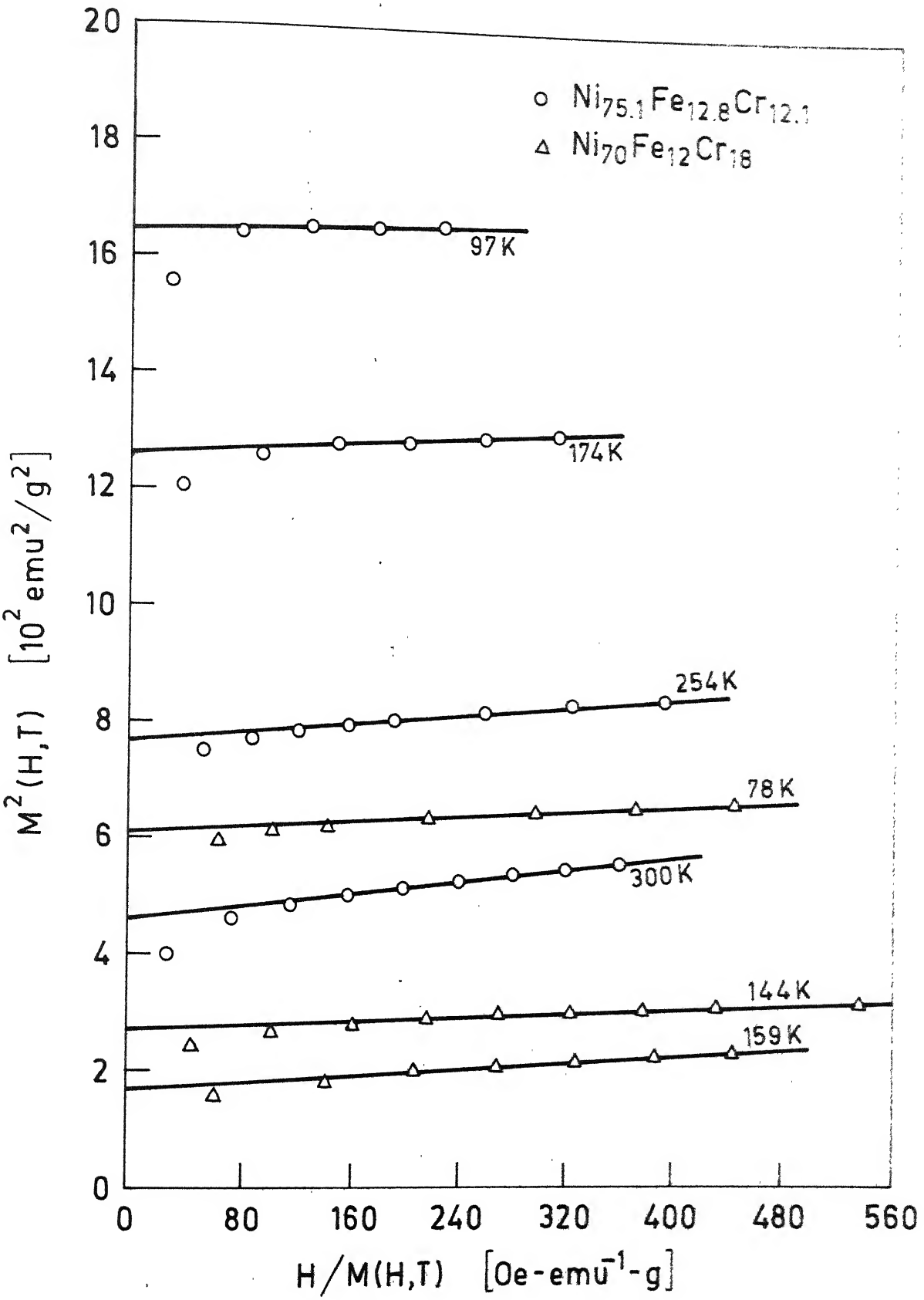
o Ni75.1Fe12.8Cr12.1
Δ Ni70Fe12Cr18
97K
174K
254K
78K
300K
144K
159K
M²(H,T) [10² emu²/g²]
H/M(H,T) [Oe-emu⁻¹-g]
0
2
4
6
8
10
12
14
16
18
20
0
80
160
240
320
400
480
560

Fig. 3.13

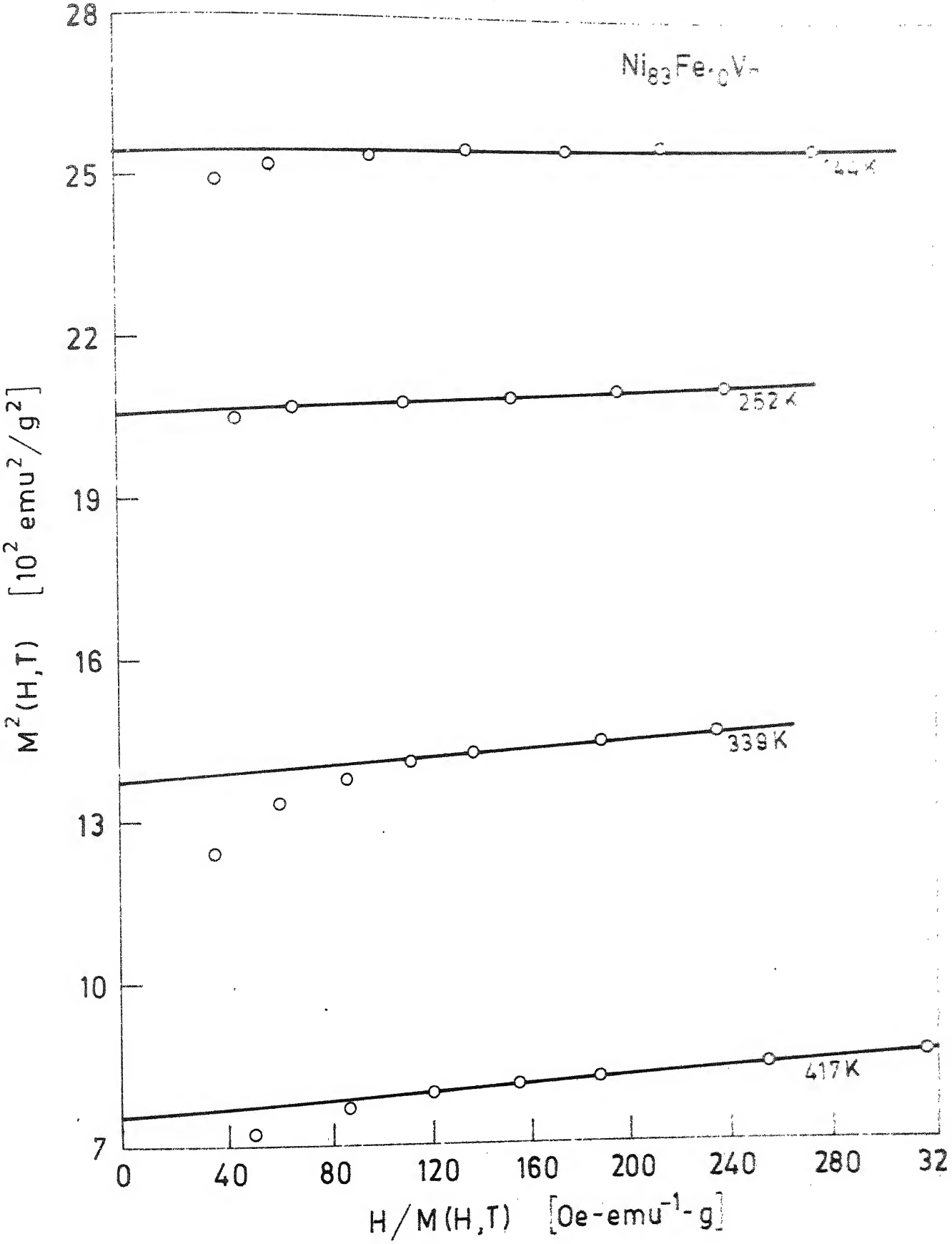
Ni83Fe7V10
252 K
339 K
417 K
M²(H,T) [10² emu²/g²]
H/M(H,T) [Oe-emu⁻¹-g]
28
25
22
19
16
13
10
7
0
40
80
120
160
200
240
280
32

Fig. 3.14

dependence of the slope is not altogether unexpected since by any consideration, these alloys cannot be considered to be perfectly weak ferromagnets. Such behaviour has also been observed in Ni-Pt[114] and in Fe-Ni[115] Invar alloys. Finally, though the slopes of Arrott plots appear as temperature dependent, the linear behaviour over a wide temperature range definitely suggest that the alloy systems under consideration behave very much similar to itinerant weak ferromagnets.

It was also pointed out by Wohlfarth[102,116] that in an itinerant weak system T_c, $\sigma(0,0)$, spin wave stiffness constant (D_o), etc. should have a common relationship with the exchange energy and hence composition, i.e.,

$$T_c^2 \sim M(0,0)^2 \sim D_o^2 \sim |C - C_o| \qquad (3.21)$$

where C_o is the critical concentration for which ferromagnetism disappears. In the case of the two ternary alloy systems under investigation, a meaningful comparison of the above mentioned quantities can be only through the concentration of Cr/V in a series of alloys with fixed Fe content. This is because, addition of Fe increases the magnitude of those quantities whereas a decrease is observed with Cr or V. Since in the present study we had very few alloys with the same Fe content but increasing Cr/V concentration, such kind of analysis was not possible. But even then, we recall that the rate of change of D_o, T_c, $\bar{\mu}$, e^2 etc. with concentration were less for the alloys with higher Cr/V content. But for the

alloys with lower Cr/V, they decreased almost linearly with concentration. So there is additional evidence in the light of Eqn.(3.21) that the alloys with higher Cr/V behave more like itinerant weak ferromagnets.

Chapter IV

Transport Properties

In this chapter we present mainly the results of extra-ordinary Hall co-efficient (R_s) as a function of composition for the two systems, Ni-Fe-Cr/V, measured at room temperature and at 77 K. Main emphasis was on studying the change of sign of R_s and thereby establishing the $R_s = 0$ line for the two ternary alloy systems. An attempt has also been made to explain the residual resistivity of these alloys in terms of the "two-current" model.

4.1 Change of Sign of the Extra-ordinary Hall Co-efficient in Ni-Fe-Cr Alloys

As has been already discussed in Chapter I, according to the S.B. model due to Berger[29], the extra-ordinary Hall co-coefficient R_s of ternary Ni-Fe-Me (Me = Ti, V, Cr, Mo, W, etc.) alloys should change sign when the Fermi level crosses the boundary between the Ni and Fe spin-down bands, and hence the line should follow Eqn.(1.8). Guided by this information, along with the already existing experimental data for $\lambda_s \sim 0$ line for Ni-Fe-Cr alloys[55], about fifteen alloys for this ternary system were prepared and the extra-ordinary Hall co-efficient was measured at room temperature and at 77K. Data for $R_s M_s$, resistivity ρ, and extra-ordinary Hall conductivity $\gamma_{HS} = \frac{R_s M_s}{\rho^2}$ are presented in Table 4.1. The values given, are the averages over several measurements of the same piece of a given sample and where necessary on different pieces of the same sample.

Reproduc ibility in R_sM_s was within about 2% and the total error in R_sM_s was estimated to be about 4%. The actual sign of R_sM_s was determined with respect to pure Ni, whose extra-ordinary Hall co-efficient is negative. As has been pointed out by Berger[24], since in concentrated alloys "side-jump" mechanism is more important (implying $R_s \propto \rho^2$), it is more meaningful to talk in terms of the extra-ordinary Hall conductivity γ_{HS} rather that R_s, since γ_{HS} is almost temperature independent except for a weak dependence through M_s. Accordingly, γ_{HS} is a better parameter when a comparison is necessary among various compositions. The error in resistivity mostly comes from dimension measurements, of which the smallest quantity, i.e. the thickness contributes the maximum. In most of the cases the total error in ρ was of the order of 3%. On the other hand γ_{HS}, being a function of ρ^2, inherits maximum uncertainty through ρ ; the typical error bar in γ_{HS} was about 10%. It can be seen from the table that out of the fifteen alloys studied, seven have positive Hall conductivity. For some of the alloys, the values of γ_{HS} are slightly different from the results presented[117] at the initial stages of this investigation. The results for sample number 9 and 24, within experimental uncertainty, are in agreement with the data of Sinha and Majumdar[118]. For sample number 50, since the temperature of measurement was very close to T_c, except for the sign, not much significance should be attached on its absolute value of γ_{HS}.

Sample No.	Composition of Ni-Fe-Cr alloys (at.%)	T_c (K)	ρ (10^{-7} Ω m)		R_sM_s (10^{-9} Ω m)		γ_{HS} (10^{3} $\Omega^{-1}m^{-1}$)	
			77K	300K	77K	300K	77K	300K
42	78-6-16	185±5	8.4±0.4	8.8±0.4	-(0.71±0.03)	0	-(10±1.0)	0
50	72-8-20	93±3	10.7±0.3	11.1±0.3	+ 0.02	0	+ 0.02	0
9	85.5-11-3.5	620±3	5.2±0.15	5.8±0.15	-(6.6±0.2)	-(5.6±0.15)	-(24.4±2)	-(16.6±1.5)
24	81-11-8	470±4	8.8±0.25	9.3±0.3	-(8.0±0.3)	-(4.6±0.2)	-(10.3±0.8)	-(5.3±0.5)
40	73.5-11.5-15	260±5	10.3±0.4	10.7±0.4	-(2.9±0.1)	0	-(2.7±0.3)	0
29	75.1-12.8-12.1	365±3	9.3±0.2	9.8±0.2	-(3.6±0.1)	-(1.20±0.05)	-(4.2±0.3)	-(1.25±0.1)
48	70-12-18	179±2	10.6±0.3	11.0±0.3	+(1.10±0.05)	0	+(1.05±0.1)	0
34	72.5-13.7-13.8	315±7	9.9±0.2	10.2±0.2	-(0.72±0.02)	-0.01	-(0.73±0.05)	-0.01
26	80-16-4	693±3	6.3±0.3	6.9±0.3	-(1.50±0.05)	-(0.73±0.05)	-(3.8±0.3)	-(1.5±0.15)
28	75-17-8	543±3	7.7±0.2	8.3±0.2	-(1.90±0.08)	-(0.84±0.04)	-(3.2±0.3)	-(1.20±0.1)
33	68.1-17.4-14.5	320±6	10.4±0.5	10.8±0.5	+(2.7±0.1)	+(1.25±0.05)	+(2.5+0.2)	+(1.03±0.1)
35	76.8-21.2-2	778±4	4.3±0.1	5.3±0.1	+(0.90±0.04)	+(1.40+0.03)	+(4.9±0.4)	+(5.0±0.3)
27	75.5-20.3-4.2	717±3	6.1±0.2	7.0±0.2	+(1.54±0.04)	+(2.5±0.07)	+(4.1±0.4)	+(5.1±0.4)
51	67-21-12	470±2	10.4±0.3	11.0±0.3	+(5.9±0.1)	+(5.1±0.1)	+(5.4±0.4)	+(4.2±0.3)
32	69.6-22.8-7.6	635±5	9.0±0.15	9.6±0.15	+(4.9±0.1)	+(5.4±0.1)	+(6.0±0.3)	+(5.8±0.3)

Using the positive and negative values of γ_{HS} at 77K one can easily draw the $\gamma_{HS} \simeq 0$ line in the ternary phase diagram of this system. Figure 4.1 shows such a diagram along with the already existing zero line for the linear co-efficient of magnetostriction ($\lambda_S \simeq 0$)[55] and the one predicted from the S.B. model (Eqn.(1.8)). The numbers associated with the solid circles represent the sample numbers as given in Table 4.1 and those in the brackets represent γ_{HS}($\times 10^{-3}$ $\Omega^{-1}m^{-1}$) values at 77K with appropriate signs. The experimental $\gamma_{HS} \simeq 0$ line in the regions of low Fe concentration (<5 at.%), shown by dotted line, has been drawn by mere extrapolation and hence is a little uncertain. The alloys in this concentration range, which are expected to show a change in sign, have T_c below 77K and thus beyond the reach of our present experimental facility. From the nature of our $\gamma_{HS} \simeq 0$ line, it appears that in binary Ni-Cr alloys a sign change in γ_{HS} cannot be observed since ferromagnetism is destroyed before such a composition is reached. This is also consistent with the literature[94], where no such sign change have been reported so far. The main points those emerge from Figure 4.1, are the following:

i) The experimental $\gamma_{HS} \simeq 0$ line definitely lies much below the theoretical line and essentially in disagreement with Berger's model. The experimental $\lambda_S \simeq 0$ line is also at variance with the theoretical line, but to a lesser extent.

ii) The deviation from the S.B. model is more pronounced in the Cr-rich region, implying that the presence of

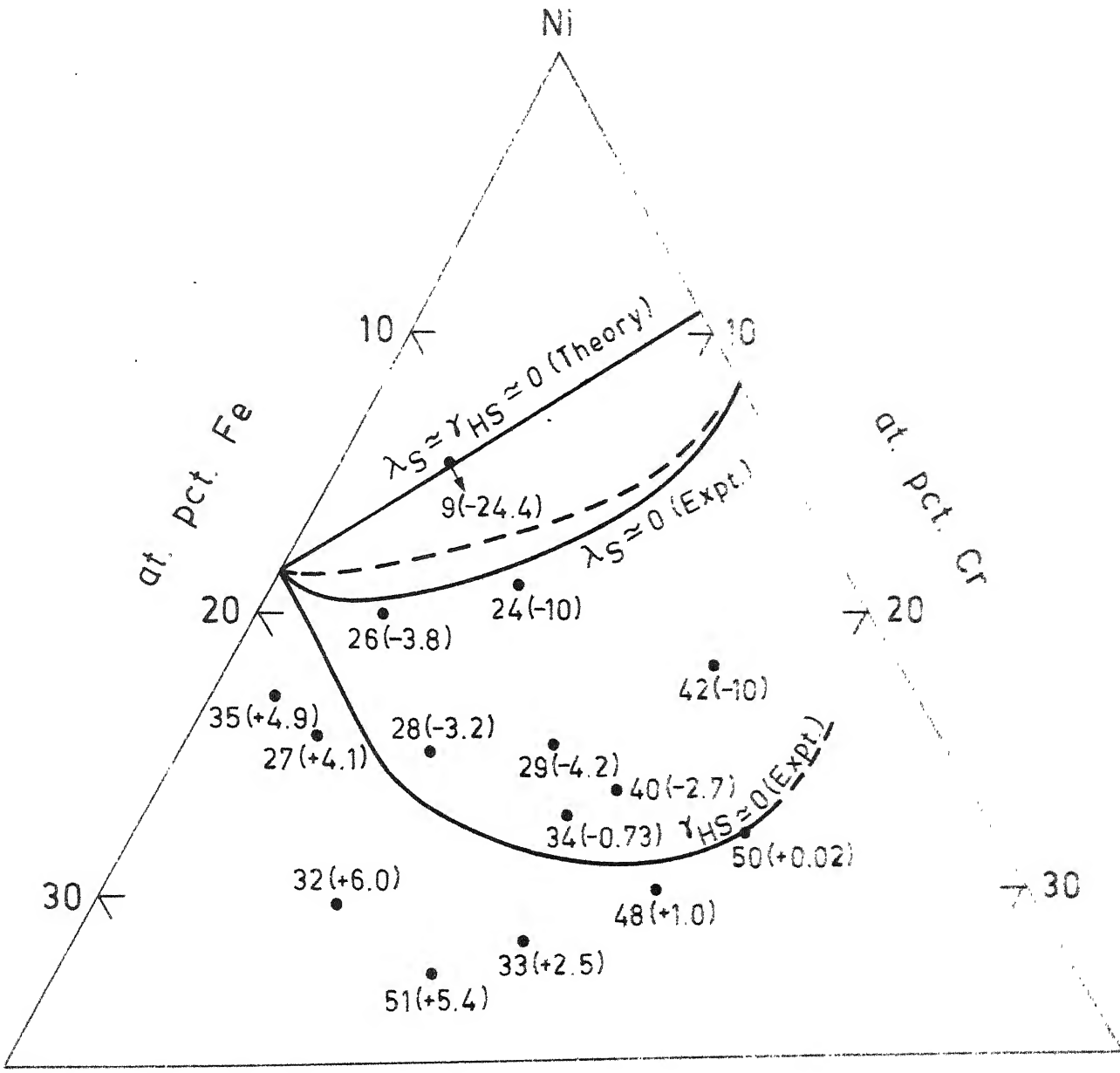

Fig. 4.1. Ternary phase diagram for Ni-Fe-Cr alloys

Cr is the cause of disagreement with a model which has been so far found to be useful in several binary and ternary alloys.

iii) Both the experimental $\gamma_{HS} \simeq 0$ and $\lambda_s \simeq 0$ lines show considerable curvature in contrary to the straight line behaviours expected from the simple S.B. model.

iv) λ_s and γ_{HS} are expected to change sign simultaneously. But in this case as one approaches the zero line from the Ni-rich side, λ_s changes sign long before γ_{HS}. Thus if a γ_{HS} vs. λ_s plot is made, the curve should have a negeative intercept on the γ_{HS}-axis. This is in contrast with the other crystalline binary and ternary systems[29] as well as some amorphous systems[48] where the intercept is positive.

In search of a plausible explanation for the deviation of our experimental results from those expected from the S.B. model, it was natural to reflect on the saturation magnetization data at OK (Section 3.3.1), since basically both the phenomena are related to band-filling. Magnetization results have clearly shown that the actual number of electrons added by the addition of Cr atoms $(Z)_{eff.}$, is far from the ideal value of (10+Z) and instead of being a constant, is itself a function of composition. As discussed earlier (Section 3.3.1), $(Z)_{eff.}$ have been found to be decreasing with increasing concentration of Cr for a series of alloys with approximately the same Fe content.

Cr is the cause of disagreement with a model which has been so far found to be useful in several binary and ternary alloys.

iii) Both the experimental $\gamma_{HS} \simeq 0$ and $\lambda_s \simeq 0$ lines show considerable curvature in contrary to the straight line behaviours expected from the simple S.B. model.

iv) λ_s and γ_{HS} are expected to change sign simultaneously. But in this case as one approaches the zero line from the Ni-rich side, λ_s changes sign long before γ_{HS}. Thus if a γ_{HS} vs. λ_s plot is made, the curve should have a negeative intercept on the γ_{HS}-axis. This is in contrast with the other crystalline binary and ternary systems[29] as well as some amorphous systems[48] where the intercept is positive.

In search of a plausible explanation for the deviation of our experimental results from those expected from the S.B. model, it was natural to reflect on the saturation magnetization data at OK (Section 3.3.1), since basically both the phenomena are related to band-filling. Magnetization results have clearly shown that the actual number of electrons added by the addition of Cr atoms $(Z)_{eff.}$, is far from the ideal value of (10+Z) and instead of being a constant, is itself a function of composition. As discussed earlier (Section 3.3.1), $(Z)_{eff.}$ have been found to be decreasing with increasing concentration of Cr for a series of alloys with approximately the same Fe content.

To check whether this could be a reason for the deviation of our $(\gamma_{HS})_{exp.} \simeq 0$ line from the one predicted by the S.B. model, what was done is the following. A few alloy compositions in the ternary diagram near the experimental $\lambda_s \simeq 0$ line were selected and the corresponding experimental values of $\bar{\mu}$ were obtained from the data of Menshikov et al.[61]. The $(Z)_{eff.}$ values for these alloys were estimated by using Eqn.(3.13). Now in turn, the new values of $(Z)_{eff.}$ were substituted in Eqn.(1.8) in place of (10+Z) and then the compositions for which a sign change in λ_s and γ_{HS} are expected (according to Eqn.(1.8)), were estimated. Eqn.(1.8), thus modified, predicts a curve shown dotted in Figure 4.1. In Table 4.2 are shown the data used for such analysis. The reason for such cumbersome analysis is the compositional dependence of $(Z)_{eff.}$.

The important outcome of this analysis is that when the non-linearity in $\bar{\mu}$ vs. concentration curves is empirically incorporated into Eqn.(1.8), theoretical line comes much closer to the experimental $\lambda_s \simeq 0$ line and essentially reproduces its curvature. But still it lies for away from the experimental $\gamma_{HS} \simeq 0$ line. From this one could safely conclude that the curvatures of experimental $\lambda_s \simeq 0$ line and possibly also that of $\gamma_{HS} \simeq 0$ line are the off-shoot of the non-oinearity in the $\bar{\mu}$ vs. C curves. In this context, it is also important to point out that for those systems, where S.B. model could account for the sign change of γ_{HS} and λ_s, saturation magnetization is a linear function of concentration.

Table 4.2 : Results of re-analysis of $(\lambda_s)_{exp.} \simeq 0$ data for Ni-Fe-Cr alloys in terms of the S.B. model, modified to incorporate the compositional dependence of $(Z)_{eff.}$

Ni-Fe-Cr alloy compositions (at%) at which $(\lambda_s)_{exp.} \simeq 0$	$(\bar{\mu})^*_{exp.}$ (units of μ_B)	$(Z)_{eff.}$	Ni-Fe-Cr compositions (at.%) for which λ_s and γ_{HS} should change sign according to modified Eqn.(1.8)
85.7-2-12.3	0.13	4.2	86.3-2-11.7
83.5-5-11.5	0.26	3.9	84.7-5-10.3
81.8-8-10.2	0.39	3.7	83.6-8-8.4
81-10-9	0.47	3.8	83.4-10-6.6
80.4-12-7.6	0.57	3.7	82.9-12-5.1
80-14-6	0.70	3.2	81.9-14-4.1
80-16-4	0.81	3.0	81.7-16-2.3
80.5-18-1.5	0.92	3.3	81.7-18-0.3

*Estimated from Reference (61).

Thus it appears that though the S.B. model can explain the position of the $(\lambda_s)_{exp.} \simeq 0$ line fairly well, it cannot do so for the $\gamma_{HS} \simeq 0$ line. The disagreement between the S.B. model and the experimental $\gamma_{HS} \simeq 0$ line, then essentially boils down to the disagreement between the experimental λ_s and $\gamma_{HS} \simeq 0$ lines.

4.2 Change of Sign of the Extra-ordinary Hall Co-efficient in Ni-Fe-V alloys

In Table 4.3 are given the values of ρ, $R_s M_s$ and γ_{HS} for twelve alloys of ternary Ni-Fe-V system, measured at 77K and room temperature. As in the case of Ni-Fe-Cr system, prior information about the position of $\lambda_s \simeq 0$ line[56] helped us in choosing the composition ranges where a sign change in $R_s M_s$ (or γ_{HS}) might be expected. Out of the twelve alloys studied, seven of them were found to be having a positive extra-ordinary Hall co-efficient. The absolute value of γ_{HS} for alloy number 49 is a bit uncertain since the temperature of measurement was very close to its T_c. Using the values of γ_{HS} at 77K for the various alloys, the experimental $\gamma_{HS} \simeq 0$ line was drawn by linear extrapolation and is shown in Figure 4.2. Also shown are the already established $\lambda_s \simeq 0$ line and the straight line predicted by the S.B. model for the sign change of γ_{HS} and λ_s. It is quite apparent that for Ni-Fe-V alloys the behaviour of all the lines ($\gamma_{HS}, \lambda_s \simeq 0$, etc.) are essentially similar to those of Ni-Fe-Cr alloys and all the observations (i to iv) made in Section 4.1 in connection with the experimental and

Table 4.3 : ρ, R_sM_s and γ_{HS} at 77 and 300K for some Ni-Fe-V Alloys

Sample No.	Compositions (at.%) for Ni-Fe-Alloys	T_c (K)	ρ (10^{-7} Ωm)		R_sM_s (10^{-9} Ωm)		γ_{HS} (10^3 $\Omega^{-1}m^{-1}$)	
			77K	300K	77K	300K	77K	300K
49	78-4-18	90±4	13.2±0.3	13.4±0 3	+(0.1±0.01)	0	+0.06	0
46	82.5-7.5-10	362±3	8.2±0.15	8.8±0.15	-(5.0±0.1)	-(2.3±0.05)	-(7.4±0.5)	-(3.0±0.2)
45	76.8-7.2-16	167±5	12.2±0.2	12.3±0.2	+(2.1±0.05)	0	+(1.4±0.07)	0
19	83-10-7	486±2	8.1±0.2	9.0±0.2	-(2.5±0.1)	-(1.20±0.04)	-(3.8±0.3)	-(1.5±0.1)
20	80.5-10.5-9	417±3	10.5±0.3	10.7±0.3	-(0.87±0.03)	-0.03	-(0.80±0.08)	-0.03
18	85-11-4	609±5	5.4±0.2	6.3±0.2	-(3.3±0.1)	-(3.1±0.1)	-(11.2±1)	-(7.8±0.8)
39	77.4-11.9-10.7	393±1	9.8±0.2	10.6±0.2	+(0.75±0.03)	+(1.09±0.03)	+(0.78±0.06)	+(0.97±0.07)
37	80.9-14-5.1	640±4	6.7±0.2	7.4±0.2	-(0.72±0.03)	-(0.06±0.01)	-(1.6±0.2)	-(0.11±0.02)
38	76.5-14-9.5	462±1	9.3±0.3	10.1±0.3	+(3.1±0.1)	+(3.3±0.1)	+(3.6±0.3)	+(3.2±0.3)
36	81-17-2	746±3	3.4±0.1	4.4±0.1	+(0.53±0.02)	+(0.82±0.03)	+(4.6±0.4)	+(4.2±0.4)
30	79.4-17-3.6	691±2	4.9±0.15	6.0±0.2	+(0.77±0.02)	+(1.30±0.03)	+(3.2±0.3)	+(3.6±0.3)
31	74-22-4	741±3	5.8±0.2	7.1±0.3	+(2.2±0.05)	+(3.2±0.1)	+(6.5±0.6)	+(6.3±0.6)

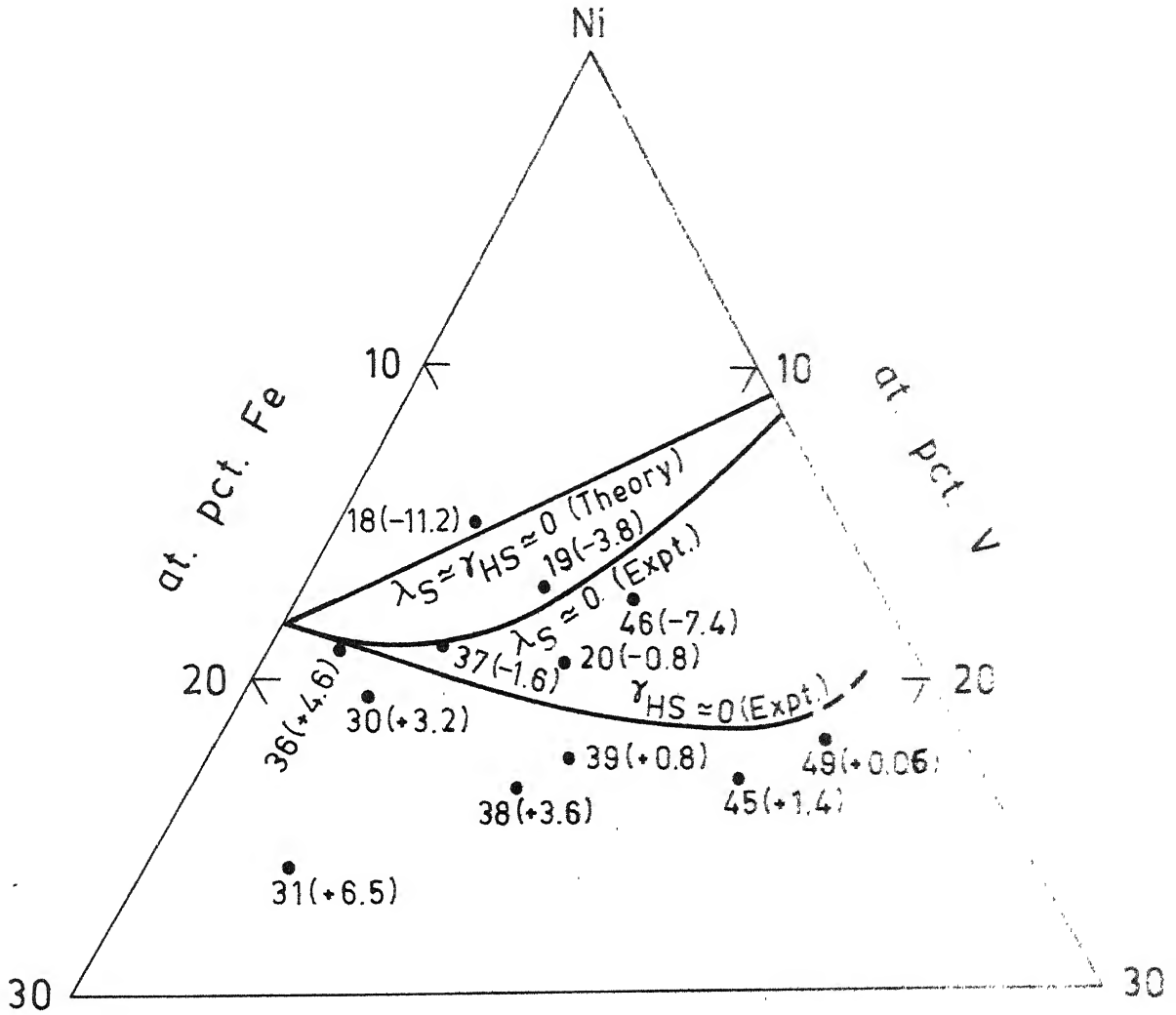

Fig. 4.2. Ternary phase diagram for Ni-Fe-V alloys.

theoretical lines for γ_{HS} and λ_s for Ni-Fe-Cr are equally valid for Ni-Fe-V alloys; differences, if any, are merely quantitative. Contrary to the Ni-Fe-Cr system, the experimental $\lambda_s \simeq 0$ and $\gamma_{HS} \simeq 0$ lines are almost coincident in the Fe-rich region of this ternary diagram. However, deviations from the S.B. model as also from the experimental $\lambda_s \simeq 0$ line become more as V-concentration is increased. But the quantitative deviation from the S.B. model for this system is much less than that for Ni-Fe-Cr alloys. This can be expected if one remembers that vanadium is one more step away from Ni than Cr in the periodic table and hence band splitting should be more complete in the former than in the latter. It also appears that in binary Ni-V, as in Ni-Cr, sign change in γ_{HS} cannot be observed experimentally since ferromagnetism is destroyed before such a composition is reached. This is consistent with the literature data[94] where no sign change has been observed.

As discussed in Section 3.3.2, $\bar{\mu}$ vs. C curves show considerable non-linearity in Ni-Fe-V alloys also and $(Z)_{eff.}$ has been found to be concentration dependent, having a value much less than the ideal value of 5. However, it could not be checked whether this non-linearity could be a possible reason for the curvature of the λ_s and $\gamma_{HS} \simeq 0$ lines as we do not have enough magnetization data ($\bar{\mu}$) available. But even with the few available data, it appears that $(Z)_{eff.}$ for this system also have the same kind of compositional dependence as in Ni-Fe-Cr and hence could possibly account for the curvature of the λ_s and $\gamma_{HS} \simeq 0$ lines.

Thus it appears that the S.B. model can fairly well explain the position of the $\lambda_s \simeq 0$ line for both the ternary (Cr/V) systems. The apparent discrepancy between the theoretically predicted and experimentally observed lines seems to be due to the non-linear concentration dependence of saturation magnetization. Because, this apparent discrepancy, at least in the case of Ni-Fe-Cr alloys, is removed to a large extent when the above mentioned non-linearity is empirically incorporated into the S.B, model. However, the S.B. model fails to justify the position of the experimental $\gamma_{HS} \simeq 0$ line simply because γ_{HS} and λ_s do not change sign simultaneously, contrary to expectation. The ternary systems studied so far (Ni-Fe-Cu/Cr/V), have all shown that experimental $\lambda_s \simeq 0$ line is always in better agreement with the S.B. model than the $\gamma_{HS} \simeq 0$ line. This point will be further elaborated in the next section.

4.3 Relationship between λ_s and γ_{HS}

Due to their common origin in S.O. coupling, λ_s and γ_{HS} have been found to bear a common relationship in the case of various binary systems like Ni-Fe, Cu-Ni, and also in ternary Ni-Fe-Cu system[29] and even in Fe-Ni-B metallic

glasses[48], as has been already discussed in Section 1.2.2. In all the crystalline materials mentioned earlier, approximately a constant ratio of $\approx 2\times10^{9}\,\Omega^{-1}m^{-1}$ have been found for γ_{HS}/λ_s; in glassy systemsthe ratio being slightly lower.

On the basis of the above results, it was natural to check whether any such relationship at all exists between γ_{HS} and λ_s for these two ternary systems, specially when the ternary diagrams in Figures 4.1 and 4.2 show a large separation between the experimental $\lambda_s \simeq 0$ and $\gamma_{HS} \simeq 0$ lines. The problems encountered in such an analysis are the following. The earlier data on linear magnetostriction are mainly confined near the region of $\lambda_s \simeq 0$ line and the corresponding data for γ_{HS} are absent. On the other hand, λ_s values corresponding to most of the alloys we have studied, do not exist in the literature. Also the earlier data of λ_s were mainly confined to single crystals. Fortunately λ_s for some of our alloys in both the ternary systems have been recently measured by Majumdar and Greenough[119]. Using their data along with a few already existing in the literature[120], a γ_{HS} vs. λ_s plot was made as shown in Figure 4.3. In Table 4.4 are presented the data used for such an analysis. γ_{HS} data for two alloys were taken from Sinha and Majumdar[118] and the rest were measured by us. Except for one alloy ($Ni_{85.5}Fe_{11}Cr_{3.5}$)[120], all the other values of λ_s were taken from Majumdar and Greenough[119], measured on the same polycrystalline samples on which γ_{HS} were measured by us. This makes the comparison of γ_{HS} and λ_s more meaningful. Since all the

Table 4.4 : Data for λ_s and γ_{HS} for some Ni-Fe-Cr and Ni-Fe-V alloys

Compositions (at.%)	γ_{HS} (10^3 $\Omega^{-1}m^{-1}$) at 77K	λ_s (10^{-6}) at 77K
Ni_{84}-Fe_6-Cr_{10}	-12.0[a]	-1.6[b]
$Ni_{85.5}$-Fe_{11}-$Cr_{3.5}$	-24.4	-6.0[c]
Ni_{83}-Fe_{11}-Cr_6	-14[a]	-2.5[b]
Ni_{81}-Fe_{11}-Cr_8	-10.3	-0.75[b]
Ni_{80}-Fe_{16}-Cr_4	-3.8	+0.6[b]
Ni_{85}-Fe_{11}-V_4	-11.2	-4.4[b]
Ni_{83}-Fe_{10}-V_7	-3.8	+0.75[b]
$Ni_{80.5}$-$Fe_{10.5}$-V_9	-0.8	+1.7[b]
$Ni_{80.9}$-Fe_{14}-$V_{5.1}$	-1.6	+0.4[b]
$Ni_{79.4}$-Fe_{17}-$V_{3.6}$	+3.2	+3.0[b]

a Reference (118)

b Reference (119)

c Reference (120)

alloys have fairly high resistivity (dominated by impurity scattering), the relationship $R_s M_s \propto \rho^2$ is expected to hold good even at low temperatures. Because of this and the lower T_c of some of the alloys, 77K data were taken for any such comparison.

In Figure 4.3 the straight line drawn using the open circles is for the Ni-Fe-V alloys and the one with solid circles is for the Ni-Fe-Cr alloys. The dot-dashed line is for Ni-Fe alloys[52,53,46] which has been included for comparison. Though the number of points is not sufficient, it appears that a rough straight line can be drawn for both the systems. However, for Ni-Fe-V alloys, one point (corresponding to $Ni_{83}Fe_{10}V_7$) lies away from the straight line. This deviation is unlikely to be an off-shoot of experimental error. No comment can be made on it at present, except for the fact that in Ni-Fe-Cu[29] system also all the points do not fall on the same straight line but form two separate branches. The main points that can be made from Figure 4.3 are the following:

i) γ_{HS} seems to be proportional to λ_s for both the ternary systems; the ratio γ_{HS}/λ_s is about $2.8\times10^{9}\,\Omega^{-1}m^{-1}$ for Ni-Fe-Cr and $1.8\times10^{9}\,\Omega^{-1}m^{-1}$ for Ni-Fe-V. This is comparable to the value of $2\times10^{9}\,\Omega^{-1}m^{-1}$ for Ni-Fe and other systems. At the same breath it is also pointed out that the value of the slope for Ni-Fe-Cr alloys should be taken cautiously since the diagram is incomplete in the absence of any data for λ_s in the region of positive γ_{HS}.

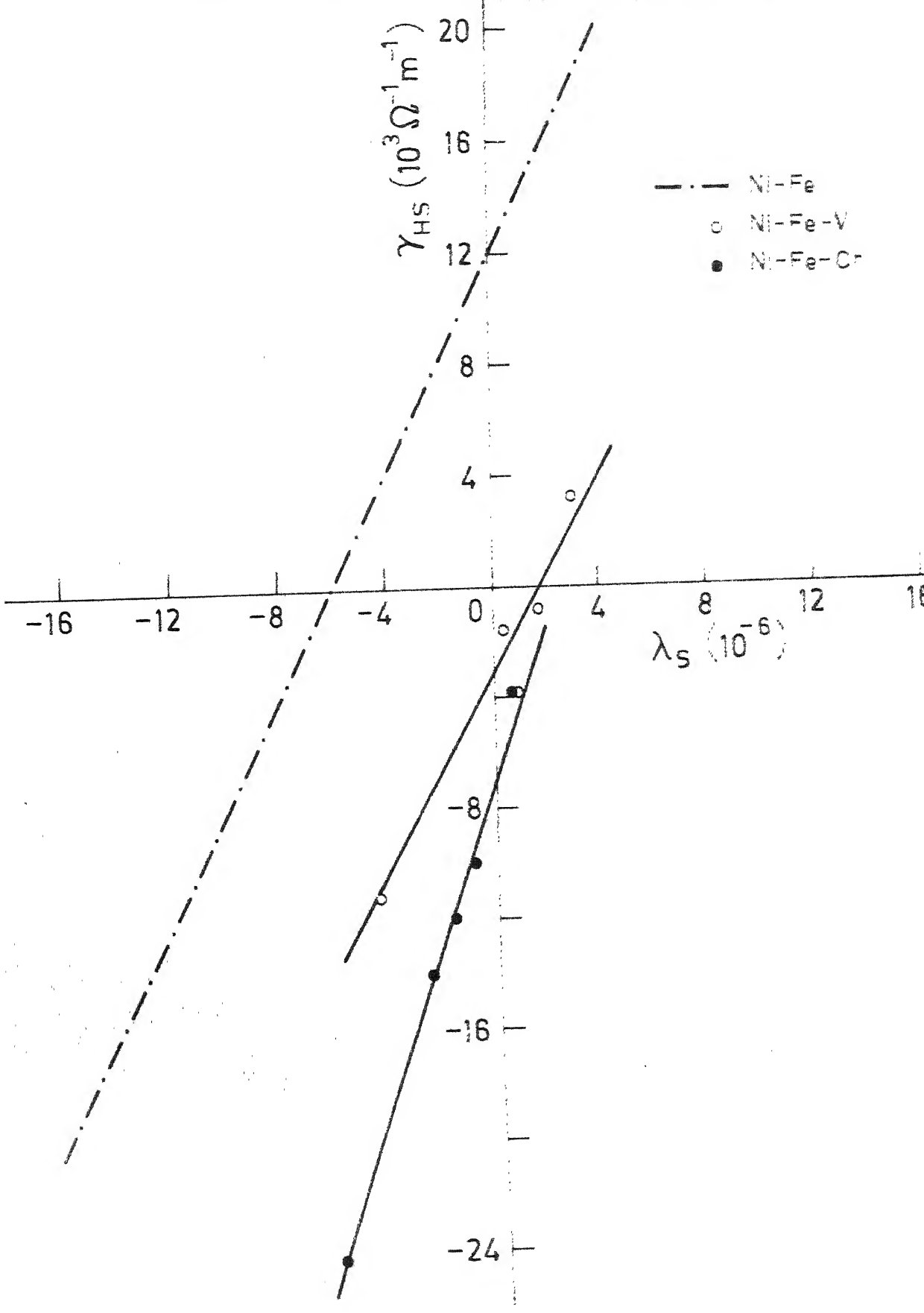
γ_{HS} $(10^3 \Omega^{-1} m^{-1})$
20
16
12
8
4
-8
-16
-24
-16
-12
-8
-4
0
4
8
12
λ_S (10^{-6})
Ni-Fe
Ni-Fe-V
Ni-Fe-Cr

ii) Usually the intercept the line makes on the γ_{HS} -axis is positive. But here for both the ternary systems the intercepts are negative being about $-3x10^{3}\ \Omega^{-1}m^{-1}$ for Ni-Fe-V and about $-7x10^{3}\Omega^{-1}m^{-1}$ for Ni-Fe-Cr alloys, in contrast to $+12x10^{3}\Omega^{-1}m^{-1}$ for Ni-Fe alloys. According to Berger's theory, the lines should all pass through the origin, which has in fact never been realized in practice.

Thus the fact that the slope and intercept are both ~~more~~ nearer to the theoretical values for Ni-Fe-V than Ni-Fe-Cr alloys, once again proves that the former is a better candidate to follow the S.B. model, probably because of more complete band-splitting. Another interesting aspect of the problem is that the large deviation of $\gamma_{HS} \simeq 0$ line from $\lambda_s \simeq 0$ line in the ternary diagrams (Figures 4.1 and 4.2) would have led one to expect that even if a proportionality relationship existed between λ_s and γ_{HS}, the intercepts of the straight lines on the γ_{HS}-axis would have been sufficiently large, compared to other alloys. But on the contrary, we find them even much smaller than in other alloys. Physically this means that the change of sign of γ_{HS} with composition is very gradual. A small negative intercept on γ_{HS}-axis means that as one approaches the $\lambda_s \simeq 0$ line from the Ni-rich side, first λ_s changes sign and the γ_{HS} value for the corresponding composition still remains negative but small in magnitude. But to reduce this small negative γ_{HS} to zero, the change of composition necessary is rather large as can be seen from the large separation of the experimental λ_s and $\gamma_{HS} \simeq 0$ lines in the ternary diagrams.

The above statement will be much more clear if one looks at Figure 4.4 where γ_{HS} and λ_s are plotted as a function of increasing Fe + Cr/V concentration for a series of ternary alloys whose Fe contents are roughly the same. In this figure are also included the corresponding quantities for Ni-Fe alloys as a function of Fe concentration, for comparison. The values of γ_{HS} for Ni-Fe alloys were taken from the data of Jellinghaus and De Andres[46] and λ_s from Bozorth et al.[52] and Hall[53]. Since magnetostriction data for Ni-Fe alloys in the literature are all for single crystals, they were converted by the relation $\lambda_s = \frac{2}{5} \lambda_{100} + \frac{3}{5} \lambda_{111}$, to compare with our polycrystalline samples. It can be seen from the figure that the rate of change of λ_s with concentration of impurity is hardly affected by the impurity type (Fe, Cr, V). But the change of γ_{HS} with the addition of Cr/V in ternary Ni-Fe-Cr/V alloys is much slower near $\gamma_{HS} \simeq 0$ region than in corresponding binary Ni-Fe alloys. This is as if the transition from negative to positive γ_{HS} is smeared out due to the addition of Cr/V in Ni-Fe alloys. In this connection we recall that Berger[44] pointed out that if the d-band has lower than spherical symmetry, then the transition from positive to negative γ_{HS} could get smeared out. Since transport properties like γ_{HS} depend only on the electrons near the Fermi level, this effect should be more pronounced in the case of γ_{HS} than λ_s. So there seems to be a possibility that the presence of Cr/V alters the d-band in such a manner as to lower its symmetry which in turn smears out the sign change of γ_{HS}.

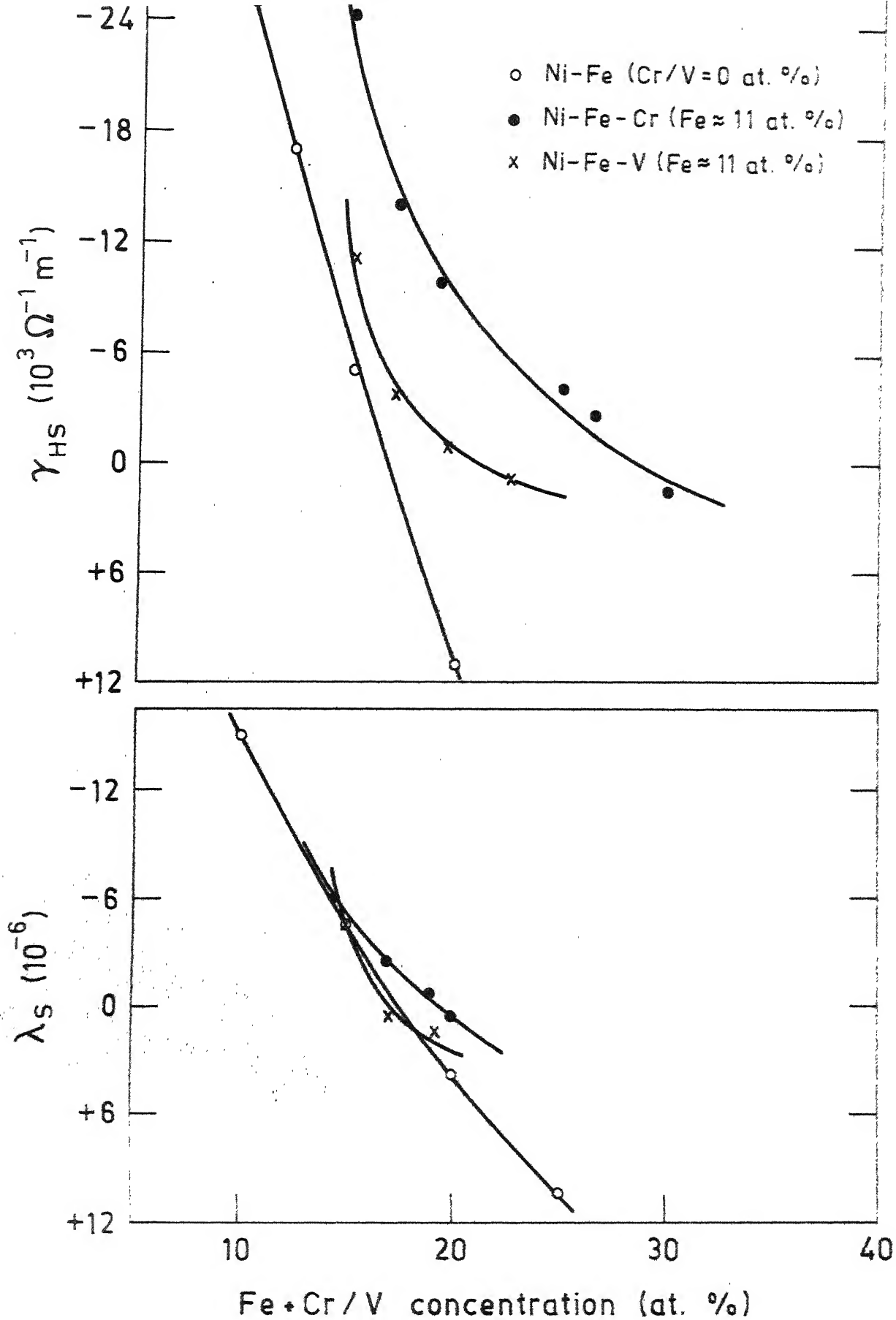

Fig. 4.4. Variation of γ_{HS} and λ_S with Cr/V

If this is true, then one should also expect that the maximum in ferromagnetic anisotropy of resistance, found for compositions near the vicinity of $\lambda_s \simeq \gamma_{HS} \simeq 0$ line, should also get smeared out being a transport property . Unfortunately the absence of any such data for the two ternary systems, rules out the possibility for a check. It seems, the effect should be more prominent in the case of Ni-Fe-Cr alloys than Ni-Fe-V, as the smearing out appears to be less in the latter case.

To summarise, from all the experimental data available so far, γ_{HS} and λ_s do never change sign exactly at the same composition (since γ_{HS} and λ_s plots have never been found to pass exactly through the origin), but approximately at the same compositions. Our systems are also no exception to this end. But there is a possibility, that the small discrepancy found in other systems regarding the compositions at which λ_s and γ_{HS} change sign, gets many times magnified in these ternary alloys because of the slow variation of γ_{HS} as a function of Cr/V concentrations. So the small separation between the $\lambda_s \simeq 0$ and $\gamma_{HS} \simeq 0$ lines in the ternary diagram found in the other systems, gets highly magnified in the case of Ni-Fe-Cr/V alloys, which gives an impression as if no relation exists between λ_s and γ_{HS} in these systems.

4.4 Magnetization data and Sign change of γ_{HS} and λ_s

The problem can also be looked at from a different point of view. As has been already shown in Section 3.5, magnetic measurements in the ferro as well as paramagnetic regions gave ample evidence that both the ternary systems behave as weak (not very weak) itinerant ferromagnets. Increasing concentration of Cr/V drives it more towards weak ferromagnetism. This behaviour is incompatible with the band model suggested by Berger. Probably such a model is an oversimplification of the reality. Unfortunately, so far no rigorous calculations have been carried out to give an idea about the band structure of these ternary systems; mainly computational problems have thwarted such attempts so far. But long back CPA calculation of band structures for the corresponding binary systems (e.g. Ni-Fe, Ni-Cr, Fe-Cr, etc.) were carried out by Hasegawa and Kanamori[36,38]. Their results show that in the case of Ni-Cr alloys[37], a distinctly separate band of Cr emerges above the Ni-spin-down band, which grows in size with increasing Cr-concentration, ultimately merging with the Ni-spin-down band. In the case of Fe-Cr alloys[38], since the energy difference of an electron sitting at the Cr-site from the one at the Fe-site ($E_{Cr} - E_{Fe}$) is very small for the down-spin electrons, on alloying, the down-spin band of Fe is hardly modified. On the other hand the up-spin band of Fe, though gets considerably deformed, hardly shows any sign of splitting. Under these circumstances,

Berger's model for ternary Ni-Fe-Cr alloys, seems to be over-simplified. It seems logical to think that the Cr spin-down band does not get separated out from the Fe-spin-down band, in contrast to what was suggested by Berger. Also the Cr spin-up band should not lie for away from the Fe spin-down band and there should be a considerable overlap between the two. With increasing Cr-concentration, the Cr sub-bands should grow in size and move towards the Ni-spin-down band. On the other hand the Fermi level of the system is also pushed up due to electron transfer. Thus at higher Cr concentrations, when the Fermi-level is near the edge of Ni-spin-down band, the assumption that all spin-up bands in the system are full, breaks down. In Eqn.(1.8), then one has to take into account the contribution of states in the spin-up bands also. Probably the large disagreement between our experimentally observed $\gamma_{HS} \simeq 0$ line and the one predicted by the S.B. model is due to this reason. Also the slow variation of γ_{HS} with Cr-concentration near the $\gamma_{HS} \simeq 0$ line seems to be in agreement with this picture. If this picture is correct, the alloys with increasing Cr content should behave more as itinerant weak ferromagnets simply because part of both up-spin and down-spin states above E_F remain empty. This is consistent with our magnetic measurements as discussed earlier.

In the case of Ni-Fe-V system, due to the absence of any such band structure calculations even for binary Ni-V, Fe-V, etc., nothing much could be said. Nevertheless, similar type of findings for γ_{HS} and magnetization for this system

suggest that similar mechanism could also be responsible for this system. Because of larger charge difference between Fe and V, band splitting for Fe-V alloys should be more complete and hence in ternary Ni-Fe-V alloys, the overlap between the Fe-spin-down and the V-spin-up bands should be lesser. The smaller discrepancy between the theoretical and our experimental $\gamma_{HS} \simeq 0$ line probably points to the same direction.

4.5 Residual Resistivity of Ternary Ni-Fe-Cr and Ni-Fe-V Alloys and the "Two-Current Model"

To explain the anomalous temperature dependence of resistivity in Ni and Pd, Mott[121] suggested that conduction takes place in parallel, through spin-up and spin-down electrons in transition metals. The idea was developed further by Fert and Campbell[122] and extended considerably by Dorleijn[123], Gautier et al.[124] andothers. The basic philosophy is that in transition metals, the relaxations times of the S↑ and S↓ electrons (which are the main current carriers) are quite different and they conduct in parallel. The large deviation of Mathiessen's rule (DMR) in transition metal alloys lend support to this hypothesis. Different band occupancies of the d-electrons, which are split into spin-up and spin-down bands in the presence of ferromagnetic exchange field, provide the main reason for the different relaxation times of the spin-up and spin-down conduction (s) electrons. Basically three processes are mainly responsible for the resistivity:

(i) the direct S-S scattering as in normal metals, (ii) the indirect S-d-S scattering, and (iii) the S-d scattering where the scattered state (d) is non-conducting. If in a particular metal, like Ni, the spin-up band is full, then the resistivity of the spin-up electrons ($\rho\uparrow$) will be considerably less than $\rho\downarrow$ since the third process cannot take place for the S$\uparrow$ electrons.

This "two-current model" has been found to be quite satisfactory in explaining the resistivities of transition metals and alloys (reference (123) and references therein), thermo-electric power in various Ni and Co-based transition metal alloys (3d, 4d and 5d series)[125], ferromagnetic anisotropy of resistance and anomalous Hall effect in dilute Ni and Fe based transition metal alloys[123,126], and so on. The so called "period effect", characterised by: (i) a maximum in $\rho\uparrow$ [127], (ii) sign change of the thermo-electric power[125], and (iii) a maximum in the specific increment of electronic specific heat co-efficient[128] also finds suitable explanation in the framework of the "two-current model". Actually the "period-effect" is observed when various elements, starting from the beginning of the transition metal series are added to Ni (or in some other element) and the changes in the various physical properties mentioned earlier, are monitored. A distinct anomaly is observed with the co-incidence of the virtual-bound state of the impurity atom with the Fermi-level of Ni (or the host material) and this occurs with Cr in the first transition series, Ru in the second and Os in the third.

According to the two current model, the total electrical resistivity ρ, is given by

$$\rho = \frac{\rho_{\downarrow}\rho_{\uparrow} + \rho_{\uparrow\downarrow}(\rho_{\uparrow} + \rho_{\downarrow})}{\rho_{\uparrow} + \rho_{\downarrow} + 4\rho_{\uparrow\downarrow}} \qquad (4.1)$$

where $\rho_{\sigma}(\sigma = \uparrow, \downarrow)$ are the resistivities associated with each sub-band σ, and $\rho_{\uparrow\downarrow}$ is the term which takes care of the mixing of the two parallel currents due to spin-flip scattering (electron-magnon interaction) and is important only at fairly high temperatures. It is assumed that though Matthiessen's rule is not valid for the total resistivity, each sub-band resistivity follows the same. Thus in a binary alloy $A_{100-x}B_x$, the sub-band resistivities are given by

$$\rho_{\sigma}(T) = \rho_{m\sigma}(T) + x\rho_{B\sigma} \qquad (4.2)$$

where the first term in the right hand side signifies the pure matrix resistivity and the second term, the impurity resistivity which is assumed to be temperature independent. It should also be noted that in the linear relationship between impurity resistivity and concentration x, is inherent the implication that Eqn.(4.2) should be valid in the dilute alloy limit where the impurity-impurity interaction is insignificant. Experimental results[123] show that Eqn.(4.2) is valid upto about 5 at.% of total impurity content in most of the Ni and Fe based alloys.

Now in the dilute alloy limit and at low temperatures, the pure matrix resistivity term and the spin-mixing term $\rho_{\uparrow\downarrow}$ are insignificant compared to this impurity resistivity[129].

Under this condition, combining Eqns. (4.1) and (4.2) the expression for the residual resistivity is given by

$$\rho_o = \frac{x\,\rho_{B\uparrow}\,\rho_{B\downarrow}}{\rho_{B\uparrow} + \rho_{B\downarrow}} \qquad (4.3)$$

In case of a ternary alloy $A_{100-x-y}B_xC_y$, in the low temperature limit, ρ_σ is given by

$$\rho_\sigma = x\,\rho_{C\sigma} + y\,\rho_{B\sigma} \qquad (4.4)$$

So if $\rho_{B\sigma}$, $\rho_{C\sigma}$ are known, the residual resistivities could be easily calculated. Studying hundreds of binary and ternary alloys based on Ni and Fe, Dorleign[123] has tabulated the values of ρ_σ for different transition metal impurities. Using the values of ρ_σ for Fe, Cr, V etc. in Ni, one could estimate the residual resistivities and compare with our experimental values. But one should not expect very good agreement with Eqn.(4.3) simply because our alloys are fairly concentrated and due to impurity-impurity interactions, the linear relationship between impurity resistivity and concentration (Eqn.(4.4)) cannot be expected to hold good. In Table 4.5 are presented the theoretically calculated values of residual resistivity and our 77K results. Since our alloys are concentrated, the change in resistivity between 77K and 4K is expected to be not more than a few percent, which is within the error-limit of our measurements. This makes the comparison between 77K data and the theoretically calculated resistivity values quite meaningful. According to Dorleijn et al.[123] $\rho_{Fe\uparrow} = 0.41$,

Table 4.5 : Experimental values of the resistivity of Ni-Fe-Cr/V alloys at 77K and those predicted by the "two-current model" (Eqn.(4.4))

Composition of Ni-Fe-Cr/V alloys (at.%)	$\rho_{exp.}$ ($\mu\Omega$-m) at 77K	$(\rho_{th})_{residual}$ ($\mu\Omega$-m)
Cr-series		
78-6-16	0.84±0.04	1.00
72-8-20	1.07±0.03	1.26
85.5-11-3.5	0.52±0.015	0.43
81-11-8	0.88±0.025	0.71
73.5-11.5-15	1.03±0.04	1.10
70-12-18	1.06±0.03	1.27
75.1-12.8-12.1	0.93±0.02	0.98
72.5-13.7-13.8	0.99±0.02	1.10
80-16-4	0.63±0.03	0.56
75-17-8	0.77±0.02	0.84
68.1-17.4-14.5	1.04±0.05	1.23
75.5-20.3-4.2	0.61±0.02	0.63
76.8-21.2-2	0.43±0.01	0.41
67-21-12	1.04±0.03	1.17
69.6-22.8-7.6	0.90±0.015	0.92
V-series		
83-10-7	0.81±0.02	0.49
85-11-4	0.54±0.02	0.35
81-17-2	0.34±0.01	0.26
79.4-17-3.6	0.49±0.015	0.37
74-22-4	0.58±0.02	0.44

$\rho_{Fe\downarrow}$ = 4.9 $\mu\Omega$ cm.; $\rho_{Cr\uparrow}$ = 28 and $\rho_{Cr\downarrow}$ = 6.2 $\mu\Omega$ cm.; $\rho_{V\uparrow}$ = 14 and $\rho_{V\downarrow}$ = 6.5 $\mu\Omega$ cm, respectively. These values were used for our resistivity calculations and are presented in Table 4.5 along with the experimental data.

Table 4.5 shows that for Ni-Fe-Cr alloys, the calculated values are in fairly good agreement with the experimental ones for alloys with low Cr-content (< 8 at.%), though the total impurity concentration often exceeds more than 20 at%. But the agreement becomes poorer with increasing Cr-content. The reasons are two-fold:

(i) Theoretical calculations[130] have shown that in binary Ni-Fe alloys, $\rho_{Fe\downarrow}$ is approximately linear even upto about 15 at.% Fe after which it starts bending and ultimately decreases after passing through a maximum around 30 at.% of Fe. But $\rho_{Fe\uparrow}$ remains very small until about 60 at.% of Fe.

(ii) Since the contribution of Cr atoms to the total resistivity is much larger than that of Fe atoms ($\rho_{Cr\uparrow} \gg \rho_{Fe\uparrow}$ and $\rho_{Cr\downarrow} \sim \rho_{Fe\downarrow}$), in ternary Ni-Fe-Cr alloys the effect of small non-linearity in $\rho_{Fe\downarrow}$ should not influence the total resistivity much. Hence even for alloys with high Fe content (< 30 at.%) but with low Cr, the theoretical and experimental values should agree reasonably well, as has been observed by us.

But in the case of alloys with high Cr-content (> 7 to 8 at.%), theoretical values are always larger than the experimental ones. This is because of the following reasons. Theoretical[130], as well as experimental results[123] have pointed out that in binary Ni-Cr alloys, resistivity

increases linearly with concentration upto about 5 to 6 at.% of Cr and then the rate of increase slows down. So if one calculates ρ for the concentrated allows, using the values of $\rho_{Cr\uparrow}$ and $\rho_{Cr\downarrow}$ in the linear range ($C < 5$ at.%), it is quite obvious that the calculated values will be larger than the actual ones. Since the resistivity is dominated by Cr contribution, the disagreement between theoretical and experimental values will be more for the alloys richer in Cr-content. This is consistent with our observation.

However, the same type of calculations, when extended to Ni-Fe-V alloys, hardly met with any success. Even for the alloy with low V-content, the disagreements were enormously large, as can be seen from Table 4.5 . Since for the alloys with higher V-content, the disagreements were even larger, they are not included in the table. One interesting observation that comes out from Table 4. 5 is that the calculated values are always much smaller than the observed ones. As discussed earlier, if deviation from linearity of the ρ vs. concentration curves (i.e. violation of Eqn.(4.4)) would have been the reason, one should have expected the calculated values to be larger than the observed ones. Again as $\rho_{V\uparrow} < \rho_{Cr\uparrow}$ and $\rho_{V\downarrow} \sim \rho_{Cr\downarrow}$, one should expect that the ternary Ni-Fe-V alloys should have lower resistivities compared to the same compositions for the corresponding Ni-Fe-Cr alloys. But surprisingly, we observe from our experimental results that ρ for the alloys in both the series with similar compositions, have comparable magnitudes. At present we are unable to give any satisfactory explanation for these observations.

Chapter V

In this chapter we will briefly summarise the highligh of the present study, followed by a short discussion on the s for future work.

5.1 Conclusions

These can be broadly classified into two categories: i) those derived from the magnetization measurements and ii) ones from the Hall effect studies.

The important outcome of the magnetization measurement are the following:

i) At low temperatures, though the change in magnetization with temperature could very well be accounted for by spin-wave theories, the values of the spin-wave stiffness constants (D) in Ni-Fe-Cr alloys were always found to be less than those obtained from neutron scattering experiments. For Ni-Fe-V system no such comparison could be made because of the absence of any neutron scattering data.

ii) For the Ni-Fe-Cr system, this discrepancy can be ve well explained if one assumes that along with spin-waves there also present an additional excitation, which in this case seems to be Stoner's single particle excitations corresponding to wea itinerant ferromagnets. The co-efficient of the Stoner term increases sharply as the Cr concentration is increased.

iii) The overall behaviour of reduced magnetization vs reduced temperature curves are not of the usual Brillouin function type, but they resemble those of amorphous ferromagnets. These data can be explained only in terms of modif Brillouin functions corresponding to that of a highly "disordered" system.

iv) Our data for $\bar{\mu}$ as a function of composition, show considerable deviation from linearity for both the ternary systems and once again confirm the findings of Menshikov et.a for Ni-Fe-Cr alloys.

v) Rhodes-Wohlfarth ratio (q_c/q_s) have been found to be always greater than unity and it shows a systematic increa with increasing Cr/V concentrations (i.e. with decreasing T_c) The values are also comparable to other itinerant systems wit comparable T_c.

vi) All the above observations including the fairly go straight line behaviour of Arrott plots over a wide temperatu range, indicate that both the ternary systems behave more like itinerant weak systems as the concentration of Cr/V is increas This is inconsistent with the S.B. picture since according to it one should expect them to behave like strong ferromagnets.

On the other hand, the conclusions that could be drawn from the Hall effect measurements are as follows:

i) The present study enabled us to establish the (γ_{HS}) line for the two ternary systems. But the position of the line is far away from the one expected from the S.B. model as well as from the $(\lambda_s)_{exp} \simeq 0$ line. Also our $\gamma_{HS} \simeq 0$ line and

the already established $\lambda_s \simeq 0$ line show considerable curvature contrary to what is expected from the S.B. model.

ii) The inconsistency of the S.B. model with the magnetization data and also its failure in explaining the $\gamma_{HS} \simeq 0$ line, points to the oversimplification of the actual band picture in the S.B. model. It seems that the assumption that Fe and Cr/V bands are completely distinct and separate, is far from the reality.

5.2 Scope for Further Work

Anybody conversant with the history of the development of science will admit, that in most cases an investigator has never knows what lies at the end of the road, although the path is always chosen with certain expectations, based mostly on rational judgement. At the end of the journey some expectations are realized, but not before giving birth to a host of new ones. The present investigation can be categorised into this class.

As discussed in Section 3.5, our magnetization measurements strongly supported the idea that the addition of Cr/V in Ni-Fe alloys drives it more towards itinerant weak ferromagnetism. But because of our present experimental limitations (viz. inaccessibility to temperatures below 77K), this idea could not be placed beyond doubt. For that it would be necessary to study some more alloys with even lower T_c (i.e. with more Cr/V content).

In the case of Ni-Fe-V alloys it is highly advisable carry out some inelastic neutron scattering experiments to ob the spin wave stiffness constants (D) and compare it with ou magnetization derived values. We have a strong suspicion tha even in Ni-Fe-V alloys, the D values obtained by us are small than actual ones due to the presence of excitations other tha spin waves at low temperatures. This can also be verified fr more accurate magnetization measurements.

We found that the Curie-Weiss behaviour, specially for Cr/V-rich alloys (i.e. with lower T_c), starts at temperatures much above T_c. However, this temperature does not seem to be high enough to exceed the degeneracy temperature, as expected from the itinerant models. Whether this deviation is actuall due to some short range ordering or due to some other reason be verified from small-angle neutron scattering experiments.

The non-linearity in the $\bar{\mu}$ vs. concentration curves, for both the systems, also do not find any suitable explanation in the existing theories. We draw the attention of the theoretic to this problem. Probably CPA type band structure calculation could shed some light on this point.

From our Hall effect measurements, we found that due to the addition of Cr/V in Ni-Fe alloys, the transition from negative to positive R_s gets smeared out compared to binary Ni-Fe alloys. Correspondingly one should expect, if at all, a broad maximum in ferromagnetic anisotropy of resistance in con with a fairly sharp one observed in other systemsat the

compositions where R_s changes sign. But so far, except for a few sketchy data[60], no systematic study has been made in search of this maximum for the two ternary systems.

Finally our data on extra-ordinary Hall effect and magnetization show that the S.B. model is inadequate, probably because of oversimplification of the band structure. A clear picture can emerge only when some actual band structure calculations for the two systems are available.

References

(1) J.M. Lavine, Phys. Rev. 123, 1273 (1961).

(2) R.W. Kaffy and R.V. Coleman, Phys. Rev. B 10, 2915 (1974).

(3) E.I. Kondorskii, Sov. Phys. JETP 28, 1256 (1969).

(4) D.I. Volkov and T.M. Kozlova, Fiz. Met. Metalloved. 20, 355 (1965).

(5) J.J. Rhyne, Phys. Rev. 172, 523 (1968).

(6) J.J. Rhyne, J. Appl. Phys. 40, 1001 (1969).

(7) C.M. Hurd, The Hall Effect in Metals and Alloys (Plenum, New York, 1972).

(8) The Hall Effect and its Applications, edited by C.L. Chien and C.R. Westgate (Plenum, New York, 1980).

(9) R. Karplus and J.M. Luttinger, Phys. Rev. 95, 1154 (1954).

(10) J. Smit, Physica 21, 877 (1955).

(11) J. Smit, Physica 24, 39 (1958).

(12) J.M. Luttinger, Phys. Rev. 112, 739 (1958).

(13) J. Smit, Phys. Rev. B 17, 1450 (1978).

(14) Yu. P. Irkhin and V.G. Shavrov, Sov. Phys. JETP 15, 854 (1962).

(15) E.I. Kondorskii, A.V. Cheremushkina and N. Kurbaniyazov, Sov. Phys. Solid State 6, 422 (1964).

(16) J. Kondo, Prog. Theoret. Phys. (Japan) 27, 772 (1962).

(17) N.V. Volkenshtein and G.V. Fedorov, Sov. Phys. JETP 11, 48 (1960).

(18) Sh.Sh. Abel'skii and Yu.P. Irkhin, Phys. Met. Metall. 14, 1 (1962).

(19) Yu.Kagan and L.A.Maksimov, Sov. Phys. Solid State 7, 422 (1965).

(20) F.E. Maranzana, Phys. Rev. 160, 421 (1967).

(21) R.C. Fivaz, Phys. Rev. 183, 586 (1969).

(22) A. Fert and A. Friederich, Phys. Rev. B13, 397 (1976).

(23) A. Fert and O. Jaoul, Phys. Rev. Lett. 28, 303 (1972).

(24) L. Berger, Phys. Rev. B2, 4559 (1970).

(25) S.K. Lyo and T. Holstein, Phys. Rev. Lett. 29, 423 (1972).

(26) P. Nozieres and C. Lewiner, J. Phys. (Paris), 34, 901 (1973).

(27) E.I. Kondorskii, Sov. Phys. JETP 28, 291 (1969).

(28) S. Soffer, J.A. Dreesen and E.M. Pugh, Phys. Rev. 140, A668 (1965).

(29) H. Ashworth, D. Sengupta, G. Schnakenberg, L. Shapiro and L.Berger, Phys. Rev. 185, 792 (1969).

(30) E.I. Kondorskii, A.V. Vedayev and A.B. Granovskiy, Fiz. Met. Metalloved. 40, 455 (1975).

(31) ibid 40, 688 (1975).

(32) ibid 40, 903 (1975).

(33) N.F. Mott, Phil. Mag. 22, 287 (1936).

(34) J. Friedel, Nuovo Cimento Suppl. 7, 287 (1958).

(35) J. Friedel, Can. Journ. Phys. 34, 1190 (1956).

(36) H. Hasegawa and J. Kanamori, J. Phys. Soc. Japan 31, 382 (1971).

(37) H. Hasegawa and J. Kanamori, J. Phys. Soc. Japan. 33, 1599 (1972).

(38) H. Hasegawa and J. Kanamori, J. Phys. Soc. Japan. 33, 1607 (1972).

(39) B. Velicky, S. Kirkpatrick and H. Ehrenreich, Phys. Rev. 175, 747 (1968).

(40) D.H. Seib and W.E. Spicer, Phys. Rev. Lett. 20, 1441 (1968)

(41) K.Y. Yu, C.R. Helms, W.E. Spicer and P.W. Chye, Phys. Rev. B15, 1629 (1977).

(42) G.M. Stocks, R.W. Williams and J.S. Faulkner, Phys. Rev. B4, 4390 (1971).

(43) P. Oelhafen, E. Hauser, H.J. Güntherodt and K.H.Bennemann, Phys. Rev. Lett. 43, 1134 (1979).

(44) L. Berger, Physica 30, 1141 (1964) and the references cited therein.

(45) L. Berger and G. Bergmann, in The Hall effect and its applications, edited by C.L.Chien and C.R.Westgate (Plenum, New York, 1980).

(46) W. Jellinghaus and M.P. De Andres, Ann. Physik 5, 187 (1960).

(47) L. Berger, AIP Conf. Proc. 34, 355 (1976).

(48) R.C. O' Handley, Phys. Rev. B18, 2577 (1978).

(49) L. Berger, Physica 91B, 31 (1977).

(50) C.H. Cheng, C.T. Wei and P.A. Beck, Phys. Rev. 120, 426 (1960).

(51) L. Berger, Phys. Rev. 138, A1083 (1965).

(52) R.M. Bozorth and J.G. Walker, Phys. Rev. 89, 624 (1953).

(53) R.C. Hall, J. Appl. Phys. 30, 816 (1959).

(54) O. Von Auwers and H. Neumann, Wiss. Veroeffentl. a.d. Siemens-Werken 14, 93 (1935).

(55) I.M. Puzej, Izv. Akad. Nauk SSSR, Ser.Fiz. 16, 549 (1952); I.M. Puzej and B.V.Molotilov, ibid. 22, 1244 (1958).

(56) U. Hofmann, Z. Angew. Phys. 21, 425 (1966).

(57) R.C. O'Handley and L. Berger, Inst. Phys. Conf. 39, 477 (1978).

(58) R.C. O'Handley, Sol. State Commun. 21, 1119 (1977).

(59) J. Smit, Physica 17, 612 (1951).

(60) H.C. Van Elst, Physica 25, 708 (1959).

(61) A.Z. Menshikov and A. Ye. Teplykh, Phys. Met. Metall. 44, 78 (1977).

(62) P. Rhodes and E.P. Wohlfarth, Proc. Roy. Soc. A 273, 247 (1963).

(63) The Hall Effect and Related Phenomena, E.H. Putley, p.45 (Butterworths, London, 1960).

(64) A.Z. Menshikov, N.N. Kuzmin, V.A. Kazantsev, S.K.Sidorov and V.M. Kalinin, Phys. Met. Matall. 40, 174 (1975).

(65) M.J. Besnus, Y. Gottehrer and G. Munschy, Phys. Stat. Sol. B 49, 597 (1972).

(66) I.P. Gregory and D.E. Moody, J. Phys. F5, 36 (1975).

(67) F. Böling, Phys. Kondens, Mater. 7, 162 (1968).

(68) F. Keffer in Handbuch der Physik, Vol. XVIII/2, edited by S. Flügge (Springer-Verlag, Berlin, 1966).

(69) F.J. Dyson, Phys. Rev. 102, 1217 (1956); ibid. 102, 1230 (1956).

(70) J.A. Copeland and H.A. Gersch, Phys. Rev. 143, 236 (1966).

(71) T. Izuyama and R. Kubo, J. Appl. Phys. 35, 1074 (1964).

(72) J. Mathon and E.P. Wohlfarth, Proc. Roy. Soc. London A 302, 409 (1968).

(73) M.W. Stringfellow, J. Phys. C1, 950 (1968).

(74) V.J. Minkiewicz, M.F. Collins, R. Nathans and G. Shirane, Phys. Rev. 182, 624 (1969).

(75) H.A. Mook, J.W. Lynn and R.M. Nicklow, Phys. Rev. Lett. 30, 556 (1973).

(76) A.T. Aldred, Phys. Rev. B 11, 2597 (1975).

(77) B.E. Argyle, S.H. Charap and E.W. Pugh, Phys. Rev. 132, 2051 (1963).

(78) I. Nakai, J. Phys. Soc. Japan. 52, 1781 (1983).

(79) I. Nakai, F. Ono and O. Yamada, J. Phys. Soc. Japan 52, 1791 (1983)

(80) B. Antonini and F. Menzinger, Solid State Commun. 9, 417 (1971).

(81) M. Hennion, B. Hennion, A. Castets and D. Tocchetti, Sol. State Commun. 17, 899 (1975).

(82) Y. Ishikawa, S. Onodera and K. Tajima, J. Magn. and Magn. Mater. 10, 183 (1979).

(83) C.L. Chien and R. Hasegawa, Phys. Rev. B 16, 2115 (1977); and the references cited therein.

(84) A.K. Majumdar, V. Oestreich, D. Weschenfelder and F.E. Luborsky, Phys. Rev. B27, 5618 (1983).

(85) P.C. Riedi, Phys. Rev. B 15, 5197 (1977).

(86) P.C. Riedi, Physica 91B, 43 (1977).

(87) A.T. Aldred, Phys. Rev. B 14, 219 (1976).

(88) E.C. Stoner, Proc. Roy. Soc. A165, 372 (1938).

(89) C. Herring, in Magnetism, Vol. IV, Chapter VI, edited by G.T. Rado and H. Suhl (Academic Press, New York, 1966).

(90) T. Moriya, J. Magn. and Magn. Mater. 31-34, 10 (1983); and the references cited therein.

(91) E.D. Thompson, E.P. Wohlfarth and A.C. Bryan, Proc. Phys. Soc. 83, 59 (1964).

(92) A.V. Gold, J. Low Temp. Phys. 16, 3 (1974).

(93) O. Yamada, F. Ono, I. Nakai, H.Maruyama, K. Ohta and M. Suzuki, J. Magn. and Magn. Mater. 31-34, 105 (1983).

(94) W. Köster and W. Gmöhling, Z. Metallk. 52, 713 (1961).

(95) F. Acker and R. Huguenin, Phys. Letts.53A, 167 (1975).

(96) A. Arrott, Phys. Rev. 108, 1394 (1957).

(97) C.C. Tsuei and H. Lilienthal, Phys. Rev. B 13, 4899 (1976).

(98) S.N. Kaul, Phys. Rev. B 24, 6550 (1981); and the references cited therein.

(99) K. Handrich, Phys. Status Solidi 32, K55 (1969).

(100) C.G. Montgomery, J.I. Krugler and R.M. Stubbs, Phys. Rev. Lett. 25, 669 (1970).

(101) J. Richter, K. Handrich and J. Schreiber, Phys. Status Solidi B 68, K61 (1975).

(102) E.P. Wohlfarth, J. Magn. and Magn. Mater. 7, 113 (1978).

(103) H.J. Blythe, Phys. Letts. 21, 144 (1966).

(104) G.S. Knapp, J. Appl. Phys. 41, 1073 (1970).

(105) W.E. Gardner, T.F.Smith, B.W.Howlett, C.W.Chu and A.Sweedler, Phys. Rev.166, 577 (1968).

(106) D.M. Edwards and E.P. Wohlfarth, Proc. Roy. Soc. A 303, 127 (1968).

(107) P.F. De Chatel and F.R. De Boer, Physica 48, 331 (1970).

(108) E.P. Wohlfarth, J. Appl. Phys. 39, 1061 (1968).

(109) T. Moriya and A. Kawabata, J. Phys. Soc. Japan.34, 639 (1973); ibid 35, 669 (1973).

(110) G.S. Knapp, F.Y. Fradin and H.V. Culbert, J. Appl. Phys. 42, 1341 (1971).

(111) M.C. Cadeville, Thesis, University of Strasbourg (1965).

(112) D.A. Read, E.H. Thomas and J.B. Forsythe, J. Phys. Chem. Solids 29, 1569 (1968).

(113) S. Ogawa and N. Sakamoto, J. Phys. Soc. Japan 22, 1214 (1967).

(114) H.L. Alberts, J. Beille, D. Bloch and E.P. Wohlfarth, Phys. Rev. B 9, 2233 (1974).

(115) O. Yamada, F. Ono and I. Nakai, Physica 91B, 298 (1977).

(116) E.P. Wohlfarth, Physica 91B, 305 (1977).

(117) A.K. Gangopadhyay, R.K. Ray and A.K. Majumdar, Ind. J. Cryogenics (to be published).

(118) A. Sinha and A.K. Majumdar, J. Appl. Phys. 50, 7533 (1979).

(119) A.K. Majumdar and R.D. Greenough, unpublished.

(120) J.J. Went, Physica 17, 98 (1951).

(121) N.F. Mott, Proc. R. Soc. A 153, 699 (1936).

(122) A. Fert and I.A. Campbell, Phys. Rev. Letts. 21, 1190 (1968).

(123) J.W.F. Dorleijn, Philips Res. Repts. 31, 287 (1976).

(124) P. Leonard, M.C. Cadeville, J. Durand and F. Gautier, J. Phys. Chem. Solids 30, 2169 (1969).

(125) M.C. Cadeville and J. Roussel, J. Phys. F 1, 686 (1971).

(126) J.W. F. Dorleijn and A.R. Miedema, AIP Conf. Proc. 34, 50 (1976); ibid. J. Magn. and Magn. Mater. 12, 26 (1979).

(127) J. Durand and F. Gautier, J. Phys. Chem. Solids, 31, 2773 (1970).

(128) R. Caudron, R. Caplain, J. Meunier and P. Costa, Phys. Rev. B 8, 5247 (1973).

(129) B. Loegel and F. Gautier, J. Phys. Chem. Solids 32, 2723 (1971).

(130) H. Akai, Physica 86-88B, 539 (1977).

87521

PHY-1983-D-GAN-EXT